NASA/TP–2012-217342

The Exact Solution for Linear Thermoelastic Axisymmetric Deformations of Generally Laminated Circular Cylindrical Shells

Michael P. Nemeth and Marc R. Schultz
Langley Research Center, Hampton, Virginia

February 2012

NASA STI Program . . . in Profile

Since its founding, NASA has been dedicated to the advancement of aeronautics and space science. The NASA scientific and technical information (STI) program plays a key part in helping NASA maintain this important role.

The NASA STI program operates under the auspices of the Agency Chief Information Officer. It collects, organizes, provides for archiving, and disseminates NASA's STI. The NASA STI program provides access to the NASA Aeronautics and Space Database and its public interface, the NASA Technical Report Server, thus providing one of the largest collections of aeronautical and space science STI in the world. Results are published in both non-NASA channels and by NASA in the NASA STI Report Series, which includes the following report types:

- TECHNICAL PUBLICATION. Reports of completed research or a major significant phase of research that present the results of NASA programs and include extensive data or theoretical analysis. Includes compilations of significant scientific and technical data and information deemed to be of continuing reference value. NASA counterpart of peer-reviewed formal professional papers, but having less stringent limitations on manuscript length and extent of graphic presentations.

- TECHNICAL MEMORANDUM. Scientific and technical findings that are preliminary or of specialized interest, e.g., quick release reports, working papers, and bibliographies that contain minimal annotation. Does not contain extensive analysis.

- CONTRACTOR REPORT. Scientific and technical findings by NASA-sponsored contractors and grantees.

- CONFERENCE PUBLICATION. Collected papers from scientific and technical conferences, symposia, seminars, or other meetings sponsored or co-sponsored by NASA.

- SPECIAL PUBLICATION. Scientific, technical, or historical information from NASA programs, projects, and missions, often concerned with subjects having substantial public interest.

- TECHNICAL TRANSLATION. English-language translations of foreign scientific and technical material pertinent to NASA's mission.

Specialized services also include creating custom thesauri, building customized databases, and organizing and publishing research results.

For more information about the NASA STI program, see the following:

- Access the NASA STI program home page at *http://www.sti.nasa.gov*

- E-mail your question via the Internet to help@sti.nasa.gov

- Fax your question to the NASA STI Help Desk at 443-757-5803

- Phone the NASA STI Help Desk at 443-757-5802

- Write to:
  NASA STI Help Desk
  NASA Center for AeroSpace Information
  7115 Standard Drive
  Hanover, MD 21076-1320

NASA/TP–2012-217342

The Exact Solution for Linear Thermoelastic Axisymmetric Deformations of Generally Laminated Circular Cylindrical Shells

Michael P. Nemeth and Marc R. Schultz
Langley Research Center, Hampton, Virginia

National Aeronautics and
Space Administration

Langley Research Center
Hampton, Virginia 23681-2199

February 2012

Available from:

NASA Center for AeroSpace Information
7115 Standard Drive
Hanover, MD 21076-1320
443-757-5802

Summary

A detailed exact solution based on the Sanders-Koiter linear shell theory is presented for laminated-composite circular cylinders that undergo axisymmetric deformations. The overall solution is formulated in a general, systematic way and is obtained from the solution of a single fourth-order, nonhomogeneous ordinary differential equation with constant coefficients in which the radial displacement is the dependent variable. Moreover, the full response-coupling effects associated with generally laminated wall construction are included in the solution. A key element of the analysis is the use of the positive-definiteness of the strain energy to define uniquely the form of the basis functions spanning the solution space of the ordinary differential equation. Loading conditions are considered that include axisymmetric edge loads, surface tractions, and temperature fields. Likewise, all possible axisymmetric displacement and traction boundary conditions are considered.

Results are presented for five examples that demonstrate a wide range of behavior for specially orthotropic and fully anisotropic cylinders. Several of the results illustrate how laminated-wall construction, loading and support conditions, and cylinder length affect the size of localized zones of bending deformations that typically occur near the cylinder ends. For some of the examples, the results indicate highly localized bending deformations that attenuate rapidly. For other examples, the bending deformations exhibit very little attenuation. Approximate solutions are also given for several of the examples that add credibility to the corresponding results obtained from the exact solution and that provide insight into the possible pitfalls of making certain types of simplifications in a preliminary-design process. For example, several results are presented that illustrate conditions for which sizing a laminated-composite cylinder based on an approximate linear membrane analysis is inappropriate.

Results obtained from the exact solution presented herein also have the potential to serve as fundamental benchmarks for the validation of numerical solution methods such as the finite-element method. Likewise, results obtained from the exact solution have the potential to provide insight into the extent of discretization that might be needed for analyzing accurately shells with zones of localized bending caused by cutouts, stiffeners, or other types of discontinuities and gradients.

Symbols

$\bar{a}_{11}, \bar{a}_{16}, \bar{a}_{66}$	modified compliances defined by equations (15)
$A_{11}, A_{12}, A_{16}, A_{22}, A_{26}, A_{66}$	laminate membrane stiffnesses
$\overline{A}_{16}, \overline{A}_{26}, \overline{A}_{66}$	modifed laminate stiffnesses defined by equations (12)
$\ell_1(x), \ell_2(x), \ell_3(x), \ell_4(x)$	solution basis functions defined by equations (45)

$\bar{\ell}_{12}, \bar{\ell}_{62}$	modified compliances defined by equations (15)
$B_{11}, B_{12}, B_{16}, B_{22}, B_{26}, B_{66}$	laminate membrane-bending coupling stiffnesses
$\overline{B}_{16}, \overline{B}_{26}, \overline{B}_{66}$	modified laminate stiffnesses defined by equations (12) and (87)
c_1, c_2	shell-theory constants defined in Appendix A
$c_{\bar{N}}, c_{\bar{T}}$	constants defined by equations (47)
c_1^M, c_2^M	constants defined by equations (67)
c_3^M, c_4^M	constants defined by equations (85)
c_5^M, c_6^M	constants defined by equations (91)
c_3^N, c_4^N	constants defined by equations (81)
$c_1^u, c_2^u, c_1^v, c_2^v$	constants defined by equations (60)-(61)
$c_x^{Th}, c_\theta^{Th}, c_{x\theta}^{Th}$	thermal constitutive parameters defined by equation (B17)
$\bar{c}_{x\theta}^{Th}$	modified thermal constitutive parameter defined by equation (101b)
C_1, C_2, C_3	constants defined by equations (19)-(21)
$C_4(x)$	function defined by equation (22)
$\bar{e}_{12}, \bar{e}_{62}$	modified compliances defined by equations (15)
$D_{11}, D_{12}, D_{16}, D_{22}, D_{26}, D_{66}$	laminate bending stiffnesses
e	eccentricity parameter defined by equation (25)
E_1, E_2	major and minor principal lamina moduli, respectively
G_0, G_1, G_s, G_c	temperature field constants defined by equation (97b)
G_{12}	lamina shear modulus

h	cylinder wall thickness
h_{ply}	lamina ply thickness
H_0, H_1, H_s, H_c	temperature field constants defined by equation (97a)
K_1, K_2, K_3, K_4	unknown solution constants defined by equation (44)
L	cylinder length
$m_x^{Th}, m_\theta^{Th}, m_{x\theta}^{Th}$	thermal constitutive parameters defined by equation (B17)
$M_x, M_\theta, M_{x\theta}$	axial and circumferential bending and twisting stress resultants, respectively
$M_x^{Th}, M_\theta^{Th}, M_{x\theta}^{Th}$	thermal stress resultants defined by equation (B15)
$M_{xk}(x)$	stress resultant functions defined by equations (67)
M_{x5}, M_{x6}	stress resultant constants defined by equations (67)
$M_{\theta k}(x)$	stress resultant functions defined by equations (85)
$M_{\theta 5}, M_{\theta 6}$	stress resultant constants defined by equations (85)
$M_{x\theta k}(x)$	stress resultant functions defined by equations (91)
$M_{x\theta 5}, M_{x\theta 6}$	stress resultant constants defined by equations (91)
$\tilde{M}$	applied uniform end moment stress resultant defined by equation (B21)
$n_x^{Th}, n_\theta^{Th}, n_{x\theta}^{Th}$	thermal constitutive parameters defined by equation (B17)
$\bar{n}_{x\theta}^{Th}$	modified thermal constitutive parameter defined by equation (101a)
$N_x, N_\theta, N_{x\theta}$	axial, circumferential, and shear membrane stress resultants, respectively
$N_x^{Th}, N_\theta^{Th}, N_{x\theta}^{Th}$	thermal stress resultants defined by equation (B15)

$N_{\theta k}(x)$	stress resultant functions defined by equations (80)
$N_{\theta 5}$, $N_{\theta 6}$	stress resultant constants defined by equations (80)
$\bar{N}_0$	constant of integration defined by equation (1a)
$\bar{N}_1(x)$	function defined by equation (1b)
$\tilde{N}$	applied uniform axial stress resultant defined by equation (B18)
p_u	uniform ullage pressure used in Example 4
$P(x)$	loading function appearing in differential equation (26) and defined by equations (29)
P_0, $P_1(x)$	$P(x)$ terms defined by equations (29)
$q_x(x)$, $q_\theta(x)$, $q_n(x)$	applied axial, circumferential, and normal surface tractions, respectively
q_x^0, q_θ^0, q_n^0, q_x^1, q_θ^1, q_n^1, q_x^s, q_θ^s, q_n^s, q_x^c, q_θ^c, q_n^c,	surface traction amplitudes defined by equations (96)
Q_x, Q_θ	axial and circumferential transverse-shear stress resultants, respectively
$Q_{xk}(x)$	stress resultant functions defined by equations (69)
$Q_{\theta k}(x)$	stress resultant functions defined by equations (95)
R	mid-surface cylinder radius
Q, S, T	constant coefficients of differential equations (26) and (40), defined by equations (27), (28), and (39)
$\hat{T}$	modified shear stress resultant defined by equation (4)
$\hat{T}^{Th}$	thermal stress resultant defined by equation (12f)
$\tilde{T}$	value of $\hat{T}$ applied at a cylinder end (see equations (6) and (B19))

$\bar{T}_0$	constant of integration defined by equation (7a)
$\bar{T}_1(x)$	function defined by equation (7b)
$\mathcal{U}$	strain-energy density defined by equation (30)
u, v	axial and circumferential displacements, respectively
$\tilde{u}$, $\tilde{v}$	applied end displacements defined by equations (B18) and (B19)
$\bar{u}$, $\bar{v}$	constants of integration defined by equations (56) and (57)
$U_k(x)$	displacement functions defined by equations (56), (58a), and (60)
U_5', U_6'	displacement constants defined by equations (50)
$V_k(x)$	displacement functions defined by equations (57), (58b), and (61)
V_5', V_6'	displacement constants defined by equations (52)
$\tilde{V}$	applied uniform transverse-shear stress resultant defined by equation (B20)
w	radial displacement
$w_H(x)$	homogeneous solution to equation (40), defined by equation (44)
$w_p(x)$	particular solution to equation (40), defined by equations (46) and (47)
w_p^0, $\bar{w}_p(x)$	constant and variable parts of $w_p(x)$ defined by equations (46) and (47)
$\bar{w}_p^0$, $\bar{w}_p^1$, $\bar{w}_p^2$, $\bar{w}_p^{s1}$ $\bar{w}_p^{s2}$, $\bar{w}_p^{c1}$, $\bar{w}_p^{c2}$	coefficients of particular solution defined by equations (104)
W_0, W_1	coefficients of approximate solution defined by equation (E4)
$\tilde{w}$	applied radial end displacement defined by equations (B20)
x	axial coordinate of cylinder

$Y_0, Y_1, Y_2, Y_{s1}, Y_{s2}, Y_{c1}, Y_{c2}$	coefficients of $P_1(x)$ defined by equations (102)
$\beta_x^o, \beta_\theta^o, \beta_n^o$	rotations defined by equations (B9)-(B11)
$\tilde{\beta}$	applied end rotation defined by equation (B21)
γ	specific weight of a fluid
$\Delta T(x, z)$	temperature change function defined by equation (B16)
$\varepsilon_x^o, \varepsilon_\theta^o, \gamma_{x\theta}^o$	axial, circumferential, and shear membrane strains, respectively
θ	circumferential, angular coordinate
$\Theta_0(x), \Theta_1(x)$	temperature change functions defined by equation (B16)
$\kappa_x^o, \kappa_\theta^o, \kappa_{x\theta}^o$	axial and circumferential bending and twisting strains, respectively
λ	parameter appearing in equations (41)-(43)
μ	constant defining different shell theories, given by equation (3)
ν_{12}	lamina major Poisson's ratio
ϕ	lamina fiber angle

Introduction

Weight and structural performance are key elements in the design of aircraft and spacecraft. For example, weight directly affects fuel costs incurred by airlines, which affects consumers and commerce. In addition, structural performance affects the safety of the flying public. Similarly, the present cost for placing a spacecraft in Earth orbit ranges from approximately $5,000 to $10,000 per pound, depending on the altitude. Thus, structural weight is a significant design driver in launch-vehicle structures that operate near the Earth, such as the Space Shuttle external tank and solid rocket boosters shown in figure 1, and in vehicles that operate far from Earth such as the conceptual lunar lander shown in figure 2. In recent studies of newer vehicles like a lunar lander, fiber-reinforced, laminated-composite materials have received significant attention for use in primary structural members. These advanced composite materials have higher stiffness-to-density ratios, higher strength-to-density ratios, and very low coefficients of thermal expansion, compared to common isotropic materials. Additionally, because laminated composites are composed of orthotropic layers, oriented at various angles, the potential exists to tailor a laminate

to meet a specific set of high-performance, or special purpose, structural requirements. Thus, laminated composites offer a design space that is much wider than that for isotropic materials. However, along with the potential structural performance benefits of laminate tailoring comes a much more complicated analysis and design process.

Efforts to reduce structural weight while maintaining, or even enhancing, structural preformance through the use of fiber-reinforced composite materials have been underway for approximately 50 years. Although many advancements have been made, and several large-scale structures have been built and tested, advances in understanding the mechanics of composite structures, especially those with extreme orthotropies and anisotropies, need to continue. One common, fundamental structural element is the circular cylinder. For example, understanding the buckling response of stiffened cylinders is fundamental to the design of aircraft fuselages and launch-vehicle fuel tanks and interstages. Likewise, understanding how edge effects associated with end fittings on the tubular members of a lunar lander affect the structural performance is significant. When dealing with generally laminated cylinders, deformation modes associated with bending, twisting, and stretching can be highly coupled, and failure to fully understand these effects on a design can have dangerous and costly unintended consequences. Thus, continued advancement of understanding the basic behavioral characteristics of generally laminated circular cylinders is an important part of the quest to develop high performance, or special purpose, structures by exploiting orthotropies and anisotropies. Moreover, advancing this understanding can be beneficial to postmortem analysis of failures that always occur when the limits of design technology are pushed, and should help to mitigate risks. Furthermore, advancing this understanding may be beneficial to the development of material-characterization test methodology for future exotic, advanced materials. Improved understanding of fundamental structural elements also provides insight into finite element modeling of complex flight-vehicle structures.

Several analyses for predicting the stresses, strains, and displacements of laminated-composite cylinders that are relevant to the present study can be found in the literature. Perhaps, one of the first significant papers to address anisotropic cylinders was given by Dong et al.[1] In this paper, equations for the linear static response of general shells are given that are based on the simplifications attributed to Donnell, Mushtari, and Vlasov (see Brush and Almroth[2]). In addition, the general-shell equations are specialized to circular cylinders and a stress-function formulation is given. Moreover, a solution is presented for the axisymmetric bending of a semi-infinite cylinder subjected to edge moments. Similarly, an analysis for anisotropic cylinders undergoing axisymmetric deformations was given by Gulati and Essenburg[3] in 1967 that is based on a shell theory more refined than Donnell-type theories and that includes the effects of transverse shear deformation.

In 1970, Stavsky and Smolash[4] presented a detailed thermoelastic analysis of orthotropic composite cylinders. In particular, numerous results are presented for fixed-end cylinders undergoing axisymmetric deformations. Also in that year, Vicario and Rizzo[5] presented an exact solution for the axisymmetric response of symmetrically laminated cylinders with coupling between extension and shear (unbalanced). Later, in 1972, Reuter[6] presented an analytical solution for axisymmetric deformation of unbalanced symmetrically laminated circular cylindrical shells and balanced unsymmetrically laminated circular cylindrical shells that are

subjected to internal pressure and thermal loads. Reuter's solution is based on Donnell-type linear equations and numerical results are presented for filament-wound cylinders made of heat-treated carbon-carbon material.

In 1975, Hennemann[7] presented an analytical solution for the axisymmetric response of homogeneous orthotropic cylinders and unsymmetrically laminated cross-ply cylinders subjected to uniform axial-compression and lateral pressure loads. Similar results were presented by Jones and Henemann[8] later in 1980. In 1984, Cheng and He[9] derived a pair of complex conjugate, fourth-order equations, that are based on Flugge's[10] corresponding equations, for specially orthotropic cylinders that can be solved in closed form. Moreover, eigenfunction solutions were presented that include the solution for the axisymmetric bending boundary layer and several simplifed equations were presented and their relative accuracy was analyzed.

Chaudhuri et al.[11] presented an analytical solution for unbalanced unsymmetrically laminated circular cylindrical shells that are subjected to internal pressure in 1986. Their analysis is based on a variant of the Love-Kirchhoff shell theory,[12] which uses an expression for the change in surface twist that was given by Timoshenko and Gere.[13] Numerical results are also presented for a two-ply shell that demonstrate the coupling effects of the shell anisotropies. Later, in 1989, Abu-Arja and Chaudhuri[14] presented similar closed-form solutions for unbalanced, symmetrically laminated cylinders and balanced unsymmetrically laminated angle-ply cylinders subjected to pressure loads that include the effects of transverse-shear deformation. In 1989, Butler and Hyer[15] presented an axisymmetric-shell analysis for a general unbalanced unsymmetrically laminated circular cylindrical shell that is subjected to axial compression, torsion, or thermal loading. Several results are presented that demonstrate the coupling effects of the shell anisotropies on the structural response.

In the early 1990s, Hyer and Paraska[16, 17] presented studies of the axisymmeric response of balanced symmetrically laminated and balanced unsymmetrically laminated cylinders subjected to axial compression and thermal loads. These studies are in the context of nonlinear prebuckling deformations that occur as a result of the compression and thermal loads considered. In particular, the effects of laminate stacking sequence on the extent and character of the bending boundary layers are presented for two groups of three similar laminates. Two of the laminates are unsymmetric. Birman[18] presented equations for axisymmetric thermal-stress analysis of ring-stiffened orthotropic cylinders in 1991 that include the first-order effects of transverse-shear deformation. In 1992, Birman[19] extended this work to symmetrically laminated cross-ply and specially orthotropic cylinders, and developed axisymmetric solutions based on a refined shear-deformation shell theory. Additionally, Birman[20] extended his work to include nonlinear axisymmetric deformations of generally laminated cylinders in 1993.

In 1997, Vinson[21] presented a linear analysis that focuses mainly on balanced, symmetrically laminated cylinders, and an expression is given for the length of the bending boundary layers near the cylinder ends that is based on the Love-Kirchhoff shell equations. In contrast, McDevitt and Simmonds[22] used Goldenveizer's static-geometric duality principle[23] to reduce the Sanders-Koiter equations[24, 25] for fully anisotropic, right-circular cylindrical shells to two coupled fourth-order equations that use a stress and a curvature function as the unknown, primary field variables. The

reduction is accomplished by adding certain negligibly small terms to the stress-strain relations, which are intrinsically in error because they must be established experimentally. The approach demonstrates how the static-geometric duality principle can be used to reduce greatly the amount of algebra needed to obtain results. Eigenfunction solutions are also presented for specially orthotropic cylinders that are in agreement with corresponding results presented by Cheng and He.[9] Moreover, asymptotic formulas that can be used to determine axisymmetric bending boundary layer attenuation lengths and the decay of other non-axisymmetric, self-equilibrated edges loads are given.

An in-depth analytical, parametric study of the attenuation of bending boundary layers in symmetrically and unsymmetrically laminated thin cylindrical shells, including balanced and unbalanced constructions, was presented for nine contemporary material systems by Nemeth and Smeltzer[26] in 2000. Herein, and in reference 26, the term "balanced" refers to laminates that do not exhibit coupling between extension or contraction and shearing. The analysis is based on the linear Sanders-Koiter shell equations and specializations to the Love-Kirchhoff shell equations and Donnell's equations are included. Two nondimensional parameters are indentified that characterize and quantify the effects of laminate orthotropy and laminate anisotropy on the bending boundary-layer decay length in a very general and encompassing manner. In this particular study, herein, and in much of the recent literature; the term "orthotropy" refers to orthogonally anisotropic laminates that exhibit deformation and stress states in which dilatation is completely uncoupled from distortion, with respect to the given coordinate system. In contrast, the term "anisotropy" implies the presence of material-induced coupling between dilatation and distortion. By using these nondimensional parameters, a substantial number of structural design technology results are presented in reference 26 that apply to a wide range of laminated-composite cylinders. Also in 2000, Paris and Costello[27] presented equations for analyzing cord-reinforced composite cylindrical shells and closed-form solutions are given for the axisymmetric response. Their analysis is based on Flugge's equations.

In 2001, Ye[28, 29] presented a three-dimensional elasticity formulation for the decay rates of stresses and displacements in cross-ply and angle-ply laminated composite cylinders subjected to self-equilibrated end loads. Analyses for the axisymmetric response of semi-infinite laminated cylinders that are based on three-dimensional elasticity theory, on a refined shear-deformation shell theory, and on classical Love-Kirchhoff shell theory were presented by Bhaskar and Balasubramanyam[30] in 2002. Somewhat unique to their study is a sizeable collection of tabular results in addition to figures. In 2003, Paris and Costello[31] extended their previous work on cord-reinforced composite cylindrical shells to include generally laminated wall constructions. This later analysis is also based on Flugge's equations and closed-form solutions are given for the axisymmetric response. Also in 2003, Kollar and Springer[32] gave a relatively terse presentation of the general closed-form solution for the axisymmetric response of fully anisotropic cylinders subjected to mechanical and thermal loads that are also based on Flugge's equations.

The literature described previously herein contains many elements of a general formulation for the axisymmetric behavior of cylindrical shells. However, none of the studies is complete and many details of the solutions are omitted. The objective of the present study is to give a detailed, complete formulation for axisymmetric deformations of a generally laminated circular cylindrical shell subjected to combined mechanical and thermal loads. As a first element of a building block

process to obtain improved theories, the analysis presented herein is based on the linear Sanders-Koiter shell equations, which neglects transverse-shear deformations. Moreover, the analysis is an extension of that presented by Nemeth and Smeltzer[26] in that it uses positive-definiteness of the strain energy density to determine the specific form of the analytical solution. This approach results in a significant simplification of the analysis procedure. To accomplish this objective, the Sanders-Koiter equations for axisymmetric deformations are given and then manipulated into a convenient form that facilitates obtaining the analytical solution. Then, a systematic presentation of the exact solution is given, followed by examples that demonstrate the typical solution processes. Approximate solutions are also presented to add credibility to the present study and to illustrate potential pitfalls of using approximate solutions in the analysis and design of laminated-composite cylinders.

Equations Governing Axisymmetric Behavior

The ordinary differential equation that governs the axisymmetric bending behavior of a right-circular cylinder that is subjected to edge loads or displacements and surface tractions is obtained by first specializing the linear Sanders-Koiter shell equations, that are given in Appendix A, for axial symmetry. For the equations presented herein, x and θ denote the axial and circumferential coordinates of a right-circular cylinder, respectively, as shown in figure 3. The z-coordinate shown in the figure is positive in the radially outward direction, and $z = 0$ corresponds to the middle surface of the shell. The cylinder has length L, radius R, and uniform thickness h. The specialization to axial symmetry is obtained by eliminating all terms in the equations that are differentiated with respect to the circumferential coordinate, θ. The resulting set of equations for axisymmetric behavior is given in Appendix B.

The particular equations used in the present study to obtain the exact solution for axisymmetric behavior are obtained by first noting that integration of equation (B1) yields

$$N_x(x) = \overline{N}_0 + \overline{N}_1(x) \tag{1a}$$

where $\overline{N}_0$ is a constant of integration and

$$\overline{N}_1(x) = -\int q_x(x)\,dx \tag{1b}$$

Next, equations (B2) and (B5) are combined to get

$$N_{x\theta}'(x) + \frac{1}{R}\left(c_1 + \frac{1}{2}c_2\right)M_{x\theta}'(x) + q_\theta(x) = 0 \tag{2}$$

where the prime mark denotes differentiation with respect to the independent variable, x. For convenience, the parameter

$$\mu = c_1 + \frac{1}{2}c_2 \tag{3}$$

is introduced such that the Sanders-Koiter equations are given by $\mu = 3/2$ and the Love-Kirchhoff equations are given by $\mu = 1$. Donnell's equations are given by $\mu = 0$. Similarly, the function

$$\hat{T}(x) = N_{x\theta}(x) + \frac{\mu}{R}M_{x\theta}(x) \tag{4}$$

is introduced so that equation (2) becomes

$$\hat{T}'(x) + q_\theta(x) = 0 \tag{5}$$

and the corresponding boundary condition given by equation (B19) becomes

$$\hat{T} = \tilde{T} \quad \text{or} \quad v = \tilde{v} \tag{6}$$

at $x = 0$ and $x = L$. Integration of equation (5) yields

$$\hat{T}(x) = \bar{T}_0 + \bar{T}_1(x) \tag{7a}$$

where $\bar{T}_0$ is a constant of integration and

$$\bar{T}_1(x) = -\int q_\theta(x)\, dx \tag{7b}$$

Next, equations (B3) and (B4) are combined to get

$$M_x''(x) - \frac{N_\theta(x)}{R} + q_n(x) = 0 \tag{8}$$

The next step in the analysis is the simplification of the constitutive equations. First, by using equations (B8) and (3), equation (B14) is expressed as

$$\kappa^o_{x\theta} = \frac{\mu}{R}\gamma^o_{x\theta} \tag{9}$$

By using equations (4) and (9), the constitutive equations given by matrix equation (B15) are expressed as

$$\begin{Bmatrix} N_x \\ N_\theta \\ \hat{T} \\ M_x \end{Bmatrix} = \begin{bmatrix} A_{11} & A_{12} & \bar{A}_{16} & B_{11} \\ A_{12} & A_{22} & \bar{A}_{26} & B_{12} \\ \bar{A}_{16} & \bar{A}_{26} & \bar{A}_{66} & \bar{B}_{16} \\ B_{11} & B_{12} & \bar{B}_{16} & D_{11} \end{bmatrix} \begin{Bmatrix} \varepsilon^o_x \\ \varepsilon^o_\theta \\ \gamma^o_{x\theta} \\ \kappa^o_x \end{Bmatrix} - \begin{Bmatrix} N_x^{Th} \\ N_\theta^{Th} \\ \hat{T}^{Th} \\ M_x^{Th} \end{Bmatrix} \tag{10}$$

and

$$M_\theta = B_{12}\varepsilon_x^o + B_{22}\varepsilon_\theta^o + \overline{B}_{26}\gamma_{x\theta}^o + D_{12}\kappa_x^o - M_\theta^{Th} \tag{11}$$

where

$$\overline{A}_{16} = A_{16} + \mu\left(\frac{h}{R}\right)\frac{B_{16}}{h} \tag{12a}$$

$$\overline{A}_{26} = A_{26} + \mu\left(\frac{h}{R}\right)\frac{B_{26}}{h} \tag{12b}$$

$$\overline{A}_{66} = A_{66} + 2\mu\left(\frac{h}{R}\right)\frac{B_{66}}{h} + \mu^2\left(\frac{h}{R}\right)^2\frac{D_{66}}{h^2} \tag{12c}$$

$$\overline{B}_{16} = B_{16} + \mu\left(\frac{h}{R}\right)\frac{D_{16}}{h} \tag{12d}$$

$$\overline{B}_{26} = B_{26} + \mu\left(\frac{h}{R}\right)\frac{D_{26}}{h} \tag{12e}$$

$$\hat{T}^{Th} = N_{x\theta}^{Th} + \frac{\mu}{R}M_{x\theta}^{Th} \tag{12f}$$

where the subscripted A, B, and D terms appearing in these equations are the usual laminate stiffnesses of classical plate and shell theory (see reference 34), in which the fiber orientation of a typical ply is denoted by the angle ϕ shown in figure 3. The motivation for writing the constitutive equations in this form is that the matrix equation given by equation (10) is the only part of the full constitutive equations that appears in the strain energy density function, which is used in the present paper to determine the corresponding positive-definiteness conditions. Noting that $\varepsilon_x^o = u'(x)$ and $\gamma_{x\theta}^o = v'(x)$ are the only strains in equation (10) that depend on the axial displacement u(x) and the circumferential displacement v(x), it is useful to extract

$$\begin{Bmatrix} N_x + N_x^{Th} \\ \hat{T} + \hat{T}^{Th} \end{Bmatrix} = \begin{bmatrix} A_{11} & \overline{A}_{16} \\ \overline{A}_{16} & \overline{A}_{66} \end{bmatrix}\begin{Bmatrix} \varepsilon_x^o \\ \gamma_{x\theta}^o \end{Bmatrix} + \begin{Bmatrix} A_{12} \\ \overline{A}_{26} \end{Bmatrix}\varepsilon_\theta^o + \begin{Bmatrix} B_{11} \\ \overline{B}_{16} \end{Bmatrix}\kappa_x^o \tag{13a}$$

from equation (10). Using equations (1a), (7a), (B6) - (B8), and (B12) with equation (13a) gives

$$\begin{Bmatrix} \overline{N}_0 + \overline{N}_1(x) + N_x^{Th}(x) \\ \overline{T}_0 + \overline{T}_1(x) + \hat{T}^{Th}(x) \end{Bmatrix} = \begin{bmatrix} A_{11} & \overline{A}_{16} \\ \overline{A}_{16} & \overline{A}_{66} \end{bmatrix}\begin{Bmatrix} u'(x) \\ v'(x) \end{Bmatrix} + \begin{Bmatrix} A_{12} \\ \overline{A}_{26} \end{Bmatrix}\frac{w(x)}{R} - \begin{Bmatrix} B_{11} \\ \overline{B}_{16} \end{Bmatrix}w''(x) \tag{13b}$$

Solving for the derivatives of the axial displacement u(x) and the circumferential displacement v(x) gives

$$\begin{Bmatrix} u'(x) \\ v'(x) \end{Bmatrix} = \begin{bmatrix} \bar{a}_{11} & \bar{a}_{16} \\ \bar{a}_{16} & \bar{a}_{66} \end{bmatrix} \begin{Bmatrix} \overline{N}_0 + \overline{N}_1(x) + N_x^{Th}(x) \\ \overline{T}_0 + \overline{T}_1(x) + \hat{T}^{Th}(x) \end{Bmatrix} + \begin{Bmatrix} \bar{\ell}_{12} \\ \bar{\ell}_{62} \end{Bmatrix} \frac{w(x)}{R} - \begin{Bmatrix} \bar{\varepsilon}_{12} \\ \bar{\varepsilon}_{62} \end{Bmatrix} w''(x) \tag{14}$$

where

$$\begin{bmatrix} \bar{a}_{11} & \bar{a}_{16} \\ \bar{a}_{16} & \bar{a}_{66} \end{bmatrix} = \begin{bmatrix} A_{11} & \overline{A}_{16} \\ \overline{A}_{16} & \overline{A}_{66} \end{bmatrix}^{-1} = \frac{1}{A_{11}\overline{A}_{66} - \overline{A}_{16}^2} \begin{bmatrix} \overline{A}_{66} & -\overline{A}_{16} \\ -\overline{A}_{16} & A_{11} \end{bmatrix} \tag{15a}$$

$$\begin{Bmatrix} \bar{\ell}_{12} \\ \bar{\ell}_{62} \end{Bmatrix} = -\begin{bmatrix} \bar{a}_{11} & \bar{a}_{16} \\ \bar{a}_{16} & \bar{a}_{66} \end{bmatrix} \begin{Bmatrix} A_{12} \\ \overline{A}_{26} \end{Bmatrix} = \frac{1}{A_{11}\overline{A}_{66} - \overline{A}_{16}^2} \begin{Bmatrix} \overline{A}_{16}\overline{A}_{26} - A_{12}\overline{A}_{66} \\ A_{12}\overline{A}_{16} - A_{11}\overline{A}_{26} \end{Bmatrix} \tag{15b}$$

$$\begin{Bmatrix} \bar{\varepsilon}_{12} \\ \bar{\varepsilon}_{62} \end{Bmatrix} = -\begin{bmatrix} \bar{a}_{11} & \bar{a}_{16} \\ \bar{a}_{16} & \bar{a}_{66} \end{bmatrix} \begin{Bmatrix} B_{11} \\ \overline{B}_{16} \end{Bmatrix} = \frac{1}{A_{11}\overline{A}_{66} - \overline{A}_{16}^2} \begin{Bmatrix} \overline{A}_{16}\overline{B}_{16} - B_{11}\overline{A}_{66} \\ B_{11}\overline{A}_{16} - A_{11}\overline{B}_{16} \end{Bmatrix} \tag{15c}$$

and where $w(x)$ is the radial deflection that is positive-valued when outward. Equations (14) and (15) indicate that the circumferential displacement $v(x)$ becomes uncoupled from the axial displacement $u(x)$ and the radial displacement $w(x)$ when $\overline{A}_{16} = \overline{A}_{26} = \overline{B}_{16} = 0$, which implies that $A_{16} = A_{26} = B_{16} = D_{16} = 0$. In addition, the constitutive equation, equation (10), indicates that N_x, N_θ, and M_x become uncoupled from the torsional, shear strain $\gamma^o_{x\theta}$ when $\overline{A}_{16} = \overline{A}_{26} = \overline{B}_{16} = 0$, and that $\hat{T}$, that is defined by equation (4), becomes uncoupled from ε^o_x, ε^o_θ, and κ^o_x. Furthermore, equation (11) indicates that M_θ becomes uncoupled from $\gamma^o_{x\theta}$ when $\overline{B}_{26} = 0$, which implies $B_{26} = D_{26} = 0$.

Next, equations (14) are then substituted into $\varepsilon^o_x = u'(x)$ and $\gamma^o_{x\theta} = v'(x)$, and the resulting expressions for ε^o_x and $\gamma^o_{x\theta}$, along with equations (B7) and (B12) are substituted into the constitutive equations given by equation (10). This action converts the strains and stress resultants in equation (10) into functions of the radial displacement $w(x)$. In particular,

$$N_\theta(x) = A_{12}u'(x) + A_{22}\frac{w(x)}{R} + \overline{A}_{26}\,v'(x) - B_{12}\,w''(x) - N_\theta^{Th}(x) \tag{16a}$$

becomes

$$\begin{aligned} N_\theta(x) = {} & \left(A_{12}\bar{a}_{11} + \overline{A}_{26}\bar{a}_{16}\right)\left[\overline{N}_0 + \overline{N}_1(x) + N_x^{Th}(x)\right] + \left(A_{12}\bar{a}_{16} + \overline{A}_{26}\bar{a}_{66}\right)\left[\overline{T}_0 + \overline{T}_1(x) + \hat{T}^{Th}(x)\right] \\ & + \left(A_{22} + A_{12}\bar{\ell}_{12} + \overline{A}_{26}\bar{\ell}_{62}\right)\frac{w(x)}{R} - \left(B_{12} + A_{12}\bar{\varepsilon}_{12} + \overline{A}_{26}\bar{\varepsilon}_{62}\right)w''(x) - N_\theta^{Th}(x) \end{aligned} \tag{16b}$$

and

$$M_x(x) = B_{11}u'(x) + B_{12}\frac{w(x)}{R} + \overline{B}_{16}\,v'(x) - D_{11}\,w''(x) - M_x^{Th}(x) \tag{17a}$$

becomes

$$M_x(x) = \left(B_{11}\bar{a}_{11} + \bar{B}_{16}\bar{a}_{16}\right)\left[\bar{N}_0 + \bar{N}_1(x) + N_x^{Th}(x)\right] + \left(B_{11}\bar{a}_{16} + \bar{B}_{16}\bar{a}_{66}\right)\left[\bar{T}_0 + \bar{T}_1(x) + \hat{T}^{Th}(x)\right] + \left(B_{12} + B_{11}\bar{\ell}_{12} + \bar{B}_{16}\bar{\ell}_{62}\right)\frac{w(x)}{R} - \left(D_{11} + B_{11}\bar{\varepsilon}_{12} + \bar{B}_{16}\bar{\varepsilon}_{62}\right)w''(x) - M_x^{Th}(x) \tag{17b}$$

Substituting equations (16b) and (17b) into equation (8) yields

$$C_1\, w''''(x) + C_2\, w''(x) + C_3\, w(x) = C_4(x) \tag{18}$$

The constant coefficients are given by

$$C_1 = D_{11}\boldsymbol{e} \quad \text{and} \quad \boldsymbol{e} = 1 + \frac{B_{11}\bar{\varepsilon}_{12} + \bar{B}_{16}\bar{\varepsilon}_{62}}{D_{11}} \tag{19}$$

$$C_2 = -\frac{1}{R}\left(2B_{12} + A_{12}\bar{\varepsilon}_{12} + \bar{A}_{26}\bar{\varepsilon}_{62} + B_{11}\bar{\ell}_{12} + \bar{B}_{16}\bar{\ell}_{62}\right) \tag{20}$$

$$C_3 = \frac{1}{R^2}\left(A_{22} + A_{12}\bar{\ell}_{12} + \bar{A}_{26}\bar{\ell}_{62}\right) \tag{21}$$

The function $C_4(x)$ is given by

$$C_4(x) = q_n(x) - M_x^{Th\,\prime\prime}(x) + \frac{1}{R}N_\theta^{Th}(x) - \frac{1}{R}\left(A_{12}\bar{a}_{11} + \bar{A}_{26}\bar{a}_{16}\right)\left[\bar{N}_0 + \bar{N}_1(x) + N_x^{Th}(x)\right] - \frac{1}{R}\left(A_{12}\bar{a}_{16} + \bar{A}_{26}\bar{a}_{66}\right)\left[\bar{T}_0 + \bar{T}_1(x) + \hat{T}^{Th}(x)\right] + \left(B_{11}\bar{a}_{11} + \bar{B}_{16}\bar{a}_{16}\right)\left[\bar{N}_1{}''(x) + N_x^{Th\,\prime\prime}(x)\right] + \left(B_{11}\bar{a}_{16} + \bar{B}_{16}\bar{a}_{66}\right)\left[\bar{T}_1{}''(x) + \hat{T}^{Th\,\prime\prime}(x)\right] \tag{22}$$

Equations (19) - (21) are expressed in terms of elements appearing in matrix equation (10) further by using equations (15); that is,

$$C_2 = -\frac{2}{R}\left[B_{12} + \frac{\left(\bar{A}_{16}\bar{A}_{26} - A_{12}\bar{A}_{66}\right)B_{11} + \left(A_{12}\bar{A}_{16} - A_{11}\bar{A}_{26}\right)\bar{B}_{16}}{A_{11}\bar{A}_{66} - \bar{A}_{16}^2}\right] \tag{23}$$

$$C_3 = \frac{1}{R^2}\,\frac{\left(A_{11}A_{22} - A_{12}^2\right)\bar{A}_{66} - A_{11}\bar{A}_{26}^2 - A_{22}\bar{A}_{16}^2 + 2A_{12}\bar{A}_{16}\bar{A}_{26}}{A_{11}\bar{A}_{66} - \bar{A}_{16}^2} \tag{24}$$

$$\boldsymbol{e} = 1 - \frac{\overline{A}_{66}B_{11}^2 + A_{11}\overline{B}_{16}^2 - 2\overline{A}_{16}B_{11}\overline{B}_{16}}{\left(A_{11}\overline{A}_{66} - \overline{A}_{16}^2\right)D_{11}} \tag{25}$$

Next, equation (18) is divided by the coefficient C_1 given by equation (19) to get

$$w''''(x) + 4S\, w''(x) + 4Q\, w(x) = P(x) \tag{26}$$

where the constants S and Q are given by

$$S = \frac{C_2}{4C_1} = -\frac{1}{2RD_{11}\boldsymbol{e}}\left[B_{12} + \frac{\left(\overline{A}_{16}\overline{A}_{26} - A_{12}\overline{A}_{66}\right)B_{11} + \left(A_{12}\overline{A}_{16} - A_{11}\overline{A}_{26}\right)\overline{B}_{16}}{A_{11}\overline{A}_{66} - \overline{A}_{16}^2}\right] \tag{27}$$

$$Q = \frac{C_3}{4C_1} = \frac{\left(A_{11}A_{22} - A_{12}^2\right)\overline{A}_{66} - A_{11}\overline{A}_{26}^2 - A_{22}\overline{A}_{16}^2 + 2A_{12}\overline{A}_{16}\overline{A}_{26}}{4R^2D_{11}\,\boldsymbol{e}\left(A_{11}\overline{A}_{66} - \overline{A}_{16}^2\right)} \tag{28}$$

The function P(x) is given by

$$P(x) = \frac{C_4(x)}{C_1} \equiv P_0 + P_1(x) \tag{29a}$$

where

$$P_0 = -\frac{1}{RD_{11}\,\boldsymbol{e}}\left[\left(A_{12}\bar{a}_{11} + \overline{A}_{26}\bar{a}_{16}\right)\overline{N}_0 + \left(A_{12}\bar{a}_{16} + \overline{A}_{26}\bar{a}_{66}\right)\overline{T}_0\right] \tag{29b}$$

$$\begin{aligned} P_1(x) = {} & \frac{1}{D_{11}\,\boldsymbol{e}}\left[q_n(x) - M_x^{Th}{}''(x) + \frac{1}{R}N_\theta^{Th}(x)\right] \\ & - \frac{1}{RD_{11}\,\boldsymbol{e}}\left[\left(A_{12}\bar{a}_{11} + \overline{A}_{26}\bar{a}_{16}\right)\left(\overline{N}_1(x) + N_x^{Th}(x)\right) + \left(A_{12}\bar{a}_{16} + \overline{A}_{26}\bar{a}_{66}\right)\left(\overline{T}_1(x) + \hat{T}^{Th}(x)\right)\right] \\ & + \frac{1}{D_{11}\,\boldsymbol{e}}\left(B_{11}\bar{a}_{11} + \overline{B}_{16}\bar{a}_{16}\right)\left[\overline{N}_1{}''(x) + N_x^{Th}{}''(x)\right] + \frac{1}{D_{11}\,\boldsymbol{e}}\left(B_{11}\bar{a}_{16} + \overline{B}_{16}\bar{a}_{66}\right)\left[\overline{T}_1{}''(x) + \hat{T}^{Th}{}''(x)\right] \end{aligned} \tag{29c}$$

Exact Solution

Equation (26) is a linear, nonhomogeneous, fourth-order ordinary differential equation with constant coefficients, and the form of its solution depends on the numerical values of the constants S and Q. To determine the specific form of the solution, it is useful to examine the positive-definiteness conditions on the strain-energy density function. The strain energy density function $\mathcal{U}$ for this problem is given by (e.g., see Paraska,[17] p. 16)

$$2\mathcal{U} = \left(N_x - N_x^{Th}\right)\varepsilon_x^o + \left(N_\theta - N_\theta^{Th}\right)\varepsilon_\theta^o + \left(N_{x\theta} - N_{x\theta}^{Th}\right)\gamma_{x\theta}^o + \left(M_x - M_x^{Th}\right)\kappa_x^o + \left(M_{x\theta} - M_{x\theta}^{Th}\right)\kappa_{x\theta}^o \tag{30}$$

By using equations (4) and (9), the strain-energy density function is expressed as

$$2\mathcal{U} = \left(N_x - N_x^{Th}\right)\varepsilon_x^o + \left(N_\theta - N_\theta^{Th}\right)\varepsilon_\theta^o + \left(\hat{T} - \hat{T}^{Th}\right)\gamma_{x\theta}^o + \left(M_x - M_x^{Th}\right)\kappa_x^o \tag{31}$$

The strain energy density is expressed in terms of the total strains, mechanical plus thermal, and constitutive terms by using the constitutive equation given by equation (10); that is,

$$\mathcal{U} = \frac{1}{2}\begin{Bmatrix} \varepsilon_x^o \\ \varepsilon_\theta^o \\ \gamma_{x\theta}^o \\ \kappa_x^o \end{Bmatrix}^T \begin{bmatrix} A_{11} & A_{12} & \overline{A}_{16} & B_{11} \\ A_{12} & A_{22} & \overline{A}_{26} & B_{12} \\ \overline{A}_{16} & \overline{A}_{26} & \overline{A}_{66} & \overline{B}_{16} \\ B_{11} & B_{12} & \overline{B}_{16} & D_{11} \end{bmatrix} \begin{Bmatrix} \varepsilon_x^o \\ \varepsilon_\theta^o \\ \gamma_{x\theta}^o \\ \kappa_x^o \end{Bmatrix} \tag{32}$$

The stiffness terms in equation (32) that have overbars are defined by equations (12) and are functions of the shell wall thickness-to-radius parameter, h/R. Because the strain energy density function is positive valued, the matrix appearing in equation (32) is positive definite. As a result (e.g., see Zwillinger[33], pp. 133-134), the diagonal terms A_{11}, A_{22}, $\overline{A}_{66}$, and D_{11} are positive-valued, and the following determinants are positive valued

$$\begin{vmatrix} A_{11} & A_{12} \\ A_{12} & A_{22} \end{vmatrix} = A_{11}A_{22} - A_{12}^2 > 0 \tag{33}$$

$$\begin{vmatrix} A_{11} & A_{12} & \overline{A}_{16} \\ A_{12} & A_{22} & \overline{A}_{26} \\ \overline{A}_{16} & \overline{A}_{26} & \overline{A}_{66} \end{vmatrix} = \left(A_{11}A_{22} - A_{12}^2\right)\overline{A}_{66} - A_{11}\overline{A}_{26}^2 - A_{22}\overline{A}_{16}^2 + 2A_{12}\overline{A}_{16}\overline{A}_{26} > 0 \tag{34}$$

in addition to the determinant of the constitutive matrix in equation (32). Moreover, by rearranging the strain energy density function into the form

$$\mathcal{U} = \frac{1}{2} \begin{Bmatrix} \varepsilon_x^o \\ \gamma_{x\theta}^o \\ \varepsilon_\theta^o \\ \kappa_x^o \end{Bmatrix}^T \begin{bmatrix} A_{11} & \overline{A}_{16} & A_{12} & B_{11} \\ \overline{A}_{16} & \overline{A}_{66} & \overline{A}_{26} & \overline{B}_{16} \\ A_{12} & \overline{A}_{26} & A_{22} & B_{12} \\ B_{11} & \overline{B}_{16} & B_{12} & D_{11} \end{bmatrix} \begin{Bmatrix} \varepsilon_x^o \\ \gamma_{x\theta}^o \\ \varepsilon_\theta^o \\ \kappa_x^o \end{Bmatrix} \tag{35}$$

the following additional positive-definiteness condition is obtained

$$\begin{vmatrix} A_{11} & \overline{A}_{16} \\ \overline{A}_{16} & \overline{A}_{66} \end{vmatrix} = A_{11}\overline{A}_{66} - \overline{A}_{16}^2 > 0 \tag{36}$$

The homogeneous solution for equation (26) involves the square root of the quantity $Q - S^2$. By using equations (27) and (28), this quantity is given by

$$Q - S^2 = \frac{4C_1C_3 - C_2^2}{16C_1^2} \tag{37}$$

Substituting equations (19) and (23) - (25) into equation (37) and simplifying, the quantity $Q - S^2$ is found to be given by

$$Q - S^2 = \frac{1}{4C_1^2R^2\left(A_{11}\overline{A}_{66} - \overline{A}_{16}^2\right)} \begin{vmatrix} A_{11} & A_{12} & \overline{A}_{16} & B_{11} \\ A_{12} & A_{22} & \overline{A}_{26} & B_{12} \\ \overline{A}_{16} & \overline{A}_{26} & \overline{A}_{66} & \overline{B}_{16} \\ B_{11} & B_{12} & \overline{B}_{16} & D_{11} \end{vmatrix} \tag{38}$$

It follows logically, that $Q - S^2 > 0$ because the positive definiteness of the strain energy density function requires that the determinants in equations (36) and (38) be positive valued. Moreover, $Q - S^2 > 0$ implies that $Q > 0$, and $Q > 0$ implies that $C_3/C_1 > 0$. Equations (34), (36), and (24) indicate that $C_3 > 0$. Thus, $C_3/C_1 > 0$ yields the condition that $C_1 = D_{11}\,e > 0$ (see equations (19) and (25)). Because $D_{11} > 0$, $e > 0$. To reinforce the postive valuedness of Q, it is convenient to introduce the expression

$$T^2 = Q = \frac{\left(A_{11}A_{22} - A_{12}^2\right)\overline{A}_{66} - A_{11}\overline{A}_{26}^2 - A_{22}\overline{A}_{16}^2 + 2A_{12}\overline{A}_{16}\overline{A}_{26}}{4R^2D_{11}\,e\left(A_{11}\overline{A}_{66} - \overline{A}_{16}^2\right)} \tag{39}$$

such that $T^2 - S^2 > 0$, and to express equation (26) as

$$w''''(x) + 4S\,w''(x) + 4T^2\,w(x) = P_0 + P_1(x) \tag{40}$$

Equation (40) is a linear, fourth-order, nonhomogeneous ordinary differential equation with constant coefficients. The characteristic equation of equation (40) is given by

$$\lambda^4 + 4S\,\lambda^2 + 4T^2 = 0 \tag{41}$$

Using the knowledge that $T^2 - S^2 > 0$, the roots of the characteristic equation are obtained from the quadratic formula; that is,

$$(\lambda^2)_{1,2} = 2\left(-S \pm i\,\sqrt{T^2 - S^2}\right) \tag{42}$$

where $i = \sqrt{-1}$. Solution of this equation for λ yields four roots of equation (41) that are pairs of complex conjugates that are given by

$$\lambda_{1,2,3,4} = \pm\left(\sqrt{T - S} \pm i\,\sqrt{T + S}\right) \tag{43}$$

The homogeneous solution of equation (40) can be written as follows

$$w_H(x) = K_1 \mathscr{G}_1(x) + K_2 \mathscr{G}_2(x) + K_3 \mathscr{G}_3(x) + K_4 \mathscr{G}_4(x) \tag{44}$$

where

$$\mathscr{G}_1(x) = e^{-\sqrt{T - S}\,x} \sin\left(\sqrt{T + S}\,x\right) \tag{45a}$$

$$\mathscr{G}_2(x) = e^{-\sqrt{T - S}\,x} \cos\left(\sqrt{T + S}\,x\right) \tag{45b}$$

$$\mathscr{G}_3(x) = e^{-\sqrt{T - S}\,(L - x)} \sin\left(\sqrt{T + S}\,x\right) \tag{45c}$$

$$\mathscr{G}_4(x) = e^{-\sqrt{T - S}\,(L - x)} \cos\left(\sqrt{T + S}\,x\right) \tag{45d}$$

are basis function spanning the solution space and where $0 \le x \le L$. The symbols K_1, K_2, K_3, and K_4 are real-valued constants that are determined from the boundary conditions. The solution given by equation (44) represents a damped, oscillatory response that decays from each end of the cylinder. The regions near the edges of the cylinder, where the amplitude of $w_H(x)$ typically varies the most, are called the bending boundary layers. This particular form for the basis functions was selected to prevent numerical issues associated with evaluating exponential functions with a large positive-valued argument.

Next, it is important to observe that the constant-valued term P_0 in equation (29a) contains

two of the unknown constants of integration, $\overline{N}_0$ and $\overline{T}_0$. Thus, it is convenient to partition the particular solution of equation (40) into

$$w_p(x) = w_p^0 + \overline{w}_p(x) \tag{46}$$

where w_p^0 is a constant obtained as the particular solution associated with P_0 and $\overline{w}_p(x)$ is the part of the particular solution associated with $P_1(x)$. Moreover, it is convenient to express

$$w_p^0 = R\left(c_{\overline{N}}\overline{N}_0 + c_{\overline{T}}\overline{T}_0\right) \tag{47a}$$

where

$$c_{\overline{N}} = \frac{\overline{A}_{16}\overline{A}_{26} - A_{12}\overline{A}_{66}}{\left(A_{11}A_{22} - A_{12}^2\right)\overline{A}_{66} - A_{11}\overline{A}_{26}^2 - A_{22}\overline{A}_{16}^2 + 2A_{12}\overline{A}_{16}\overline{A}_{26}} \tag{47b}$$

$$c_{\overline{T}} = \frac{\overline{A}_{16}A_{12} - A_{11}\overline{A}_{26}}{\left(A_{11}A_{22} - A_{12}^2\right)\overline{A}_{66} - A_{11}\overline{A}_{26}^2 - A_{22}\overline{A}_{16}^2 + 2A_{12}\overline{A}_{16}\overline{A}_{26}} \tag{47c}$$

The form of $\overline{w}_p(x)$ depends on the specific functional representations of the applied surface tractions and thermal fields. By using equations (44), (46), and (47a), the general solution to equation (40) is expressed as

$$w(x) = K_1\ell_1(x) + K_2\ell_2(x) + K_3\ell_3(x) + K_4\ell_4(x) + R\left(c_{\overline{N}}\overline{N}_0 + c_{\overline{T}}\overline{T}_0\right) + \overline{w}_p(x) \tag{48}$$

With the form of $w(x)$ known, the first of equations (14) is expressed as

$$u'(x) = U_0'(x) + U_1'(x)\,K_1 + U_2'(x)\,K_2 + U_3'(x)\,K_3 + U_4'(x)\,K_4 + U_5'\overline{N}_0 + U_6'\overline{T}_0 \tag{49}$$

where

$$U_0'(x) = \bar{a}_{11}\left[\overline{N}_1(x) + N_x^{Th}(x)\right] + \bar{a}_{16}\left[\overline{T}_1(x) + \hat{T}^{Th}(x)\right] + \bar{\ell}_{12}\frac{\overline{w}_p(x)}{R} - \bar{\varepsilon}_{12}\overline{w}_p''(x) \tag{50a}$$

$$U_k'(x) = \bar{\ell}_{12}\frac{\ell_k(x)}{R} - \bar{\varepsilon}_{12}\ell_k''(x) \quad \text{with } k = 1, 2, 3, \text{ and } 4 \tag{50b}$$

$$U_5' = \bar{a}_{11} + \bar{\ell}_{12}c_{\overline{N}} \tag{50c}$$

$$U_6' = \bar{a}_{16} + \bar{\ell}_{12} c_{\bar{T}} \tag{50d}$$

Likewise, the second of equations (14) is expressed as

$$v'(x) = V_0'(x) + V_1'(x)\, K_1 + V_2'(x)\, K_2 + V_3'(x)\, K_3 + V_4'(x)\, K_4 + V_5' \bar{N}_0 + V_6' \bar{T}_0 \tag{51}$$

where

$$V_0'(x) = \bar{a}_{16}\left[\bar{N}_1(x) + N_x^{Th}(x)\right] + \bar{a}_{66}\left[\bar{T}_1(x) + \hat{T}^{Th}(x)\right] + \bar{\ell}_{62}\frac{\bar{w}_p(x)}{R} - \bar{\varepsilon}_{62}\bar{w}_p''(x) \tag{52a}$$

$$V_k'(x) = \bar{\ell}_{62}\frac{\ell_k(x)}{R} - \bar{\varepsilon}_{62}\ell_k''(x) \quad \text{with } k = 1, 2, 3, \text{ and } 4 \tag{52b}$$

$$V_5' = \bar{a}_{16} + \bar{\ell}_{62} c_{\bar{N}} \tag{52c}$$

$$V_6' = \bar{a}_{66} + \bar{\ell}_{62} c_{\bar{T}} \tag{52d}$$

Next, the derivatives of the basis functions, given by equations (45), are expressed as

$$\ell_1'(x) = \sqrt{T+S}\,\ell_2(x) - \sqrt{T-S}\,\ell_1(x) \tag{53a}$$

$$\ell_2'(x) = -\sqrt{T+S}\,\ell_1(x) - \sqrt{T-S}\,\ell_2(x) \tag{53b}$$

$$\ell_3'(x) = \sqrt{T+S}\,\ell_4(x) + \sqrt{T-S}\,\ell_3(x) \tag{53c}$$

$$\ell_4'(x) = -\sqrt{T+S}\,\ell_3(x) + \sqrt{T-S}\,\ell_4(x) \tag{53d}$$

$$\ell_1''(x) = -2S\,\ell_1(x) - 2\sqrt{T^2-S^2}\,\ell_2(x) \tag{53e}$$

$$\ell_2''(x) = 2\sqrt{T^2-S^2}\,\ell_1(x) - 2S\,\ell_2(x) \tag{53f}$$

$$\ell_3''(x) = -2S\,\ell_3(x) + 2\sqrt{T^2-S^2}\,\ell_4(x) \tag{53g}$$

$$\ell_4''(x) = -2\sqrt{T^2-S^2}\,\ell_3(x) - 2S\,\ell_4(x) \tag{53h}$$

By using these expressions for the derivatives, equations (50b) are expressed as

$$U_1'(x) = \left[\frac{\bar{\ell}_{12}}{R} + 2S\bar{\varepsilon}_{12}\right]\mathcal{L}_1(x) + 2\bar{\varepsilon}_{12}\sqrt{T^2 - S^2}\,\mathcal{L}_2(x) \tag{54a}$$

$$U_2'(x) = -2\bar{\varepsilon}_{12}\sqrt{T^2 - S^2}\,\mathcal{L}_1(x) + \left[\frac{\bar{\ell}_{12}}{R} + 2S\bar{\varepsilon}_{12}\right]\mathcal{L}_2(x) \tag{54b}$$

$$U_3'(x) = \left[\frac{\bar{\ell}_{12}}{R} + 2S\bar{\varepsilon}_{12}\right]\mathcal{L}_3(x) - 2\bar{\varepsilon}_{12}\sqrt{T^2 - S^2}\,\mathcal{L}_4(x) \tag{54c}$$

$$U_4'(x) = 2\bar{\varepsilon}_{12}\sqrt{T^2 - S^2}\,\mathcal{L}_3(x) + \left[\frac{\bar{\ell}_{12}}{R} + 2S\bar{\varepsilon}_{12}\right]\mathcal{L}_4(x) \tag{54d}$$

Likewise, equations (52b) are expressed as

$$V_1'(x) = \left[\frac{\bar{\ell}_{62}}{R} + 2S\bar{\varepsilon}_{62}\right]\mathcal{L}_1(x) + 2\bar{\varepsilon}_{62}\sqrt{T^2 - S^2}\,\mathcal{L}_2(x) \tag{55a}$$

$$V_2'(x) = -2\bar{\varepsilon}_{62}\sqrt{T^2 - S^2}\,\mathcal{L}_1(x) + \left[\frac{\bar{\ell}_{62}}{R} + 2S\bar{\varepsilon}_{62}\right]\mathcal{L}_2(x) \tag{55b}$$

$$V_3'(x) = \left[\frac{\bar{\ell}_{62}}{R} + 2S\bar{\varepsilon}_{62}\right]\mathcal{L}_3(x) - 2\bar{\varepsilon}_{62}\sqrt{T^2 - S^2}\,\mathcal{L}_4(x) \tag{55c}$$

$$V_4'(x) = 2\bar{\varepsilon}_{62}\sqrt{T^2 - S^2}\,\mathcal{L}_3(x) + \left[\frac{\bar{\ell}_{62}}{R} + 2S\bar{\varepsilon}_{62}\right]\mathcal{L}_4(x) \tag{55d}$$

Next, equations (49) and (51) are integrated directly to get

$$u(x) = U_0(x) + U_1(x)\,K_1 + U_2(x)\,K_2 + U_3(x)\,K_3 + U_4(x)\,K_4 + \left(U_5'\bar{N}_0 + U_6'\bar{T}_0\right)x + \bar{u} \tag{56}$$

and

$$v(x) = V_0(x) + V_1(x)\,K_1 + V_2(x)\,K_2 + V_3(x)\,K_3 + V_4(x)\,K_4 + \left(V_5'\bar{N}_0 + V_6'\bar{T}_0\right)x + \bar{v} \qquad (57)$$

where

$$U_0(x) = \bar{a}_{11}\int \left[\bar{N}_1(x) + N_x^{Th}(x)\right]dx + \bar{a}_{16}\int \left[\bar{T}_1(x) + \hat{T}^{Th}(x)\right]dx + \frac{\bar{\ell}_{12}}{R}\int \bar{w}_p(x)\,dx - \bar{\varepsilon}_{12}\bar{w}_p'(x) \qquad (58a)$$

$$V_0(x) = \bar{a}_{16}\int \left[\bar{N}_1(x) + N_x^{Th}(x)\right]dx + \bar{a}_{66}\int \left[\bar{T}_1(x) + \hat{T}^{Th}(x)\right]dx + \frac{\bar{\ell}_{62}}{R}\int \bar{w}_p(x)\,dx - \bar{\varepsilon}_{62}\bar{w}_p'(x) \qquad (58b)$$

$$U_k(x) = \int U_k'(x)\,dx \qquad (58c)$$

$$V_k(x) = \int V_k'(x)\,dx \qquad (58d)$$

for values of k = 1, 2, 3, and 4; and $\bar{u}$ and $\bar{v}$ are the corresponding constants of integration. Next, the integrals of the basis functions, given by equations (45), are expressed as

$$\int \ell_1(x)\,dx = -\frac{1}{2T}\left(\sqrt{T-S}\,\ell_1(x) + \sqrt{T+S}\,\ell_2(x)\right) \qquad (59a)$$

$$\int \ell_2(x)\,dx = \frac{1}{2T}\left(-\sqrt{T-S}\,\ell_2(x) + \sqrt{T+S}\,\ell_1(x)\right) \qquad (59b)$$

$$\int \ell_3(x)\,dx = \frac{1}{2T}\left(\sqrt{T-S}\,\ell_3(x) - \sqrt{T+S}\,\ell_4(x)\right) \qquad (59c)$$

$$\int \ell_4(x)\,dx = \frac{1}{2T}\left(\sqrt{T-S}\,\ell_4(x) + \sqrt{T+S}\,\ell_3(x)\right) \qquad (59d)$$

By using these expressions for the integrals, equations (58c) and (58d) are expressed as

$$U_1(x) = c_1^u\ell_1(x) - c_2^u\ell_2(x) \qquad (60a)$$

$$U_2(x) = c_2^u\ell_1(x) + c_1^u\ell_2(x) \qquad (60b)$$

$$U_3(x) = -c_1^u \mathcal{U}_3(x) - c_2^u \mathcal{U}_4(x) \tag{60c}$$

$$U_4(x) = c_2^u \mathcal{U}_3(x) - c_1^u \mathcal{U}_4(x) \tag{60d}$$

with

$$c_1^u = \frac{\sqrt{T - S}}{2T}\left[2\bar{\varepsilon}_{12}T - \frac{\bar{\ell}_{12}}{R}\right] \tag{60e}$$

$$c_2^u = \frac{\sqrt{T + S}}{2T}\left[2\bar{\varepsilon}_{12}T + \frac{\bar{\ell}_{12}}{R}\right] \tag{60f}$$

and

$$V_1(x) = c_1^v \mathcal{V}_1(x) - c_2^v \mathcal{V}_2(x) \tag{61a}$$

$$V_2(x) = c_2^v \mathcal{V}_1(x) + c_1^v \mathcal{V}_2(x) \tag{61b}$$

$$V_3(x) = -c_1^v \mathcal{V}_3(x) - c_2^v \mathcal{V}_4(x) \tag{61c}$$

$$V_4(x) = c_2^v \mathcal{V}_3(x) - c_1^v \mathcal{V}_4(x) \tag{61d}$$

with

$$c_1^v = \frac{\sqrt{T - S}}{2T}\left[2\bar{\varepsilon}_{62}T - \frac{\bar{\ell}_{62}}{R}\right] \tag{61e}$$

$$c_2^v = \frac{\sqrt{T + S}}{2T}\left[2\bar{\varepsilon}_{62}T + \frac{\bar{\ell}_{62}}{R}\right] \tag{61f}$$

Equations (48), (56), and (57) define completely the displacement fields in terms of eight constants that are determined from the boundary conditions. These constants are

$$\left\{K_1, K_2, K_3, K_4, \bar{u}, \bar{v}, \overline{N}_0, \overline{T}_0\right\} \tag{62}$$

To determine the unknown constants given by equation (62), the boundary conditions stated

by equations (B18) - (B21) must be enforced. To enforce these equations, expressions for the rotation β_x° and the stress resultants are needed. First, the expression for the slope is obtained by differentiating equation (48) and using the expressions for the derivatives of the basis functions given by equations (53). This task yields

$$\beta_x^{\circ}(x) = \beta_0(x) + K_1\beta_1(x) + K_2\beta_2(x) + K_3\beta_3(x) + K_4\beta_4(x) \tag{63}$$

where

$$\beta_0(x) = -\overline{w}_p'(x) \tag{64a}$$

$$\beta_1(x) = \sqrt{T-S}\,\mathscr{C}_1(x) - \sqrt{T+S}\,\mathscr{C}_2(x) \tag{64b}$$

$$\beta_2(x) = \sqrt{T+S}\,\mathscr{C}_1(x) + \sqrt{T-S}\,\mathscr{C}_2(x) \tag{64c}$$

$$\beta_3(x) = -\sqrt{T+S}\,\mathscr{C}_4(x) - \sqrt{T-S}\,\mathscr{C}_3(x) \tag{64d}$$

$$\beta_4(x) = \sqrt{T+S}\,\mathscr{C}_3(x) - \sqrt{T-S}\,\mathscr{C}_4(x) \tag{64e}$$

Next, equations (48), (49), and (51) are substituted into equation (17a) to get

$$M_x = M_{x0}(x) + M_{x1}(x)\,K_1 + M_{x2}(x)\,K_2 + M_{x3}(x)\,K_3 + M_{x4}(x)\,K_4 + M_{x5}\overline{N}_0 + M_{x6}\overline{T}_0 \tag{65}$$

where

$$M_{x0}(x) = B_{11}U_0'(x) + B_{12}\frac{\overline{w}_p(x)}{R} + \overline{B}_{16}V_0'(x) - D_{11}\overline{w}_p''(x) - M_x^{Th}(x) \tag{66a}$$

$$M_{xk}(x) = B_{11}U_k'(x) + \frac{B_{12}}{R}\mathscr{C}_k(x) + \overline{B}_{16}V_k'(x) - D_{11}\mathscr{C}_k''(x) \quad \text{with } k = 1, 2, 3, \text{ and } 4 \tag{66b}$$

$$M_{x5} = B_{11}U_5' + B_{12}c_{\overline{N}} + \overline{B}_{16}V_5' \tag{66c}$$

$$M_{x6} = B_{11}U_6' + B_{12}c_{\overline{T}} + \overline{B}_{16}V_6' \tag{66d}$$

Using equation (50a) for $U_0'(x)$, equation (52a) for $V_0'(x)$, equations (54) for $U_1'(x)$ through $U_4'(x)$, equations (55) for $V_1'(x)$ through $V_4'(x)$, equation (50c) for U_5', equation (50d) for U_6', equation (52c) for V_5', and equation (52d) for V_6', and equations (53) for the second derivatives of the basis functions gives

$$M_{x0}(x) = \left(B_{11}\bar{a}_{11} + \bar{B}_{16}\bar{a}_{16}\right)\left[\bar{N}_1(x) + N_x^{Th}(x)\right] + \left(B_{11}\bar{a}_{16} + \bar{B}_{16}\bar{a}_{66}\right)\left[\bar{T}_1(x) + \hat{T}^{Th}(x)\right] + \left(B_{12} + B_{11}\bar{\ell}_{12} + \bar{B}_{16}\bar{\ell}_{62}\right)\frac{\bar{w}_p(x)}{R} - \left(D_{11} + B_{11}\bar{\varepsilon}_{12} + \bar{B}_{16}\bar{\varepsilon}_{62}\right)\bar{w}_p''(x) - M_x^{Th}(x) \tag{67a}$$

$$M_{x1}(x) = c_1^M \mathcal{L}_1(x) + c_2^M \mathcal{L}_2(x) \tag{67b}$$

$$M_{x2}(x) = -c_2^M \mathcal{L}_1(x) + c_1^M \mathcal{L}_2(x) \tag{67c}$$

$$M_{x3}(x) = c_1^M \mathcal{L}_3(x) - c_2^M \mathcal{L}_4(x) \tag{67d}$$

$$M_{x4}(x) = c_2^M \mathcal{L}_3(x) + c_1^M \mathcal{L}_4(x) \tag{67e}$$

$$M_{x5} = c_{\bar{N}}\left(B_{12} + B_{11}\bar{\ell}_{12} + \bar{B}_{16}\bar{\ell}_{62}\right) + B_{11}\bar{a}_{11} + \bar{B}_{16}\bar{a}_{16} \tag{67f}$$

$$M_{x6} = c_{\bar{T}}\left(B_{12} + B_{11}\bar{\ell}_{12} + \bar{B}_{16}\bar{\ell}_{62}\right) + B_{11}\bar{a}_{16} + \bar{B}_{16}\bar{a}_{66} \tag{67g}$$

where

$$c_1^M = \frac{B_{11}\bar{\ell}_{12} + B_{12} + \bar{B}_{16}\bar{\ell}_{62}}{R} + 2S\left(B_{11}\bar{\varepsilon}_{12} + \bar{B}_{16}\bar{\varepsilon}_{62} + D_{11}\right) \tag{67h}$$

$$c_2^M = 2\sqrt{T^2 - S^2}\left(B_{11}\bar{\varepsilon}_{12} + \bar{B}_{16}\bar{\varepsilon}_{62} + D_{11}\right) \tag{67i}$$

Next, the transverse shear stress resultant $Q_x(x)$ is obtained by using equation (65) with equation (B4) to get

$$Q_x(x) = M_x'(x) \equiv Q_{x0}(x) + Q_{x1}(x)\,K_1 + Q_{x2}(x)\,K_2 + Q_{x3}(x)\,K_3 + Q_{x4}(x)\,K_4 \tag{68}$$

where $Q_{xk}(x) = M_{xk}'(x)$ for values of k = 1, 2, 3, and 4. Differentiating equation (67a) gives

$$Q_{x0}(x) = M_{x0}'(x) = \left(B_{11}\bar{a}_{11} + \bar{B}_{16}\bar{a}_{16}\right)\left[\bar{N}_1'(x) + N_x^{Th}{}'(x)\right] + \left(B_{11}\bar{a}_{16} + \bar{B}_{16}\bar{a}_{66}\right)\left[\bar{T}_1'(x) + \hat{T}^{Th}{}'(x)\right] + \left[B_{12} + B_{11}\bar{\ell}_{12} + \bar{B}_{16}\bar{\ell}_{62}\right]\frac{\bar{w}_p'(x)}{R} - \left[D_{11} + B_{11}\bar{\varepsilon}_{12} + \bar{B}_{16}\bar{\varepsilon}_{62}\right]\bar{w}_p'''(x) - M_x^{Th}{}'(x) \tag{69a}$$

Similarly, differentiating equations (67b) - (67e) and using equations (53) gives

$$Q_{x1}(x) = -\left[c_1^M \sqrt{T-S} + c_2^M \sqrt{T+S}\right] \mathcal{L}_1(x) + \left[c_1^M \sqrt{T+S} - c_2^M \sqrt{T-S}\right] \mathcal{L}_2(x) \qquad (69b)$$

$$Q_{x2}(x) = \left[c_2^M \sqrt{T-S} - c_1^M \sqrt{T+S}\right] \mathcal{L}_1(x) - \left[c_2^M \sqrt{T+S} + c_1^M \sqrt{T-S}\right] \mathcal{L}_2(x) \qquad (69c)$$

$$Q_{x3}(x) = \left[c_1^M \sqrt{T-S} + c_2^M \sqrt{T+S}\right] \mathcal{L}_3(x) + \left[c_1^M \sqrt{T+S} - c_2^M \sqrt{T-S}\right] \mathcal{L}_4(x) \qquad (69d)$$

$$Q_{x4}(x) = \left[c_2^M \sqrt{T-S} - c_1^M \sqrt{T+S}\right] \mathcal{L}_3(x) + \left[c_2^M \sqrt{T+S} + c_1^M \sqrt{T-S}\right] \mathcal{L}_4(x) \qquad (69e)$$

All expressions needed to enforce 8 of the 16 boundary conditions given by equations (B18)-(B21) have been obtained. In particular, equations (1a) and (56) are used to enforce the boundary conditions stated by equation (B18). Equations (7a) and (57) are used to enforce the boundary conditions stated by equation (6), and equivalently equation (B19). Equations (68) and (48) are used to enforce the boundary conditions stated by equation (B20), and equations (63) and (65) are used to enforce the boundary conditions stated by equation (B21). The resulting 16 possible boundary conditions, in which one must be selected from each pair, are listed as follows:

$$u(0) = \tilde{u}_0: \quad U_1(0)\,K_1 + U_2(0)\,K_2 + U_3(0)\,K_3 + U_4(0)\,K_4 + \bar{u} = \tilde{u}_0 - U_0(0) \qquad \text{or} \qquad (70a)$$

$$N_x(0) = \tilde{N}_0: \quad \bar{N}_0 = \tilde{N}_0 - \bar{N}_1(0) \qquad (70b)$$

$$v(0) = \tilde{v}_0: \quad V_1(0)\,K_1 + V_2(0)\,K_2 + V_3(0)\,K_3 + V_4(0)\,K_4 + \bar{v} = \tilde{v}_0 - V_0(0) \qquad \text{or} \qquad (71a)$$

$$\hat{T}(0) = \tilde{T}_0: \quad \bar{T}_0 = \tilde{T}_0 - \bar{T}_1(0) \qquad (71b)$$

$$w(0) = \tilde{w}_0: \quad K_1 \mathcal{L}_1(0) + K_2 \mathcal{L}_2(0) + K_3 \mathcal{L}_3(0) + K_4 \mathcal{L}_4(0) + R\left(c_{\bar{N}} \bar{N}_0 + c_{\bar{T}} \bar{T}_0\right) = \tilde{w}_0 - \bar{w}_p(0) \qquad \text{or} \qquad (72a)$$

$$Q_x(0) = \tilde{V}_0: \quad Q_{x1}(0)\,K_1 + Q_{x2}(0)\,K_2 + Q_{x3}(0)\,K_3 + Q_{x4}(0)\,K_4 = \tilde{V}_0 - Q_{x0}(0) \qquad (72b)$$

$$\beta_x^{\circ}(0) = \tilde{\beta}_0: \quad K_1 \beta_1(0) + K_2 \beta_2(0) + K_3 \beta_3(0) + K_4 \beta_4(0) = \tilde{\beta}_0 - \beta_0(0) \qquad \text{or} \qquad (73a)$$

$M_x(0) = \tilde{M}_0$:

$$M_{x1}(0)\,K_1 + M_{x2}(0)\,K_2 + M_{x3}(0)\,K_3 + M_{x4}(0)\,K_4 + M_{x5}\bar{N}_0 + M_{x6}\bar{T}_0 = \tilde{M}_0 - M_{x0}(0) \tag{73b}$$

$u(L) = \tilde{u}_L$:

$$U_1(L)\,K_1 + U_2(L)\,K_2 + U_3(L)\,K_3 + U_4(L)\,K_4 + \left(U_5'\bar{N}_0 + U_6'\bar{T}_0\right)L + \bar{u} = \tilde{u}_L - U_0(L) \quad \text{or} \tag{74a}$$

$$N_x(L) = \tilde{N}_L: \quad \bar{N}_0 = \tilde{N}_L - \bar{N}_1(L) \tag{74b}$$

$v(L) = \tilde{v}_L$:

$$V_1(L)\,K_1 + V_2(L)\,K_2 + V_3(L)\,K_3 + V_4(L)\,K_4 + \left(V_5'\bar{N}_0 + V_6'\bar{T}_0\right)L + \bar{v} = \tilde{v}_L - V_0(L) \quad \text{or} \tag{75a}$$

$$\hat{T}(x) = \tilde{T}_L: \quad \bar{T}_0 = \tilde{T}_L - \bar{T}_1(L) \tag{75b}$$

$w(L) = \tilde{w}_L$:

$$K_1\mathscr{U}_1(L) + K_2\mathscr{U}_2(L) + K_3\mathscr{U}_3(L) + K_4\mathscr{U}_4(L) + R\left(c_{\bar{N}}\bar{N}_0 + c_{\bar{T}}\bar{T}_0\right) = \tilde{w}_L - \bar{w}_p(L) \quad \text{or} \tag{76a}$$

$$Q_x(x) = \tilde{V}_L: \quad Q_{x1}(L)\,K_1 + Q_{x2}(L)\,K_2 + Q_{x3}(L)\,K_3 + Q_{x4}(L)\,K_4 = \tilde{V}_L - Q_{x0}(L) \tag{76b}$$

$$\beta_x^{\circ}(L) = \tilde{\beta}_L: \quad K_1\beta_1(L) + K_2\beta_2(L) + K_3\beta_3(L) + K_4\beta_4(L) = \tilde{\beta}_L - \beta_0(L) \quad \text{or} \tag{77a}$$

$M_x(L) = \tilde{M}_L$:

$$M_{x1}(L)\,K_1 + M_{x2}(L)\,K_2 + M_{x3}(L)\,K_3 + M_{x4}(L)\,K_4 + M_{x5}\bar{N}_0 + M_{x6}\bar{T}_0 = \tilde{M}_L - M_{x0}(L) \tag{77b}$$

For certain combinations of boundary conditions, rigid-body displacements may be present that must be eliminated in order to have a unique solution.

After determining the unknown constants given by equation (62), the displacements, strains, and stress resultants are known. The stress resultant N_θ is obtained from equation (16a). Substituting equations (48), (49), and (51) into equation (16a) gives

$$N_\theta = N_{\theta 0}(x) + N_{\theta 1}(x)\,K_1 + N_{\theta 2}(x)\,K_2 + N_{\theta 3}(x)\,K_3 + N_{\theta 4}(x)\,K_4 + N_{\theta 5}\bar{N}_0 + N_{\theta 6}\bar{T}_0 \tag{78}$$

where

$$N_{\theta 0}(x) = A_{12}U_0'(x) + A_{22}\frac{\overline{w}_p(x)}{R} + \overline{A}_{26}V_0'(x) - B_{12}\overline{w}_p''(x) - N_\theta^{Th}(x) \tag{79a}$$

$$N_{\theta k}(x) = A_{12}U_k'(x) + \frac{A_{22}}{R}\ell_k(x) + \overline{A}_{26}V_k'(x) - B_{12}\ell_k''(x) \quad \text{with } k = 1, 2, 3, \text{ and } 4 \tag{79b}$$

$$N_{\theta 5} = A_{12}U_5' + A_{22}c_{\overline{N}} + \overline{A}_{26}V_5' \tag{79c}$$

$$N_{\theta 6} = A_{12}U_6' + A_{22}c_{\overline{T}} + \overline{A}_{26}V_6' \tag{79d}$$

Using equation (50a) for $U_0'(x)$, equation (52a) for $V_0'(x)$, equations (54) for $U_1'(x)$ through $U_4'(x)$, equations (55) for $V_1'(x)$ through $V_4'(x)$, equation (50c) for U_5', equation (50d) for U_6', equation (52c) for V_5', and equation (52d) for V_6', and equations (53) for the second derivatives of the basis functions gives

$$\begin{aligned} N_{\theta 0}(x) = {} & \left(A_{12}\bar{a}_{11} + \overline{A}_{26}\bar{a}_{16}\right)\left[\overline{N}_1(x) + N_x^{Th}(x)\right] + \left(A_{12}\bar{a}_{16} + \overline{A}_{26}\bar{a}_{66}\right)\left[\overline{T}_1(x) + \hat{T}^{Th}(x)\right] \\ & + \left(A_{22} + A_{12}\bar{\ell}_{12} + \overline{A}_{26}\bar{\ell}_{62}\right)\frac{\overline{w}_p(x)}{R} - \left(B_{12} + A_{12}\bar{\varepsilon}_{12} + \overline{A}_{26}\bar{\varepsilon}_{62}\right)\overline{w}_p''(x) - N_\theta^{Th}(x) \end{aligned} \tag{80a}$$

$$N_{\theta 1}(x) = c_3^N\ell_1(x) + c_4^N\ell_2(x) \tag{80b}$$

$$N_{\theta 2}(x) = -c_4^N\ell_1(x) + c_3^N\ell_2(x) \tag{80c}$$

$$N_{\theta 3}(x) = c_3^N\ell_3(x) - c_4^N\ell_4(x) \tag{80d}$$

$$N_{\theta 4}(x) = c_4^N\ell_3(x) + c_3^N\ell_4(x) \tag{80e}$$

$$N_{\theta 5} = c_{\overline{N}}\left(A_{22} + A_{12}\bar{\ell}_{12} + \overline{A}_{26}\bar{\ell}_{62}\right) + A_{12}\bar{a}_{11} + \overline{A}_{26}\bar{a}_{16} \tag{80f}$$

$$N_{\theta 6} = c_{\overline{T}}\left(A_{22} + A_{12}\bar{\ell}_{12} + \overline{A}_{26}\bar{\ell}_{62}\right) + A_{12}\bar{a}_{16} + \overline{A}_{26}\bar{a}_{66} \tag{80g}$$

where

$$c_3^N = \frac{A_{12}\bar{\ell}_{12} + A_{22} + \overline{A}_{26}\bar{\ell}_{62}}{R} + 2S\left(A_{12}\bar{\varepsilon}_{12} + \overline{A}_{26}\bar{\varepsilon}_{62} + B_{12}\right) \tag{81a}$$

$$c_4^N = 2\sqrt{T^2 - S^2}\left(A_{12}\bar{\varepsilon}_{12} + \overline{A}_{26}\bar{\varepsilon}_{62} + B_{12}\right) \tag{81b}$$

Similarly, The stress resultant M_θ is obtained from equation (11) by using equations (B6) - (B8) and (B12); that is

$$M_\theta = B_{12}u'(x) + B_{22}\frac{w(x)}{R} + \overline{B}_{26}v'(x) - D_{12}w''(x) - M_\theta^{Th}(x) \tag{82}$$

Substituting equations (48), (49), and (51) into equation (82) gives

$$M_\theta = M_{\theta 0}(x) + M_{\theta 1}(x)\,K_1 + M_{\theta 2}(x)\,K_2 + M_{\theta 3}(x)\,K_3 + M_{\theta 4}(x)\,K_4 + M_{\theta 5}\overline{N}_0 + M_{\theta 6}\overline{T}_0 \tag{83}$$

where

$$M_{\theta 0}(x) = B_{12}U_0'(x) + B_{22}\frac{\overline{w}_p(x)}{R} + \overline{B}_{26}V_0'(x) - D_{12}\overline{w}_p''(x) - M_\theta^{Th}(x) \tag{84a}$$

$$M_{\theta k}(x) = B_{12}U_k'(x) + \frac{B_{22}}{R}\mathscr{C}_k(x) + \overline{B}_{26}V_k'(x) - D_{12}\mathscr{C}_k''(x) \quad \text{with } k = 1, 2, 3, \text{ and } 4 \tag{84b}$$

$$M_{\theta 5} = B_{12}U_5' + B_{22}c_{\overline{N}} + \overline{B}_{26}V_5' \tag{84c}$$

$$M_{\theta 6} = B_{12}U_6' + B_{22}c_{\overline{T}} + \overline{B}_{26}V_6' \tag{84d}$$

Again, using equation (50a) for $U_0'(x)$, equation (52a) for $V_0'(x)$, equations (54) for $U_1'(x)$ through $U_4'(x)$, equations (55) for $V_1'(x)$ through $V_4'(x)$, equation (50c) for U_5', equation (50d) for U_6', equation (52c) for V_5', and equation (52d) for V_6', and equations (53) for the second derivatives of the basis functions gives

$$\begin{aligned} M_{\theta 0}(x) = {} & \left(B_{12}\bar{a}_{11} + \overline{B}_{26}\bar{a}_{16}\right)\left[\overline{N}_1(x) + N_x^{Th}(x)\right] + \left(B_{12}\bar{a}_{16} + \overline{B}_{26}\bar{a}_{66}\right)\left[\overline{T}_1(x) + \hat{T}^{Th}(x)\right] \\ & + \left(B_{22} + B_{12}\bar{\mathscr{C}}_{12} + \overline{B}_{26}\bar{\mathscr{C}}_{62}\right)\frac{\overline{w}_p(x)}{R} - \left(D_{12} + B_{12}\bar{\varepsilon}_{12} + \overline{B}_{26}\bar{\varepsilon}_{62}\right)\overline{w}_p''(x) - M_\theta^{Th}(x) \end{aligned} \tag{85a}$$

$$M_{\theta 1}(x) = c_3^M\mathscr{C}_1(x) + c_4^M\mathscr{C}_2(x) \tag{85b}$$

$$M_{\theta 2}(x) = -c_4^M\mathscr{C}_1(x) + c_3^M\mathscr{C}_2(x) \tag{85c}$$

$$M_{\theta 3}(x) = c_3^M\mathscr{C}_3(x) - c_4^M\mathscr{C}_4(x) \tag{85d}$$

$$M_{\theta 4}(x) = c_4^M\mathscr{C}_3(x) + c_3^M\mathscr{C}_4(x) \tag{85e}$$

$$M_{\theta 5} = c_{\bar{N}}\left(B_{22} + B_{12}\bar{\ell}_{12} + \overline{B}_{26}\bar{\ell}_{62}\right) + B_{12}\bar{a}_{11} + \overline{B}_{26}\bar{a}_{16} \tag{85f}$$

$$M_{\theta 6} = c_{\bar{T}}\left(B_{22} + B_{12}\bar{\ell}_{12} + \overline{B}_{26}\bar{\ell}_{62}\right) + B_{12}\bar{a}_{16} + \overline{B}_{26}\bar{a}_{66} \tag{85g}$$

where

$$c_3^M = \frac{B_{12}\bar{\ell}_{12} + B_{22} + \overline{B}_{26}\bar{\ell}_{62}}{R} + 2S\left(B_{12}\bar{\varepsilon}_{12} + \overline{B}_{26}\bar{\varepsilon}_{62} + D_{12}\right) \tag{85h}$$

$$c_4^M = 2\sqrt{T^2 - S^2}\left(B_{12}\bar{\varepsilon}_{12} + \overline{B}_{26}\bar{\varepsilon}_{62} + D_{12}\right) \tag{85i}$$

The stress resultant $M_{x\theta}(x)$ is obtained by using equation (B15) and (9) to get

$$M_{x\theta}(x) = B_{16}\varepsilon_x^o + B_{26}\varepsilon_\theta^o + \overline{B}_{66}\gamma_{x\theta}^o + D_{16}\kappa_x^o - M_{x\theta}^{Th} \tag{86}$$

where

$$\overline{B}_{66} = B_{66} + \mu\left(\frac{h}{R}\right)\frac{D_{66}}{h} \tag{87}$$

Then, using equations (B6) - (B8) and (B12), equation (86) becomes

$$M_{x\theta}(x) = B_{16}u'(x) + B_{26}\frac{w(x)}{R} + \overline{B}_{66}v'(x) - D_{16}w''(x) - M_{x\theta}^{Th}(x) \tag{88}$$

Substituting equations (48), (49), and (51) into equation (88) gives

$$M_{x\theta} = M_{x\theta 0}(x) + M_{x\theta 1}(x)\,K_1 + M_{x\theta 2}(x)\,K_2 + M_{x\theta 3}(x)\,K_3 + M_{x\theta 4}(x)\,K_4 + M_{x\theta 5}\overline{N}_0 + M_{x\theta 6}\overline{T}_0 \tag{89}$$

where

$$M_{x\theta 0}(x) = B_{16}U_0'(x) + B_{26}\frac{\overline{w}_p(x)}{R} + \overline{B}_{66}V_0'(x) - D_{16}\overline{w}_p''(x) - M_{x\theta}^{Th}(x) \tag{90a}$$

$$M_{x\theta k}(x) = B_{16}U_k'(x) + \frac{B_{26}}{R}\ell_k(x) + \overline{B}_{66}V_k'(x) - D_{16}\ell_k''(x) \quad \text{with } k = 1, 2, 3, \text{ and } 4 \tag{90b}$$

$$M_{x\theta 5} = B_{16}U_5' + B_{26}c_{\bar{N}} + \overline{B}_{66}V_5' \tag{90c}$$

$$M_{x\theta 6} = B_{16}U_6' + B_{26}c_{\bar{T}} + \overline{B}_{66}V_6' \tag{90d}$$

Again, using equation (50a) for $U_0'(x)$, equation (52a) for $V_0'(x)$, equations (54) for $U_1'(x)$ through $U_4'(x)$, equations (55) for $V_1'(x)$ through $V_4'(x)$, equation (50c) for U_5', equation (50d) for U_6', equation (52c) for V_5', and equation (52d) for V_6' , and equations (53) for the second derivatives of the basis functions gives

$$\begin{aligned} M_{x\theta 0}(x) = {} & \left(B_{16}\bar{a}_{11} + \bar{B}_{66}\bar{a}_{16}\right)\left[\bar{N}_1(x) + N_x^{Th}(x)\right] + \left(B_{16}\bar{a}_{16} + \bar{B}_{66}\bar{a}_{66}\right)\left[\bar{T}_1(x) + \hat{T}^{Th}(x)\right] \\ & + \left(B_{26} + B_{16}\bar{\ell}_{12} + \bar{B}_{66}\bar{\ell}_{62}\right)\frac{\bar{w}_p(x)}{R} - \left(D_{16} + B_{16}\bar{\varepsilon}_{12} + \bar{B}_{66}\bar{\varepsilon}_{62}\right)\bar{w}_p''(x) - M_{x\theta}^{Th}(x) \end{aligned} \tag{91a}$$

$$M_{x\theta 1}(x) = c_5^M \ell_1(x) + c_6^M \ell_2(x) \tag{91b}$$

$$M_{x\theta 2}(x) = -c_5^M \ell_1(x) + c_6^M \ell_2(x) \tag{91c}$$

$$M_{x\theta 3}(x) = c_5^M \ell_3(x) - c_6^M \ell_4(x) \tag{91d}$$

$$M_{x\theta 4}(x) = c_5^M \ell_3(x) + c_6^M \ell_4(x) \tag{91e}$$

$$M_{x\theta 5} = c_{\bar{N}}\left(B_{26} + B_{16}\bar{\ell}_{12} + \bar{B}_{66}\bar{\ell}_{62}\right) + B_{16}\bar{a}_{11} + \bar{B}_{66}\bar{a}_{16} \tag{91f}$$

$$M_{x\theta 6} = c_{\bar{T}}\left(B_{26} + B_{16}\bar{\ell}_{12} + \bar{B}_{66}\bar{\ell}_{62}\right) + B_{16}\bar{a}_{16} + \bar{B}_{66}\bar{a}_{66} \tag{91g}$$

where

$$c_5^M = \frac{B_{16}\bar{\ell}_{12} + B_{26} + \bar{B}_{66}\bar{\ell}_{62}}{R} + 2S\left(B_{16}\bar{\varepsilon}_{12} + \bar{B}_{66}\bar{\varepsilon}_{62} + D_{16}\right) \tag{91h}$$

$$c_6^M = 2\sqrt{T^2 - S^2}\left(B_{16}\bar{\varepsilon}_{12} + \bar{B}_{66}\bar{\varepsilon}_{62} + D_{16}\right) \tag{91i}$$

Then, equations (4) and (7a) give

$$N_{x\theta}(x) = \bar{T}_0 + \bar{T}_1(x) - \frac{\mu}{R}M_{x\theta}(x) \tag{92}$$

The transverse shear stress resultant Q_θ is obtained from equation (B5); that is,

$$Q_\theta(x) = M_{x\theta}'(x) \tag{93}$$

Differentiating equations (89) and (91), and using equations (53) gives

$$Q_\theta(x) = Q_{\theta 0}(x) + Q_{\theta 1}(x)\, K_1 + Q_{\theta 2}(x)\, K_2 + Q_{\theta 3}(x)\, K_3 + Q_{\theta 4}(x)\, K_4 \tag{94}$$

where

$$\begin{aligned} Q_{\theta 0}(x) = {} & \left(B_{16}\bar{a}_{11} + \bar{B}_{66}\bar{a}_{16}\right)\left[\bar{N}_1'(x) + N_x^{Th\prime}(x)\right] + \left(B_{16}\bar{a}_{16} + \bar{B}_{66}\bar{a}_{66}\right)\left[\bar{T}_1'(x) + \hat{T}^{Th\prime}(x)\right] \\ & + \left(B_{26} + B_{16}\bar{\ell}_{12} + \bar{B}_{66}\bar{\ell}_{62}\right)\frac{\bar{w}_p'(x)}{R} - \left(D_{16} + B_{16}\bar{\epsilon}_{12} + \bar{B}_{66}\bar{\epsilon}_{62}\right)\bar{w}_p'''(x) - M_{x\theta}^{Th\prime}(x) \end{aligned} \tag{95a}$$

$$Q_{\theta 1}(x) = -\left[c_5^M\sqrt{T-S} + c_6^M\sqrt{T+S}\right]\mathscr{C}_1(x) + \left[c_5^M\sqrt{T+S} - c_6^M\sqrt{T-S}\right]\mathscr{C}_2(x) \tag{95b}$$

$$Q_{\theta 2}(x) = \left[c_5^M\sqrt{T-S} - c_6^M\sqrt{T+S}\right]\mathscr{C}_1(x) - \left[c_5^M\sqrt{T+S} + c_6^M\sqrt{T-S}\right]\mathscr{C}_2(x) \tag{95c}$$

$$Q_{\theta 3}(x) = \left[c_5^M\sqrt{T-S} + c_6^M\sqrt{T+S}\right]\mathscr{C}_3(x) + \left[c_5^M\sqrt{T+S} - c_6^M\sqrt{T-S}\right]\mathscr{C}_4(x) \tag{95d}$$

$$Q_{\theta 4}(x) = \left[c_5^M\sqrt{T-S} - c_6^M\sqrt{T+S}\right]\mathscr{C}_3(x) + \left[c_5^M\sqrt{T+S} + c_6^M\sqrt{T-S}\right]\mathscr{C}_4(x) \tag{95e}$$

Particular Solutions

Whenever $P_1(x)$ given by equation (29c) is nonzero, the particular solution $\bar{w}_p(x)$ must be determined. To illustrate the solution process, consider a cylinder subjected to the surface tractions

$$q_x(x) = q_x^0 + q_x^1\, x + q_x^s \sin\left(\frac{\pi x}{L}\right) + q_x^c \cos\left(\frac{2\pi x}{L}\right) \tag{96a}$$

$$q_\theta(x) = q_\theta^0 + q_\theta^1\, x + q_\theta^s \sin\left(\frac{\pi x}{L}\right) + q_\theta^c \cos\left(\frac{2\pi x}{L}\right) \tag{96b}$$

$$q_n(x) = q_n^0 + q_n^1\, x + q_n^s \sin\left(\frac{\pi x}{L}\right) + q_n^c \cos\left(\frac{2\pi x}{L}\right) \tag{96c}$$

and the temperature-change distributions

$$\Theta_0(x) = H_0 + H_1 x + H_s \sin\left(\frac{\pi x}{L}\right) + H_c \cos\left(\frac{2\pi x}{L}\right) \tag{97a}$$

$$\Theta_1(x) = G_0 + G_1\, x + G_s \sin\left(\frac{\pi x}{L}\right) + G_c \cos\left(\frac{2\pi x}{L}\right) \tag{97b}$$

where q_x^0, q_x^1, q_x^s, q_x^c, q_θ^0, q_θ^1, q_θ^s, q_θ^c, q_n^0, q_n^1, q_n^s, q_n^c, H_0, H_1, H_s, H_c, G_0, G_1, G_s, and G_c are specified constants. The first step in constructing the particular solution is to obtain all the input quantities that appear in equation (29c) for $P_1(x)$. Equations (1b) and (96a) give

$$\bar{N}_1(x) = -q_x^0 x - \frac{q_x^1}{2} x^2 + \frac{q_x^s L}{\pi} \cos\left(\frac{\pi x}{L}\right) - \frac{q_x^c L}{2\pi} \sin\left(\frac{2\pi x}{L}\right) \tag{98}$$

and equations (7b) and (96b) give

$$\bar{T}_1(x) = -q_\theta^0 x - \frac{q_\theta^1}{2} x^2 + \frac{q_\theta^s L}{\pi} \cos\left(\frac{\pi x}{L}\right) - \frac{q_\theta^c L}{2\pi} \sin\left(\frac{2\pi x}{L}\right) \tag{99}$$

Equations (B17) and (97) give

$$\begin{aligned} N_x^{Th}(x) = &\left(H_0 n_x^{Th} + G_0 c_x^{Th}\right) + \left(H_1 n_x^{Th} + G_1 c_x^{Th}\right) x \\ &+ \left(H_s n_x^{Th} + G_s c_x^{Th}\right) \sin\left(\frac{\pi x}{L}\right) + \left(H_c n_x^{Th} + G_c c_x^{Th}\right) \cos\left(\frac{2\pi x}{L}\right) \end{aligned} \tag{100a}$$

Likewise,

$$\begin{aligned} N_\theta^{Th}(x) = &\left(H_0 n_\theta^{Th} + G_0 c_\theta^{Th}\right) + \left(H_1 n_\theta^{Th} + G_1 c_\theta^{Th}\right) x \\ &+ \left(H_s n_\theta^{Th} + G_s c_\theta^{Th}\right) \sin\left(\frac{\pi x}{L}\right) + \left(H_c n_\theta^{Th} + G_c c_\theta^{Th}\right) \cos\left(\frac{2\pi x}{L}\right) \end{aligned} \tag{100b}$$

$$\begin{aligned} M_x^{Th}(x) = &\left(H_0 c_x^{Th} + G_0 m_x^{Th}\right) + \left(H_1 c_x^{Th} + G_1 m_x^{Th}\right) x \\ &+ \left(H_s c_x^{Th} + G_s m_x^{Th}\right) \sin\left(\frac{\pi x}{L}\right) + \left(H_c c_x^{Th} + G_c m_x^{Th}\right) \cos\left(\frac{2\pi x}{L}\right) \end{aligned} \tag{100c}$$

In addition, equations (B17), (12f), and (97) give

$$\begin{aligned} \hat{T}^{Th}(x) = &\left(H_0 \bar{n}_{x\theta}^{Th} + G_0 \bar{c}_{x\theta}^{Th}\right) + \left(H_1 \bar{n}_{x\theta}^{Th} + G_1 \bar{c}_{x\theta}^{Th}\right) x \\ &+ \left(H_s \bar{n}_{x\theta}^{Th} + G_s \bar{c}_{x\theta}^{Th}\right) \sin\left(\frac{\pi x}{L}\right) + \left(H_c \bar{n}_{x\theta}^{Th} + G_c \bar{c}_{x\theta}^{Th}\right) \cos\left(\frac{2\pi x}{L}\right) \end{aligned} \tag{100d}$$

where

$$\bar{n}_{x\theta}^{Th} = n_{x\theta}^{Th} + \frac{\mu}{R} c_{x\theta}^{Th} \tag{101a}$$

$$\bar{c}_{x\theta}^{Th} = c_{x\theta}^{Th} + \frac{\mu}{R} m_{x\theta}^{Th} \tag{101b}$$

Using equations (96c), (98), (99), and (100) with equation (29c) yields

$$P_1(x) = Y_0 + Y_1\, x + Y_2\, x^2 + Y_{s1}\sin\left(\frac{\pi x}{L}\right) + Y_{s2}\sin\left(\frac{2\pi x}{L}\right) + Y_{c1}\cos\left(\frac{\pi x}{L}\right) + Y_{c2}\cos\left(\frac{2\pi x}{L}\right) \tag{102a}$$

where

$$Y_0 = \frac{1}{D_{11}\,\boldsymbol{e}}\Big[q_n^0 - q_x^1\left(B_{11}\bar{a}_{11} + \bar{B}_{16}\bar{a}_{16}\right) - q_\theta^1\left(B_{11}\bar{a}_{16} + \bar{B}_{16}\bar{a}_{66}\right) + \frac{H_0}{R}\left(n_\theta^{Th} - n_x^{Th}\left(A_{12}\bar{a}_{11} + \bar{A}_{26}\bar{a}_{16}\right) - \bar{n}_{x\theta}^{Th}\left(A_{12}\bar{a}_{16} + \bar{A}_{26}\bar{a}_{66}\right)\right) + \frac{G_0}{R}\left(c_\theta^{Th} - c_x^{Th}\left(A_{12}\bar{a}_{11} + \bar{A}_{26}\bar{a}_{16}\right) - \bar{c}_{x\theta}^{Th}\left(A_{12}\bar{a}_{16} + \bar{A}_{26}\bar{a}_{66}\right)\right)\Big] \tag{102b}$$

$$Y_1 = \frac{1}{D_{11}\,\boldsymbol{e}}\Big[q_n^1 + \frac{q_x^0}{R}\left(A_{12}\bar{a}_{11} + \bar{A}_{26}\bar{a}_{16}\right) + \frac{q_\theta^0}{R}\left(A_{12}\bar{a}_{16} + \bar{A}_{26}\bar{a}_{66}\right) + \frac{H_1}{R}\left(n_\theta^{Th} - n_x^{Th}\left(A_{12}\bar{a}_{11} + \bar{A}_{26}\bar{a}_{16}\right) - \bar{n}_{x\theta}^{Th}\left(A_{12}\bar{a}_{16} + \bar{A}_{26}\bar{a}_{66}\right)\right) + \frac{G_1}{R}\left(c_\theta^{Th} - c_x^{Th}\left(A_{12}\bar{a}_{11} + \bar{A}_{26}\bar{a}_{16}\right) - \bar{c}_{x\theta}^{Th}\left(A_{12}\bar{a}_{16} + \bar{A}_{26}\bar{a}_{66}\right)\right)\Big] \tag{102c}$$

$$Y_2 = \frac{1}{2RD_{11}\,\boldsymbol{e}}\Big[q_x^1\left(A_{12}\bar{a}_{11} + \bar{A}_{26}\bar{a}_{16}\right) + q_\theta^1\left(A_{12}\bar{a}_{16} + \bar{A}_{26}\bar{a}_{66}\right)\Big] \tag{102d}$$

$$Y_{s1} = \frac{1}{D_{11}\,\boldsymbol{e}}\Big[q_n^s + \frac{H_s}{R}\left(n_\theta^{Th} - n_x^{Th}\left(A_{12}\bar{a}_{11} + \bar{A}_{26}\bar{a}_{16}\right) - \bar{n}_{x\theta}^{Th}\left(A_{12}\bar{a}_{16} + \bar{A}_{26}\bar{a}_{66}\right)\right) + H_s\frac{\pi^2}{L^2}\left(c_x^{Th} - n_x^{Th}\left(B_{11}\bar{a}_{11} + \bar{B}_{16}\bar{a}_{16}\right) - \bar{n}_{x\theta}^{Th}\left(B_{11}\bar{a}_{16} + \bar{B}_{16}\bar{a}_{66}\right)\right) + \frac{G_s}{R}\left(c_\theta^{Th} - c_x^{Th}\left(A_{12}\bar{a}_{11} + \bar{A}_{26}\bar{a}_{16}\right) - \bar{c}_{x\theta}^{Th}\left(A_{12}\bar{a}_{16} + \bar{A}_{26}\bar{a}_{66}\right)\right) + G_s\frac{\pi^2}{L^2}\left(m_x^{Th} - c_x^{Th}\left(B_{11}\bar{a}_{11} + \bar{B}_{16}\bar{a}_{16}\right) - \bar{c}_{x\theta}^{Th}\left(B_{11}\bar{a}_{16} + \bar{B}_{16}\bar{a}_{66}\right)\right)\Big] \tag{102e}$$

$$Y_{s2} = \frac{1}{D_{11}\,\boldsymbol{e}}\Big[\frac{2\pi}{L}\left(q_x^c\left(B_{11}\bar{a}_{11} + \bar{B}_{16}\bar{a}_{16}\right) + q_\theta^c\left(B_{11}\bar{a}_{16} + \bar{B}_{16}\bar{a}_{66}\right)\right) + \frac{L}{2\pi R}\left(q_x^c\left(A_{12}\bar{a}_{11} + \bar{A}_{26}\bar{a}_{16}\right) + q_\theta^c\left(A_{12}\bar{a}_{16} + \bar{A}_{26}\bar{a}_{66}\right)\right)\Big] \tag{102f}$$

$$Y_{c1} = \frac{-1}{D_{11}\,\mathcal{e}}\Big[\frac{\pi}{L}\Big(\,q_x^s\Big(B_{11}\bar{a}_{11} + \bar{B}_{16}\bar{a}_{16}\Big) + q_\theta^s\Big(B_{11}\bar{a}_{16} + \bar{B}_{16}\bar{a}_{66}\Big)\Big) + \frac{L}{\pi R}\Big(q_x^s\Big(A_{12}\bar{a}_{11} + \bar{A}_{26}\bar{a}_{16}\Big) + q_\theta^s\Big(A_{12}\bar{a}_{16} + \bar{A}_{26}\bar{a}_{66}\Big)\Big)\Big] \tag{102g}$$

$$\begin{aligned} Y_{c2} = \frac{1}{D_{11}\,\mathcal{e}}\Big[& q_n^c + \frac{H_c}{R}\Big(n_\theta^{Th} - n_x^{Th}\Big(A_{12}\bar{a}_{11} + \bar{A}_{26}\bar{a}_{16}\Big) - \bar{n}_{x\theta}^{Th}\Big(A_{12}\bar{a}_{16} + \bar{A}_{26}\bar{a}_{66}\Big)\Big) \\ & + H_c\frac{4\pi^2}{L^2}\Big(c_x^{Th} - n_x^{Th}\Big(B_{11}\bar{a}_{11} + \bar{B}_{16}\bar{a}_{16}\Big) - \bar{n}_{x\theta}^{Th}\Big(B_{11}\bar{a}_{16} + \bar{B}_{16}\bar{a}_{66}\Big)\Big) \\ & + \frac{G_c}{R}\Big(c_\theta^{Th} - c_x^{Th}\Big(A_{12}\bar{a}_{11} + \bar{A}_{26}\bar{a}_{16}\Big) - \bar{c}_{x\theta}^{Th}\Big(A_{12}\bar{a}_{16} + \bar{A}_{26}\bar{a}_{66}\Big)\Big) \\ & + G_c\frac{4\pi^2}{L^2}\Big(m_x^{Th} - c_x^{Th}\Big(B_{11}\bar{a}_{11} + \bar{B}_{16}\bar{a}_{16}\Big) - \bar{c}_{x\theta}^{Th}\Big(B_{11}\bar{a}_{16} + \bar{B}_{16}\bar{a}_{66}\Big)\Big)\Big] \end{aligned} \tag{102h}$$

By applying the method of undetermined coefficients to equation (40) with $P_0 = 0$, the particular solution $\bar{w}_p(x)$ is found to be given by

$$\begin{aligned} \bar{w}_p(x) = & \bar{w}_p^0 + \bar{w}_p^1\,x + \bar{w}_p^2\,x^2 \\ & + \bar{w}_p^{s1}\sin\Big(\frac{\pi x}{L}\Big) + \bar{w}_p^{s2}\sin\Big(\frac{2\pi x}{L}\Big) + \bar{w}_p^{c1}\cos\Big(\frac{\pi x}{L}\Big) + \bar{w}_p^{c2}\cos\Big(\frac{2\pi x}{L}\Big) \end{aligned} \tag{103}$$

where

$$\bar{w}_p^0 = \frac{1}{4T^2}\Big(Y_0 - \frac{2SY_2}{T^2}\Big) \tag{104a}$$

$$\bar{w}_p^1 = \frac{Y_1}{4T^2} \tag{104b}$$

$$\bar{w}_p^2 = \frac{Y_2}{4T^2} \tag{104c}$$

$$\bar{w}_p^{s1} = Y_{s1}\Big[\frac{\pi^4}{L^4} - \frac{4\pi^2}{L^2}\,S + 4T^2\Big]^{-1} \tag{104d}$$

$$\bar{w}_p^{s2} = Y_{s2}\Big[\frac{16\pi^4}{L^4} - \frac{16\pi^2}{L^2}\,S + 4T^2\Big]^{-1} \tag{104e}$$

$$\overline{w}_p^{c1} = Y_{c1}\left[\frac{\pi^4}{L^4} - \frac{4\pi^2}{L^2}S + 4T^2\right]^{-1} \tag{104f}$$

$$\overline{w}_p^{c2} = Y_{c2}\left[\frac{16\pi^4}{L^4} - \frac{16\pi^2}{L^2}S + 4T^2\right]^{-1} \tag{104g}$$

Examples

Five examples are presented subsequently to illustrate the utility of the exact solution presented herein and some of the behavioral characteristics of laminated-composite cylinders that exhibit general forms of anisotropy. For each example, results are presented for length-to-radius ratios L/R = 0.5 and 2, and for fixed values of the radius-to-thickness ratio R/h. Cylinders with these two L/R values exhibit the full range of variations in behavior; that is, behavior in which zones of localized bending are isolated near the ends of a cylinder and behavior in which the bending behavior is not localized at all. Zones of localized bending are referred to herein as bending boundary layers. For every laminate considered, the lamina material properties are given by the major principal modulus $E_1 = 18.5 \times 10^6$ psi, the minor principal modulus $E_2 = 1.64 \times 10^6$ psi, the shear modulus $G_{12} = 0.87 \times 10^6$ psi, the major Poisson's ratio $\nu_{12} = 0.30$, the major principal coefficient of thermal expansion $\alpha_1 = 0.25 \times 10^{-6}$ /°F, and the minor principal coefficient of thermal expansion $\alpha_2 = 16.2 \times 10^{-6}$ /°F. For all laminates considered, the ply thicknesses are identical and the ply thickness is taken as the total thickness h divided by the number of plies. From a practical standpoint, atypically thick plies are considered to be composed of groups of thinner plies with the same orientation. For all results presented, based on the exact solution, the Sanders-Koiter equations were used, which corresponds to the value $\mu = 3/2$. For several of the examples, simplified approximate solutions are also presented. Each simplified solution provides a necessary condition for establishing the correctness, and hence credibility, of the corresponding more complicated exact solution. Several examples also include the effects of temperature-change fields. For convenience, the temperature-change fields on the outside and inside of a cylinder are denoted by $\Delta T_o = \Delta T\left(x, \frac{h}{2}\right)$ and $\Delta T_i = \Delta T\left(x, -\frac{h}{2}\right)$, respectively (see equations (B16)).

Example 1: Self-Equilibrated End Loads

Perhaps one of the most fundamental problems of shell theory is the attenuation behavior of a circular cylinder subjected to self-equilibrated end loads. For the example considered herein, the boundary conditions specified in the present study are

$$N_x(0) = 0 \tag{105a}$$

$$\hat{T}(0) = 0 \tag{105b}$$

$$Q_x(0) = \tilde{V}_0 \tag{105c}$$

$$M_x(0) = \tilde{M}_0 \tag{105d}$$

at $x = 0$ and

$$u(L) = 0 \tag{106a}$$

$$v(L) = 0 \tag{106b}$$

$$w(L) = 0 \tag{106c}$$

$$\beta_x^{\circ}(L) = 0 \tag{106d}$$

at $x = L$. These boundary conditions correspond to a cylinder that is completely clamped around the circumference at $x = L$ and subjected to a uniform transverse shear stress resultant and a uniform bending moment resultant, as depicted in figure 4. For these loading conditions, the particular solution given by equation (103) is identically zero-valued.

Results were obtained for geometrically identical cylinders with two very different laminated-wall constructions, and for the applied loads given by $\tilde{M}_0 = 100$ lbs and $\tilde{V}_0 = 100$ lbs/in. The geometries considered are characterized by the radius-to-thickness ratio R/h = 100 and the length-to-radius ratios L/R = 0.5 and 2. In particular, results are presented in figures 4-7 for cylinders with laminated walls composed of all 90-degree plies and a total wall thickness h = 0.1 in. This wall construction is referred to herein as specially orthotropic because the principal axes of each orthotropic ply are aligned with the x and θ coordinate directions shown in figure 3. Therefore, these laminates exhibit no form of anisotropy associated with coupling between extension and shear, coupling between bending and twisting, or coupling between any membrane deformation and any bending deformation. As a result, the cylinders with this wall construction do not exhibit any circumferential displacements. The values of the nonzero constitutive matrices computed for this laminate are given by

$$\begin{bmatrix} A_{11} & A_{12} & A_{16} \\ A_{12} & A_{22} & A_{26} \\ A_{16} & A_{26} & A_{66} \end{bmatrix} = \begin{bmatrix} 0.165319 & 0.0495957 & 0 \\ 0.0495957 & 1.86488 & 0 \\ 0 & 0 & 0.087000 \end{bmatrix} \times 10^6 \ \frac{\text{lbs}}{\text{in.}} \tag{107a}$$

$$\begin{bmatrix} D_{11} & D_{12} & D_{16} \\ D_{12} & D_{22} & D_{26} \\ D_{16} & D_{26} & D_{66} \end{bmatrix} = \begin{bmatrix} 0.137766 & 0.0413297 & 0 \\ 0.0413297 & 1.55407 & 0 \\ 0 & 0 & 0.0725000 \end{bmatrix} \times 10^{3} \text{ in.–lbs} \tag{107b}$$

Similarly, the constitutive expressions defined by equations (15) are given by

$$\begin{bmatrix} \bar{a}_{11} & \bar{a}_{16} \\ \bar{a}_{16} & \bar{a}_{66} \end{bmatrix} = \begin{bmatrix} 6.04891 & 0 \\ 0 & 11.494 \end{bmatrix} \times 10^{-6} \frac{\text{in.}}{\text{lbs}} \tag{108a}$$

$$\begin{Bmatrix} \bar{\ell}_{12} \\ \bar{\ell}_{62} \end{Bmatrix} = - \begin{Bmatrix} 0.3 \\ 0 \end{Bmatrix} \tag{108b}$$

$$\begin{Bmatrix} \bar{c}_{12} \\ \bar{c}_{62} \end{Bmatrix} = \begin{Bmatrix} 0 \\ 0 \end{Bmatrix} \text{ in.} \tag{108c}$$

The values of S and T, defined by equations (27) and (39), respectively, that are used to determine the basis functions of the solution space are given by $S = 0$ and $T = 5.79409$ in.$^{-2}$.

In contrast to the specially orthotropic wall, results are presented in figures 8-13 for cylinders with laminated walls composed of all 10-degree plies and a total wall thickness h = 0.1 in. This wall construction exhibits anisotropy in the form of coupling between membrane expansion or contraction and shearing deformations, and coupling between pure bending and twisting deformations. The values of the nonzero constitutive matrices computed are given by

$$\begin{bmatrix} A_{11} & A_{12} & A_{16} \\ A_{12} & A_{22} & A_{26} \\ A_{16} & A_{26} & A_{66} \end{bmatrix} = \begin{bmatrix} 1.76734 & 0.0958898 & 0.272513 \\ 0.0958898 & 0.170273 & 0.0181288 \\ 0.272513 & 0.0181288 & 0.133294 \end{bmatrix} \times 10^{6} \frac{\text{lbs}}{\text{in.}} \tag{109a}$$

$$\begin{bmatrix} D_{11} & D_{12} & D_{16} \\ D_{12} & D_{22} & D_{26} \\ D_{16} & D_{26} & D_{66} \end{bmatrix} = \begin{bmatrix} 1.47278 & 0.0799082 & 0.227094 \\ 0.0799082 & 0.141894 & 0.0151073 \\ 0.227094 & 0.0151073 & 0.111078 \end{bmatrix} \times 10^{3} \text{ in.–lbs} \tag{109b}$$

Similarly, the constitutive expressions defined by equations (15) are given by

$$\begin{bmatrix} \bar{a}_{11} & \bar{a}_{16} \\ \bar{a}_{16} & \bar{a}_{66} \end{bmatrix} = \begin{bmatrix} 0.826304 & -1.6893 \\ -1.6893 & 10.9577 \end{bmatrix} \times 10^{-6} \frac{\text{in.}}{\text{lbs}} \tag{110a}$$

$$\begin{Bmatrix} \bar{\ell}_{12} \\ \bar{\ell}_{62} \end{Bmatrix} = - \begin{Bmatrix} 0.0486091 \\ 0.0366266 \end{Bmatrix} \tag{110b}$$

$$\begin{Bmatrix} \bar{\varepsilon}_{12} \\ \bar{\varepsilon}_{62} \end{Bmatrix} = \begin{Bmatrix} 0.575447 \\ 3.731960 \end{Bmatrix} \times 10^{-4} \text{ in.} \tag{110c}$$

For this anisotropic-wall construction, $S = 4.23574 \times 10^{-5}$ in.$^{-2}$ and $T = 0.529147$ in.$^{-2}$.

Graphs of the normalized radial displacement w/h, bending stress resultant $\frac{M_x}{\tilde{M}_0}$, transverse-shear stress resultant $\frac{Q_x}{\tilde{V}_0}$, and circumferential stress resultant $\frac{N_\theta}{\tilde{V}_0}$ for the cylinders with all 90-degree plies are shown in figures 4-7, respectively, as a function of the axial distance x normalized by the cylinder length L. Two curves appear in each figure that correspond to values of L/R = 0.5 and 2. These results exhibit the common trend in which the effects of the edge loads attenuate as x/L increases, with the longer cylinder exhibiting the larger attenuation rate. Likewise, graphs of the normalized axial displacement u/h, circumferential displacement v/h, radial displacement w/h, bending stress resultant $\frac{M_x}{\tilde{M}_0}$, transverse-shear stress resultant $\frac{Q_x}{\tilde{V}_0}$, and circumferential stress resultant $\frac{N_\theta}{\tilde{V}_0}$ for the cylinders with all 10-degree plies are shown in figures 8-13, respectively, as a function of the normalized axial distance x/L. The results for these cylinders with L/R = 2 also exhibit the expected response-attenuation behavior. It is noteworthy to point out that the response quantities for the shorter cylinder with all 10-degree plies do not attenuate as x/L increases, unlike the corresponding cylinders with all 90-degree plies. This difference in attenuation behavior is due to the higher axial stiffness of the cylinders with all 10-degree plies. The results in figure 9 show relatively small circumferential displacements, as expected, that are generated by the wall anisotropy. For both wall constructions, circumferential stresses (figure 13) are generated that are significantly larger in magnitude than the corresponding value of the applied transverse-shear load. Moreover, the largest magnitude of the circumferential stresses in the cylinders with all 90-degree plies (figure 7) are approximately six times larger than those in the cylinders with all 10-degree plies.

Example 2: Uniform Axial End Load

Another fundamental problem of shell theory is the response-attenuation behavior of a circular cylinder subjected to a uniform axial end load. This problem is particularly important in the study of cylinder buckling. For the corresponding example considered in the present study, the boundary conditions are given by

$$u(0) = 0 \tag{111a}$$

$$v(0) = 0 \tag{111b}$$

$$w(0) = 0 \tag{111c}$$

$$M_x(0) = 0 \tag{111d}$$

at $x = 0$ and

$$N_x(L) = \tilde{N}_L \tag{112a}$$

$$v(L) = 0 \tag{112b}$$

$$w(L) = 0 \tag{112c}$$

$$M_x(L) = 0 \tag{112d}$$

at $x = L$. For these loading conditions, the particular solution given by equation (103) is identically zero-valued.

Results for this example were also obtained for cylinders with radius-to-thickness ratio R/h = 100 and the length-to-radius ratios L/R = 0.5 and 2. Specifically, results are presented in figures 14-19 for cylinders with laminated walls composed of two inner 90-degree plies, two outer 10-degree plies, and a total wall thickness $h = 0.1$ in. This wall construction exhibits the full extent of anisotropy possible in the exact solution; that is, coupling between membrane expansion or contraction and shearing deformations, coupling between pure bending and twisting deformations, and coupling between membrane and bending-twisting deformations. The values of the constitutive matrices that were computed are given by

$$\begin{bmatrix} A_{11} & A_{12} & A_{16} \\ A_{12} & A_{22} & A_{26} \\ A_{16} & A_{26} & A_{66} \end{bmatrix} = \begin{bmatrix} 0.966328 & 0.0727428 & 0.136257 \\ 0.0727428 & 1.01758 & 0.00906441 \\ 0.136257 & 0.00906441 & 0.110147 \end{bmatrix} \times 10^6 \ \frac{\text{lbs}}{\text{in.}} \tag{113a}$$

$$\begin{bmatrix} B_{11} & B_{12} & B_{16} \\ B_{12} & B_{22} & B_{26} \\ B_{16} & B_{26} & B_{66} \end{bmatrix} = \begin{bmatrix} 2.00252 & 0.0578677 & 0.340641 \\ 0.0578677 & -2.11826 & 0.022661 \\ 0.340641 & 0.022661 & 0.0578677 \end{bmatrix} \times 10^4 \ \text{lbs} \tag{113b}$$

$$\begin{bmatrix} D_{11} & D_{12} & D_{16} \\ D_{12} & D_{22} & D_{26} \\ D_{16} & D_{26} & D_{66} \end{bmatrix} = \begin{bmatrix} 8.05273 & 0.60619 & 1.13547 \\ 0.60619 & 8.4798 & 0.0755367 \\ 1.13547 & 0.0755367 & 0.917892 \end{bmatrix} \times 10^2 \ \text{in.–lbs} \tag{113c}$$

Similarly, the constitutive expressions defined by equations (15) are given by

$$\begin{bmatrix} \bar{a}_{11} & \bar{a}_{16} \\ \bar{a}_{16} & \bar{a}_{66} \end{bmatrix} = \begin{bmatrix} 1.25506 & -1.5559 \\ -1.5559 & 10.9932 \end{bmatrix} \times 10^{-6} \frac{\text{in.}}{\text{lbs}} \tag{114a}$$

$$\begin{Bmatrix} \bar{\ell}_{12} \\ \bar{\ell}_{62} \end{Bmatrix} = \begin{Bmatrix} -0.0771401 \\ 0.0131601 \end{Bmatrix} \tag{114b}$$

$$\begin{Bmatrix} \bar{e}_{12} \\ \bar{e}_{62} \end{Bmatrix} = -\begin{Bmatrix} 1.98063 \\ 0.64773 \end{Bmatrix} \times 10^{-2} \text{ in.} \tag{114c}$$

For this laminate, S = 0.119157 in.$^{-2}$ and T = 2.55869 in.$^{-2}$.

Graphs of the normalized axial displacement u/h, radial displacement w/h, bending stress resultants $\frac{M_x}{\tilde{N}_L h}$ and $\frac{M_\theta}{\tilde{N}_L h}$, twisting stress resultant $\frac{M_{x\theta}}{\tilde{N}_L h}$, and circumferential stress resultant $\frac{N_\theta}{\tilde{N}_L}$ are shown in figures 14-19, respectively, as a function of the axial distance x normalized by the cylinder length L. Two pairs of blue and red curves appear in each figure that correspond to values of L/R = 0.5 and 2. The red curves correspond to an approximate solution, given in Appendix C, that is based on the equations of linear membrane theory, in which the bending boundary layer is ignored such that the radial displacement is presumed to be constant valued. In the figures with only one red curve, the curve corresponds to both values of L/R. For all results, a value of $\tilde{N}_L = 1000$ lbs/in. was used for the end load. The blue curves correspond to exact solution presented herein.

The results in figure 14 show a nearly linear variation in the axial displacement, with the largest displacements being exhibited by the longer cylinder. Moreover, the results indicate that the approximate solution yields nearly the same results as the exact solution for both values of L/R. The normalized axial displacements at x = L were computed as u/h = 0.216 and 0.060 for L/R = 2 and 0.5, respectively. In contrast, the results in figures 15-19 show the presence of bending boundary layers in the longer cylinders with L/R = 2 that attenuate to the approximate solution, as expected, at distances from the cylinder ends that are about 10% of the cylinder length. The results also indicate that most of the the response quantities for the shorter cylinders with L/R = 0.5 do not exhibit zones of bending attenuation and, as a result, the approximate solution is inadequate for estimating the interior response of the cylinders. The normalized radial displacements at x = L/2 were computed as w/h = -0.007 and -0.004 for L/R = 2 and 0.5, respectively.

Example 3: Uniform Temperature and Internal Pressure Fields

A very practical problem of shell theory deals with the behavior of a circular cylinder subjected to uniform internal pressure and different, uniform internal and external temperature fields. For the corresponding example considered herein, the boundary conditions are given by

$$u(0) = 0 \tag{115a}$$

$$v(0) = 0 \tag{115b}$$

$$w(0) = 0 \tag{115c}$$

$$\beta_x^\circ(0) = 0 \tag{115d}$$

at $x = 0$ and

$$u(L) = 0 \tag{116a}$$

$$v(L) = 0 \tag{116b}$$

$$w(L) = 0 \tag{116c}$$

$$\beta_x^\circ(L) = 0 \tag{116d}$$

at $x = L$. Thus, the cylinder is completely clamped around the circumference at each end. The applied internal pressure given by $q_n(x) = q_n^0 = 100$ psi and the applied thermal load is given by an external temperature increase $\Delta T_0 = 300$ °F and an internal temperature increase $\Delta T_i = 100$ °F. From equations (B16) and (97) it follows that $\Theta_0(x) = H_0 = 200$ °F and $\Theta_1(x) = G_0 = 2000$ °F/in. For these loading conditions, the particular solution given by equation (103) reduces to

$$\overline{w}_p(x) = \overline{w}_p^0 = \frac{Y_0}{4T^2} \tag{117a}$$

where Y_0 given by equation (102b) reduces to

$$Y_0 = \frac{1}{D_{11}\,e}\Big[q_n^0 + \frac{H_0}{R}\Big(n_\theta^{Th} - n_x^{Th}\Big(A_{12}\bar{a}_{11} + \overline{A}_{26}\bar{a}_{16}\Big) - \bar{n}_{x\theta}^{Th}\Big(A_{12}\bar{a}_{16} + \overline{A}_{26}\bar{a}_{66}\Big)\Big) + \frac{G_0}{R}\Big(c_\theta^{Th} - c_x^{Th}\Big(A_{12}\bar{a}_{11} + \overline{A}_{26}\bar{a}_{16}\Big) - \bar{c}_{x\theta}^{Th}\Big(A_{12}\bar{a}_{16} + \overline{A}_{26}\bar{a}_{66}\Big)\Big)\Big] \tag{117b}$$

For this example, results were obtained for cylinders with radius-to-thickness ratio $R/h = 100$ and the length-to-radius ratios $L/R = 0.5$ and 2. Selected results are presented in figures 20-27 for the previous generally anisotropic cylinders with laminated walls composed of two inner 90-degree plies, two outer 10-degree plies, and a total wall thickness $h = 0.1$ in. The values of the

constitutive matrices computed are given by equations (113) and (114) and, as before, S = 0.119157 in.$^{-2}$ and T = 2.55869 in.$^{-2}$. The values of the thermal constitutive parameters in equation (B17) that were computed are given by

$$\begin{Bmatrix} n_x^{Th} \\ n_\theta^{Th} \\ n_{x\theta}^{Th} \end{Bmatrix} = \begin{Bmatrix} 2.00154 \\ 1.9587 \\ -0.121494 \end{Bmatrix} \frac{\text{lbs}}{^0\text{F–in.}} \tag{118a}$$

$$\begin{Bmatrix} c_x^{Th} \\ c_\theta^{Th} \\ c_{x\theta}^{Th} \end{Bmatrix} = \begin{Bmatrix} -0.0172256 \\ 0.0172256 \\ -0.00303735 \end{Bmatrix} \frac{\text{lbs}}{^0\text{F}} \tag{118b}$$

$$\begin{Bmatrix} m_x^{Th} \\ m_\theta^{Th} \\ m_{x\theta}^{Th} \end{Bmatrix} = \begin{Bmatrix} 0.00166795 \\ 0.00163225 \\ -0.000101245 \end{Bmatrix} \frac{\text{in.–lbs}}{^0\text{F}} \tag{118c}$$

Graphs of the normalized axial displacement u/h, circumferential displacement v/h, radial displacement w/h, circumferential stress resultant $\frac{N_\theta}{q_n^0 R + N_\theta^{Th}}$, bending stress resultants $\frac{M_x}{\left(q_n^0 R + N_\theta^{Th}\right)h}$ and $\frac{M_\theta}{\left(q_n^0 R + N_\theta^{Th}\right)h}$, twisting stress resultant $\frac{M_{x\theta}}{\left(q_n^0 R + N_\theta^{Th}\right)h}$, and transverse-shear stress resultant $\frac{Q_x}{q_n^0 R + N_\theta^{Th}}$ are shown in figures 20-27, respectively, as a function of the axial distance x normalized by the cylinder length L. Two pairs of blue curves and coincident red lines appear in each figure that correspond to values of L/R = 0.5 and 2. The red lines correspond to an approximate solution given in Appendix D that is based on the equations of linear membrane theory, in which the bending boundary layer is ignored such that the radial displacement is presumed to be constant valued.

The results in figures 20 and 21 show relatively small-magnitude antisymmetric distributions of the axial and circumferential displacements that attenuate to a value of zero in the central region of the cylinders, with the larger magnitudes occuring near the ends. The corresponding displacements predicted by the approximate solution are zero valued, as indicated by the red line in each figure. The exact solution gives the constant values N_x = -288.68 lbs/in. and -270.10 lbs/in. for the cylinders with L/R = 0.5 and 2, respectively. In addition, the exact solution gives the constant values $\hat{T}$ = 40.15 lbs/in. and 42.47 lbs/in. for the cylinders with L/R = 0.5 and 2, respectively. The approximate solution gives N_x = -263.90 lbs/in. and $\hat{T}$ = 43.25 lbs/in., regardless of the value for L/R.

The results in figures 22-27 show the presence of bending boundary layers in the longer cylinders with L/R = 2 that attenuate to the approximate solution, as expected, at distances from the cylinder ends that are about 10% of the cylinder length. The results also indicate that most of the response quantities for the shorter cylinder with L/R = 0.5 exhibit small centrally located zones of attenuation and, as a result, the approximate solution is inadequate for estimating the interior response of these cylinders. The approximate solution yields the values w/h = 0.14,

$$\frac{N_\theta}{q_n^0 R + N_\theta^{Th}} = 0.701, \quad \frac{M_x}{\left(q_n^0 R + N_\theta^{Th}\right)h} = 0.006, \quad \frac{M_\theta}{\left(q_n^0 R + N_\theta^{Th}\right)h} = -0.255, \text{ and}$$

$$\frac{M_{x\theta}}{\left(q_n^0 R + N_\theta^{Th}\right)h} = 0.008 \text{ with } N_\theta^{Th} = 426.19 \text{ lbs/in.}$$

The values agree well with the exact solution in the central, attenuated region of the longer cylinders. However, even in the central region of the shorter cylinders, there are significant differences between the approximate and exact solutions for several of these quantities.

Example 4: Linearly Varying Temperature and Internal Pressure Fields

This example corresponds to cylinder proportions and loading conditions that are typical of a large-scale launch vehicle. Specifically, a circular cylinder subjected to an axial end load, an end circumferential shear load, a linearly varying internal pressure field, associated with a liquid fuel, and different, linearly varying internal and external temperature fields. For this example, the boundary conditions specified in the present study are

$$N_x(0) = \tilde{N}_0 \tag{119a}$$

$$\hat{T}(0) = \tilde{T}_0 \tag{119b}$$

$$w(0) = 0 \tag{119c}$$

$$M_x(0) = 0 \tag{119d}$$

at $x = 0$ and

$$u(L) = 0 \tag{120a}$$

$$v(L) = 0 \tag{120b}$$

$$w(L) = 0 \tag{120c}$$

$$M_x(L) = 0 \tag{120d}$$

at $x = L$. The values of the applied end loads used in the present example are given by $\tilde{N}_0 = 1000$ lbs/in. and $\tilde{T}_0 = 200$ lbs/in. The applied pressure load is given by $q_n(x) = p_u + \gamma(L - x)$, where p_u = 30 psi represents an ullage pressure and $\gamma = 0.04123$ lb/in.^{3} is the specific weight of the fluid inside the cylinder. Thus, equation (96c) reduces to $q_n(x) = q_n^0 + q_n^1 x$, where $q_n^0 = p_u + \gamma L$ and $q_n^1 = -\gamma$. The applied thermal load is given by an external temperature rise $\Delta T_0(x) = -500 + 100\, x/L$ °F and an internal temperature rise $\Delta T_i(x) = -500 + 50\, x/L$ °F. From equations (B16) and (97) it follows that, $\Theta_0(x) = H_0 + H_1 x$ and $\Theta_1(x) = G_0 + G_1 x$, where $H_0 = -500$ °F, $G_0 = 0$ °F/in., $H_1 = 75/L$ °F/in., and $G_1 = 50/(hL)$ °F/in.^{2}. For these loading conditions, the particular solution given by equation (103) reduces to $\bar{w}_p(x) = \bar{w}_p^0 + \bar{w}_p^1 x$, where $\bar{w}_p^0 = \frac{Y_0}{4T^2}$ and $\bar{w}_p^1 = \frac{Y_1}{4T^2}$. In addition, Y_0 and Y_1, given by equations (102), reduce to

$$Y_0 = \frac{1}{D_{11}\,e}\Big[q_n^0 + \frac{H_0}{R}\Big(n_\theta^{Th} - n_x^{Th}\big(A_{12}\bar{a}_{11} + \bar{A}_{26}\bar{a}_{16}\big) - \bar{n}_{x\theta}^{Th}\big(A_{12}\bar{a}_{16} + \bar{A}_{26}\bar{a}_{66}\big)\Big) + \frac{G_0}{R}\Big(c_\theta^{Th} - c_x^{Th}\big(A_{12}\bar{a}_{11} + \bar{A}_{26}\bar{a}_{16}\big) - \bar{c}_{x\theta}^{Th}\big(A_{12}\bar{a}_{16} + \bar{A}_{26}\bar{a}_{66}\big)\Big)\Big] \tag{121a}$$

and

$$Y_1 = \frac{1}{D_{11}\,e}\Big[q_n^1 + \frac{H_1}{R}\Big(n_\theta^{Th} - n_x^{Th}\big(A_{12}\bar{a}_{11} + \bar{A}_{26}\bar{a}_{16}\big) - \bar{n}_{x\theta}^{Th}\big(A_{12}\bar{a}_{16} + \bar{A}_{26}\bar{a}_{66}\big)\Big) + \frac{G_1}{R}\Big(c_\theta^{Th} - c_x^{Th}\big(A_{12}\bar{a}_{11} + \bar{A}_{26}\bar{a}_{16}\big) - \bar{c}_{x\theta}^{Th}\big(A_{12}\bar{a}_{16} + \bar{A}_{26}\bar{a}_{66}\big)\Big)\Big] \tag{121b}$$

For this example, results were obtained for cylinders with radius-to-thickness ratio R/h = 330 and the length-to-radius ratios L/R = 0.5 and 2. Selected results are presented in figures 28-35 for the previously considered generally anisotropic cylinders with laminated walls composed of two inner 90-degree plies, two outer 10-degree plies, but with a total wall thickness h = 0.5 in. The values of the constitutive matrices computed are given by

$$\begin{bmatrix} A_{11} & A_{12} & A_{16} \\ A_{12} & A_{22} & A_{26} \\ A_{16} & A_{26} & A_{66} \end{bmatrix} = \begin{bmatrix} 4.83164 & 0.363714 & 0.681283 \\ 0.363714 & 5.08788 & 0.045322 \\ 0.681283 & 0.045322 & 0.550735 \end{bmatrix} \times 10^6 \ \frac{\text{lbs}}{\text{in.}} \tag{122a}$$

$$\begin{bmatrix} B_{11} & B_{12} & B_{16} \\ B_{12} & B_{22} & B_{26} \\ B_{16} & B_{26} & B_{66} \end{bmatrix} = \begin{bmatrix} 5.00630 & 0.144669 & 0.851603 \\ 0.144669 & -5.29564 & 0.0566525 \\ 0.851603 & 0.0566525 & 0.144669 \end{bmatrix} \times 10^{5} \text{ lbs} \tag{122b}$$

$$\begin{bmatrix} D_{11} & D_{12} & D_{16} \\ D_{12} & D_{22} & D_{26} \\ D_{16} & D_{26} & D_{66} \end{bmatrix} = \begin{bmatrix} 100659 & 7577.37 & 14193.4 \\ 7577.37 & 105997 & 944.209 \\ 14193.4 & 944.209 & 11473.7 \end{bmatrix} \text{ in.–lbs} \tag{122c}$$

and the constitutive expressions defined by equations (15) are given by

$$\begin{bmatrix} \bar{a}_{11} & \bar{a}_{16} \\ \bar{a}_{16} & \bar{a}_{66} \end{bmatrix} = \begin{bmatrix} 2.50793 & -3.10445 \\ -3.10445 & 2.19917 \end{bmatrix} \times 10^{-6} \frac{\text{in.}}{\text{lbs}} \tag{123a}$$

$$\begin{Bmatrix} \bar{\ell}_{12} \\ \bar{\ell}_{62} \end{Bmatrix} = \begin{Bmatrix} -0.0771309 \\ 0.0131291 \end{Bmatrix} \tag{123b}$$

$$\begin{Bmatrix} \bar{z}_{12} \\ \bar{z}_{62} \end{Bmatrix} = -\begin{Bmatrix} 0.0990770 \\ 0.0321475 \end{Bmatrix} \text{ in.} \tag{123c}$$

The values of S and T, defined by equations (27) and (39), respectively, that are used to determine the basis functions of the solution space were found to be given by $S = 0.001444$ in.$^{-2}$ and $T = 0.031012$ in.$^{-2}$, and the values of the thermal constitutive parameters in equation (B17) are given by

$$\begin{Bmatrix} n_x^{Th} \\ n_\theta^{Th} \\ n_{x\theta}^{Th} \end{Bmatrix} = \begin{Bmatrix} 10.0077 \\ 9.79348 \\ -0.607469 \end{Bmatrix} \frac{\text{lbs}}{^0\text{F–in.}} \tag{124a}$$

$$\begin{Bmatrix} c_x^{Th} \\ c_\theta^{Th} \\ c_{x\theta}^{Th} \end{Bmatrix} = \begin{Bmatrix} -0.430641 \\ 0.430641 \\ -0.0759336 \end{Bmatrix} \frac{\text{lbs}}{^0\text{F}} \tag{124b}$$

$$\begin{Bmatrix} m_x^{Th} \\ m_\theta^{Th} \\ m_{x\theta}^{Th} \end{Bmatrix} = \begin{Bmatrix} 0.208494 \\ 0.204031 \\ -0.0126556 \end{Bmatrix} \frac{\text{in.–lbs}}{^0\text{F}} \tag{124c}$$

Graphs of the normalized axial displacement u/h, circumferential displacement v/h, radial

displacement w/h, circumferential stress resultant $\frac{N_\theta}{(p_u + \gamma L)R}$, bending stress resultants $\frac{M_x}{(p_u + \gamma L)Rh}$ and $\frac{M_\theta}{(p_u + \gamma L)Rh}$, twisting stress resultant $\frac{M_{x\theta}}{(p_u + \gamma L)Rh}$, and transverse-shear stress resultant $\frac{Q_x}{(p_u + \gamma L)R}$ are shown in figures 28-35, respectively, as a function of the axial distance x normalized by the cylinder length L. The denominator term $p_u + \gamma L$ represents the maximum pressure in the cylinder. Two pairs of blue and red curves appear in each figure that correspond to values of L/R = 0.5 and 2. The red curves correspond to an approximate solution given in Appendix E that is found by applying the equations of linear membrane theory, ignoring the bending boundary layer and presuming that the radial displacements vary like the pressure and temperature fields. In the figures with only one red curve, the curve corresponds to both values of L/R.

The results in figures 28 and 29 show a nearly linear variation in the axial and circumferential displacements, respectively, with the largest displacement magnitudes being exhibited by the longer cylinder. Moreover, the results indicate that the approximate solution yields nearly the same results as the exact solution for both values of L/R. In contrast, the results in figures 30-35 show the presence of bending boundary layers that attenuate to the linearly varying approximate solution at distances from the cylinder ends that are about 10% and 20% of the cylinder length for L/R = 2 and 0.5, respectively. The linear variation in the response quantities is generally more pronounced in the longer cylinders because the pressure increases with increasing cylinder length.

Example 5: Sinusoidal Pressure and Temperature Fields

This example illustrates the behavior of a circular cylinder subjected to sinusoidal internal pressure and different, sinusoidal internal and external temperature fields. The cylinder is fixed at one end and free to expand axially and twist circumferentially at the other end. The corresponding boundary conditions specified in the present study are

$$u(0) = 0 \tag{125a}$$

$$v(0) = 0 \tag{125b}$$

$$w(0) = 0 \tag{125c}$$

$$\beta_x^\circ(0) = 0 \tag{125d}$$

at $x = 0$ and

$$N_x(0) = 0 \tag{126a}$$

$$\hat{T}(0) = 0 \tag{126b}$$

$$w(L) = 0 \tag{126c}$$

$$\beta_x^{\circ}(L) = 0 \tag{126d}$$

at $x = L$. The applied mechanical load given by $q_n(x) = q_n^s \sin\left(\frac{\pi x}{L}\right)$, where $q_n^s = 1000$ psi. The applied thermal load is given by an external temperature rise $\Delta T_0(x) = 300 \sin(\pi x/L)$ °F and an internal temperature rise $\Delta T_i(x) = 100 \sin(\pi x/L)$ °F. Equations (B16) and (97) give $\Theta_0(x) = H_s \sin(\pi x/L)$ and $\Theta_1(x) = G_s \sin(\pi x/L)$ where $H_s = 200$ °F and $G_s = 200/h$ °F/in. For these loading conditions, the particular solution given by equation (103) reduces to

$$\overline{w}_p(x) = \overline{w}_p^{s1} \sin\left(\frac{\pi x}{L}\right) \tag{127}$$

where $\overline{w}_p^{s1}$ is given by equation (104d).

For this example, results were obtained for cylinders with radius-to-thickness ratio $R/h = 100$ and the length-to-radius ratios $L/R = 0.5$ and 2. Selected results are presented in figures 36-45 for generally anisotropic cylinders with laminated walls composed of two inner 90-degree plies, two outer 10-degree plies, and a total wall thickness $h = 0.1$ in. The values of the constitutive matrices are given by equations (113) and (114), and the values of the thermal constitutive parameters in equation (B17) are given by equations (118). Like before, $S = 0.119157$ in.$^{-2}$ and $T = 2.55869$ in.$^{-2}$.

Graphs of the normalized axial displacement u/h, circumferential displacement v/h, and radial displacement w/h are shown in figures 36-38, respectively, as a function of the axial distance x normalized by the cylinder length L, and the axial rotation β_x^0 is shown in figure 39 as a function of x/L. Graphs of the normalized circumferential stress resultant $\frac{N_\theta}{\overline{N}_\theta}$, bending stress resultants $\frac{M_x}{\overline{M}_x}$ and $\frac{M_\theta}{\overline{M}_\theta}$, twisting stress resultant $\frac{M_{x\theta}}{\overline{M}_x}$, and transverse-shear stress resultants $\frac{Q_x h}{\overline{M}_x}$ and $\frac{Q_\theta h}{\overline{M}_x}$ are shown in figures 40-45, respectively, as a function of x/L. In these nondimensional quantities, $\overline{N}_\theta$ is given by equation (F10b), $\overline{M}_x$ is given by equation (F7b), and $\overline{M}_\theta$ is given by equation (F11b). One blue curve and one red curve is shown in each part of the

two-part figures. The red curves correspond to a simplified exact trigonometric solution, given in Appendix F, for the corresponding cylinder with simply supported ends instead of clamped ends. The blue curves represent the exact solution obtained herein.

The results in figures 36-45 show that the difference between the exact solution (blue response curves) for the cylinders with rotation restrained at the ends and the exact trigonometric solution for simply supported ends is much smaller for the cylinders with L/R = 2 than for those with L/R = 0.5, as expected. For the longer cylinders, significant differences between most of the corresponding response curves appear to be confined to edge zones that are about 10% of the cylinder length. For the shorter cylinders, the zones of significant difference grow to about 20% of the cylinder length. For both cylinder lengths, the greatest overall discrepancies between the exact and corresponding trigonometric solutions are exhibted by the axial displacements and the bending stress resultant M_x.

Concluding Remarks

A detailed exact solution has been presented for generally laminated circular cylinders that undergo axisymmetric deformations. The cylinders exhibit the full range of anisotropy that is possible in first-approximation shell theories that neglect high-order effects such as transverse-shear deformation. The overall solution has been formulated in a general, systematic way and is based on the solution of a single fourth-order, nonhomogeneous ordinary differential equation with constant coefficients in which the radial displacement is the dependent variable. Moreover, positive-definiteness of the strain energy has been used to define uniquely the form of the basis functions spanning the solution space of the ordinary differential equation. This approach appears to be a unique feature of the analysis presented herein.

Axisymmetric loading conditions have been considered that include edge loads, surface tractions, and temperature fields. In addition, all possible corresponding boundary conditions have been considered, and several particular solutions to the fourth-order, nonhomogeneous ordinary differential equation governing the response have been presented. Results have been presented for five examples that demonstrate a wide range of behavior. Several of the results illustrate how laminated-wall construction and cylinder length affect the size of localized zones of bending deformations that occur near the cylinder ends. For some of the examples, the results indicate highly localized bending deformations that attenuate rapidly. For other examples, the bending deformations exhibit very little attenuation. In addition, approximate solutions for several of the examples have been presented that add credibility to the corresponding results obtained from the exact solution and that provide insight into the possible pitfalls of making certain types of simplifications in a preliminary-design process. For example, several results are presented that illustrate conditions for which sizing a laminated-composite cylinder based on an approximate linear membrane analysis is inappropriate.

Results obtained from the exact solution presented herein also have the potential to serve as fundamental benchmarks for the validation of numerical solution methods such as the finite-element method. Likewise, results obtained from the exact solution have the potential to provide

insight into the extent of discretization that might be needed for analyzing accurately shells with zones of localized bending caused by cutouts, stiffeners, or other types of discontinuities and gradients.

References

1. Dong, S. B.; Pister, K.. S.; and Taylor, R. L.: On the Theory of Laminated Anisotropic Shells and Plates. *Journal of the Aerospace Sciences*, vol. 29, no. 8, 1962, pp. 969-975.

2. Brush, D. O.; and Almroth, B.: *Buckling of Bars, Plates, and Shells*. McGraw-Hill, 1975.

3. Gulati, S. T.; and Essenburg, F.: Effects of Anisotropy in Axisymmetric Cylindrical Shells. *Journal of Applied Mechanics*, vol. 34, September, 1967, pp. 659-666.

4. Stavsky, Y.; and Smolash, I.: Thermoelasticity of Heterogeneous Orthotropic Cylinders. *International Journal of Solids and Structures*, vol. 6, 1970, pp. 1211-1231.

5. Vicario, A. A.; and Rizzo, R. R.: Effect of Length on Laminated Thin Tubes Under Combined Loading. *Journal of Composite Materials*, vol. 4, 1970, pp. 273-277.

6. Reuter, R. C., Jr.: Analysis of Shells Under Internal Pressure. *Journal of Composite Materials*, Vol. 6, 1972, pp. 94-113.

7. Hennemann, J. C. F.: Effect of Prebuckling Deformations on Buckling of Laminated Composite Circular Cylindrical Shells. Ph. D. Dissertation, Civil and Mechanical Engineering Dept., Southern Methodist University, Dallas, Texas, 1975.

8. Jones, R. M.; and Hennemann, J. C. F.: Effect of Prebuckling Deformations on Buckling of Laminated Composite Circular Cylindrical Shells. *Proceedings of the AIAA/ASME 19th Structures, Structural Dynamics, and Materials Conference*, Bethesda, Maryland, April 3-5, 1978, pp. 370-379.

9. Cheng, S.; and He, F. B.: Theory of Orthotropic and Composite Cylindrical Shells, Accurate and Simple Fourth-Order Governing Equations. *Journal of Applied Mechanics*, vol. 51, 1984, pp. 736-744.

10. Flügge, W.: *Stresses in Shells*, Springer-Verlag, Berlin, 1967.

11. Chaudhuri, R. A.; Balaraman, K.; and Kunukkasseril, V. X.: Arbitrarily Laminated, Anisotropic Cylindrical Shell Under Internal Pressure. *AIAA Journal*, vol. 24, no. 11, 1986, pp. 1851-1858.

12. Kraus, H.: *Thin Elastic Shells - An Introduction to the Theoretical Foundations and the Analysis of Their Static and Dynamic Behavior,* John Wiley and Sons, Inc., 1967.

13. Timoshenko, S. P.; and Gere, J. M.: *Theory of Elastic Stability*. Second ed., McGraw-Hill, 1961.

14. Abu-Arja, K. R.; and Chaudhuri, R. A.: Moderately Thick Angle-ply Cylindrical Shells Under Internal Pressure. *Journal of Applied Mechanics*, vol. 56, 1989, pp. 652-657.

15. Butler, T. A.; and Hyer, M. W.: The Structural Response of Unsymmetrically Laminated Composite Cylinders. Dept. of Mechanical Engineering, Technical Report 89-2, The University of Maryland, August 1989.

16. Hyer, M. W.; and Paraska, P. J., "Innovative Design of Composite Structures: Axisymmetric Deformations of Unsymmetrically Laminated Cylinders Loaded in Axial Compression," Dept. of Engineering Science and Mechanics, VPI-E-90-10 Report, VA Tech, June 1990.

17. Paraska, P. J.: Axisymmetric Deformations and Stresses of Unsymmetrically Laminated Composite Cylinders in Axial Compression with Thermally-Induced Preloading Effects. CARDEROCKDIV-U-SSM-65-93/03, Carderock Division, Naval Surface Warfare Center, March 1993.

18. Birman, V.: Thermal Bending of Shear-Deformable Orthotropic Cylindrical Shells Reinforced by Cylindrically-Orthotropic Rings. *International Journal of Solids and Structures*, vol. 28, no. 7, 1991, pp. 819-830.

19. Birman, V.: Exact Solution of Axisymmetric Problems of Laminated Cylindrical Shells with Arbitrary Boundary Conditions - Higher-Order Theory. *Mechanics Research Communications*, vol. 19, no. 3, 1992, pp. 219-225.

20. Birman, V.: Axisymmetric Bending of Generally Laminated Cylindrical Shells. *Journal of Applied Mechanics*, vol. 60, 1993, pp. 157-162.

21. Vinson, J. R.: Composite Shell Structures and Their Behavior. *Proceedings of the AIAA/ ASME/ASCE/AHS/ASC 38th Structures, Structural Dynamics, and Materials Conference*, Kissimmee, Florida, April 7-10, 1997, pp. 2400-2406.

22. McDevitt, T. J.; and Simmonds, J. G.: Reduction of the Sanders-Koiter Equations for Fully Anisotropic Circular Cylindrical Shells to Two Coupled Equations for a Stress and a Curvature Function. *Journal of Applied Mechanics*, vol. 66, September, 1999, pp. 593-597.

23. Goldenveizer, A. L.: *Theory of Thin Elastic Shells*, Pergamon, New York, 1961.

24. Sanders, J. L., Jr.: *An Improved First-Approximation Theory for Thin Shells*. NASA TR R-24, 1959.

25. Koiter, W. T.: A Consistent First Approximation in the General Theory of Thin Elastic Shells. *The Theory of Thin Elastic Shells, Proceedings of the IUTAM Symposium*, Delft, North-Holland, Amsterdam, The Netherlands, 1960, pp. 12-33.

26. Nemeth, M. P.; and Smeltzer, S. S., III: *Bending Boundary Layers in Laminated-Composite Circular Cylindrical Shells*. NASA/TP-2000-210549, 2000.

27. Paris, A. J.; and Costello, G. A.: Bending of Cord Composite Cylindrical Shells. *Journal of Applied Mechanics*, vol. 67, March, 2000, pp. 117-127.

28. Ye, J.: Decay Rate of Edge Effects in Cross-Ply-Laminated Hollow Cylinders. *International Journal of Mechanical Sciences*, vol. 43, 2001, pp. 455-470.

29. Ye, J.: Edge Effects in Angle-Ply Laminated Hollow Cylinders. *Composite Structures,* vol. 52, 2001, pp. 247-253.

30. Bhaskar, K.; and Balasubramanyam, G.: Accurate Analysis of End-Loaded Laminated Orthotropic Cylindrical Shells. *Composite Structures*, vol. 58, 2002, pp. 209-216.

31. Paris, A. J.; and Costello, G. A.: Bending of Cord Composite Laminate Cylindrical Shells. *Journal of Applied Mechanics*, vol. 70, May 2003, pp. 364-373.

32. Kollar, L. P.; and Springer, G. S.: *Mechanics of Composite Structures*. Cambridge University Press, 2003, pp. 368-380.

33. *Standard Mathematical Tables and Formulae*, D. Zwillinger, ed., CRC Press, 1996.

34. Jones, R. M.: *Mechanics of Composite Materials,* Second ed., Taylor and Francis, 1999.

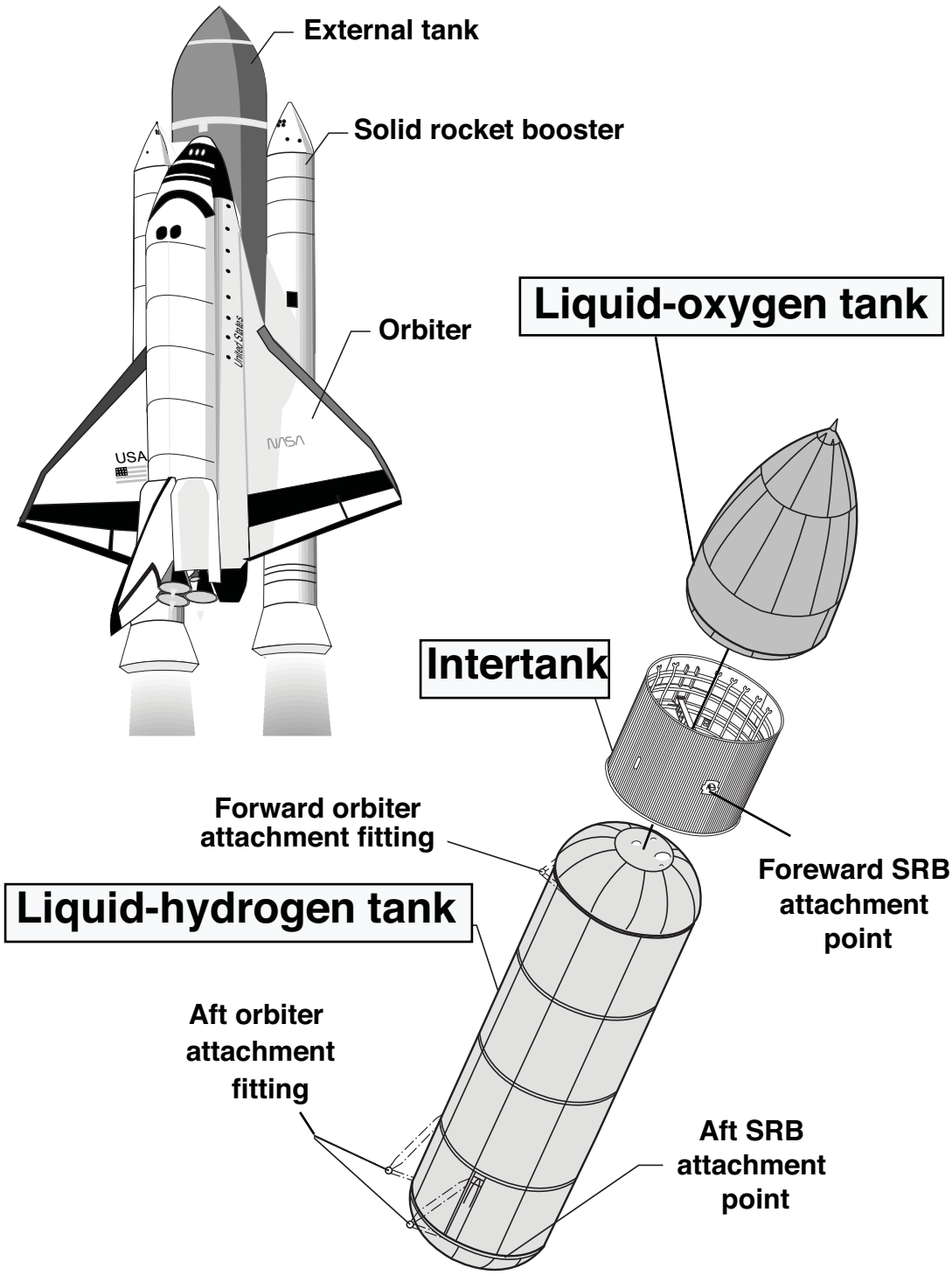

Figure 1. Space Shuttle external tank components.

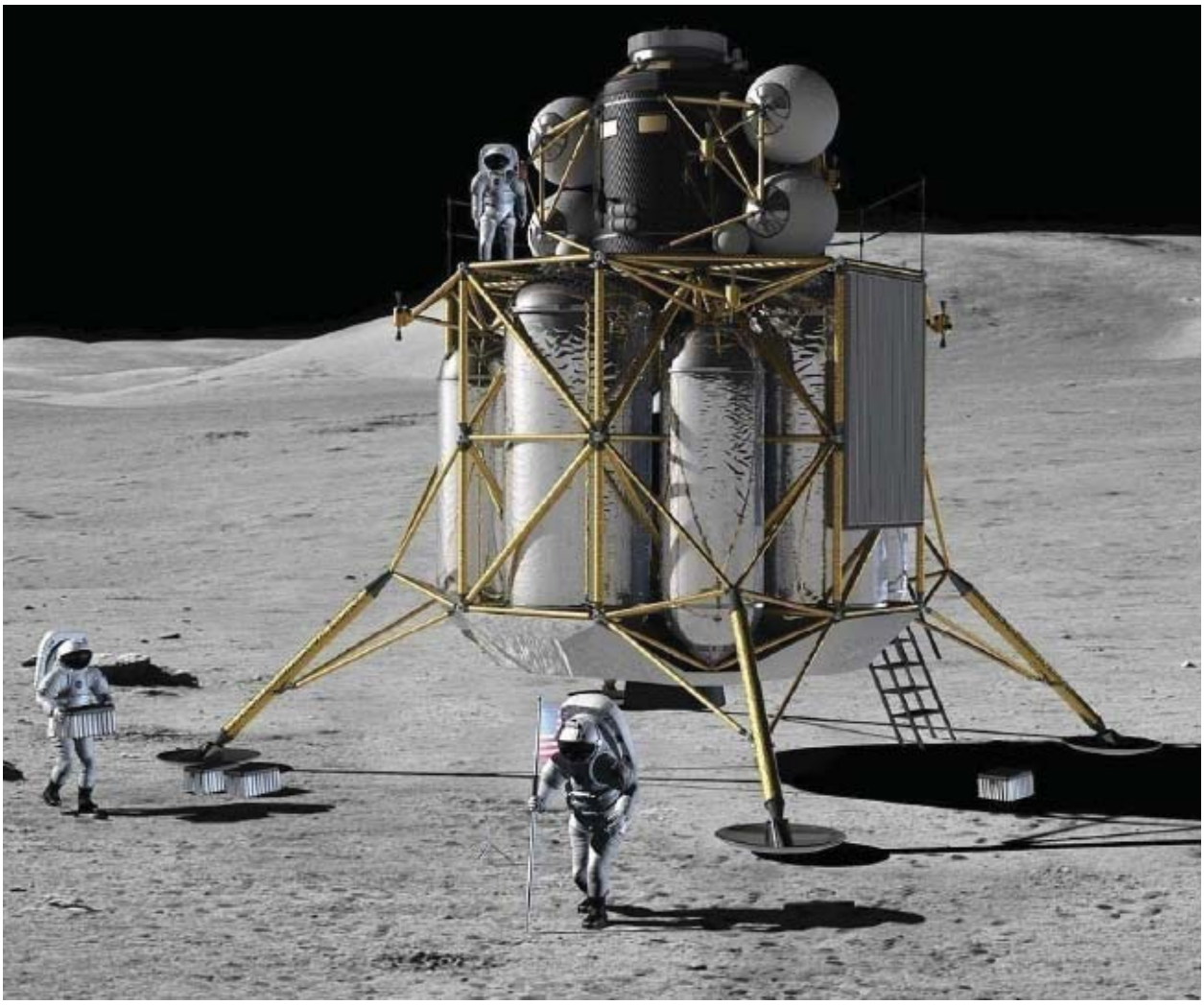

Figure 2. Conceptual lunar lander.

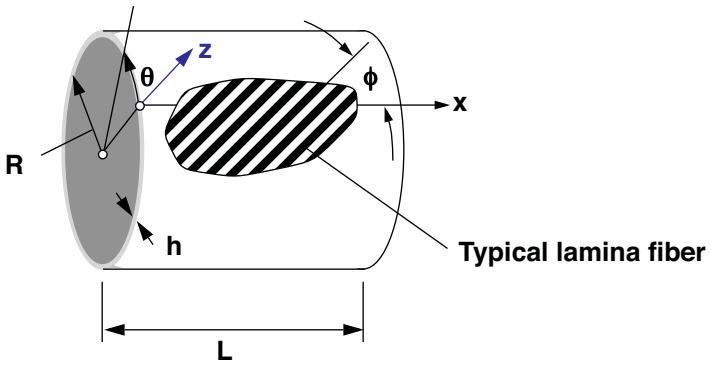

Figure 3. Cylinder geometry, surface coordinate system, and lamina fiber orientation.

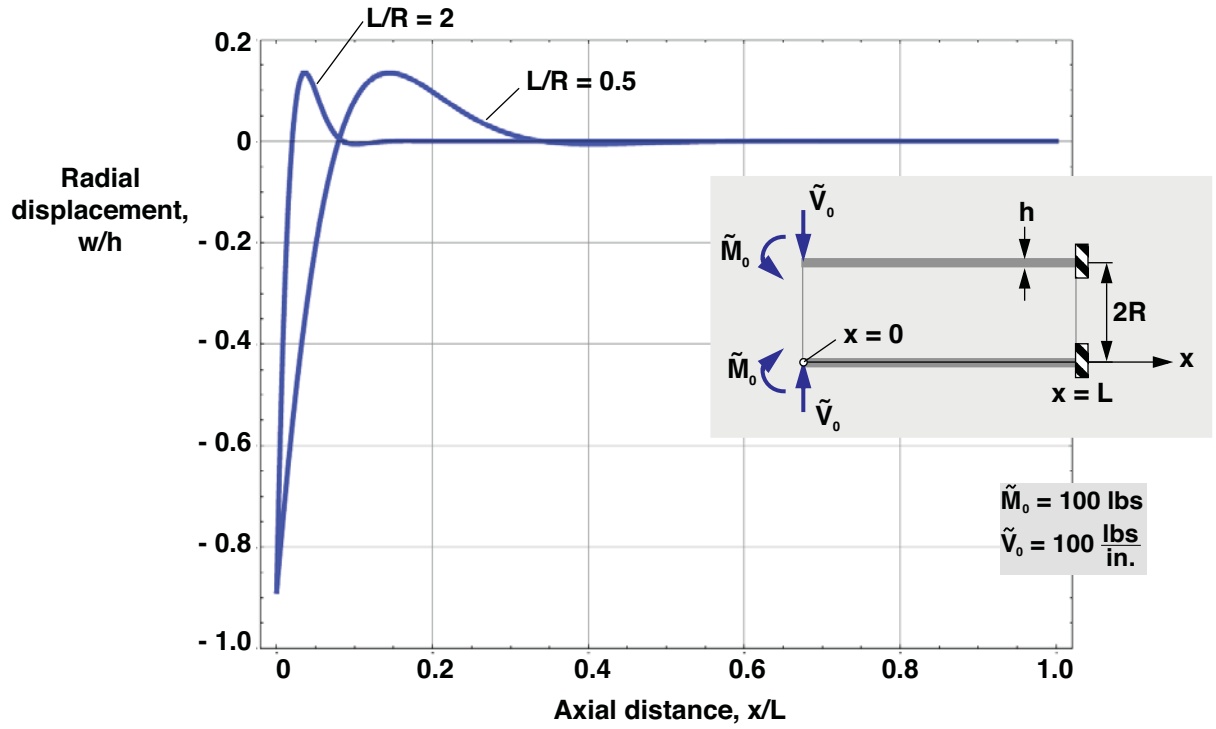

Figure 4. Radial displacement of laminated cylinder with all 90-deg plies, subjected to edge loads at x = 0, and clamped at x = L (R/h = 100).

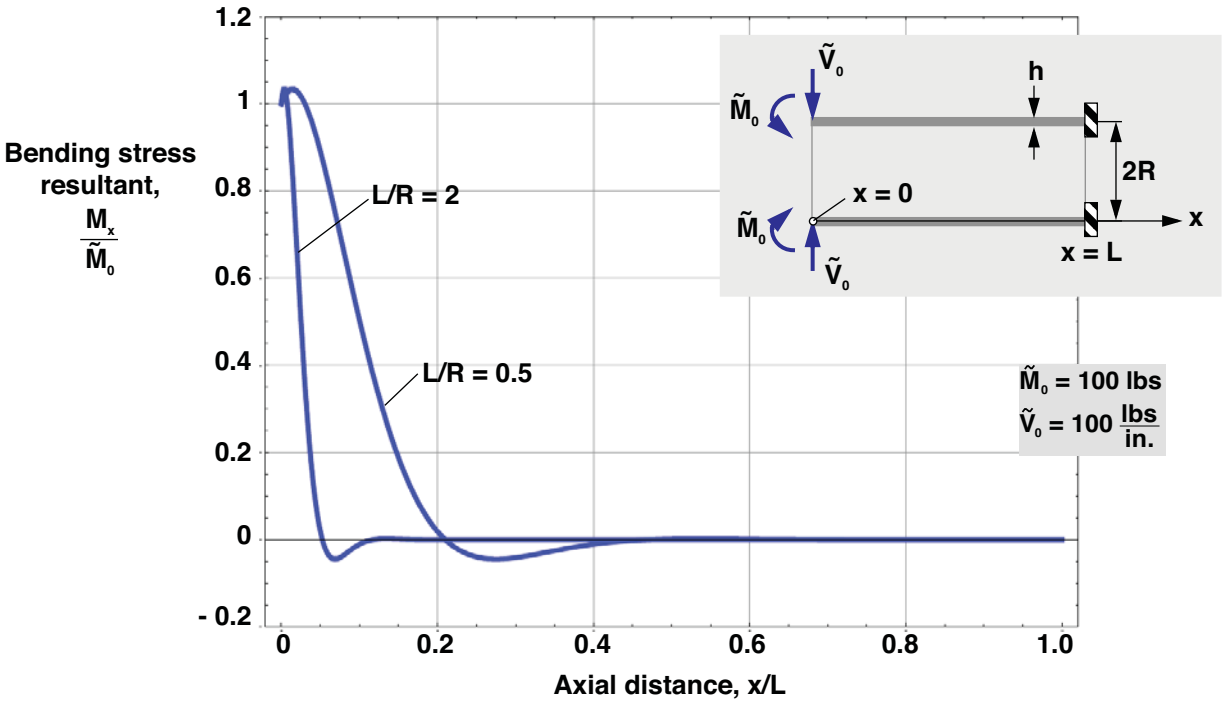

Figure 5. Bending stress resultant for laminated cylinder with all 90-deg plies, subjected to edge loads at x = 0, and clamped at x = L (R/h = 100).

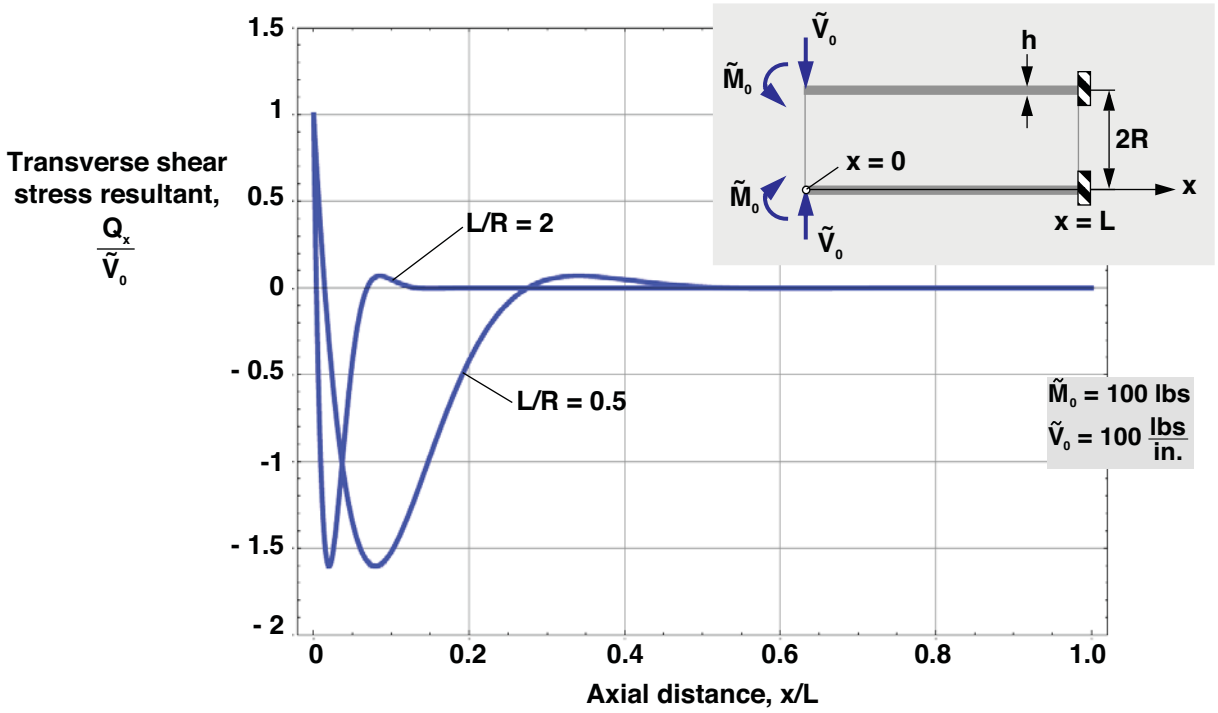

Figure 6. Transverse shear stress resultant for laminated cylinder with all 90-deg plies, subjected to edge loads at x = 0, and clamped at x = L (R/h = 100).

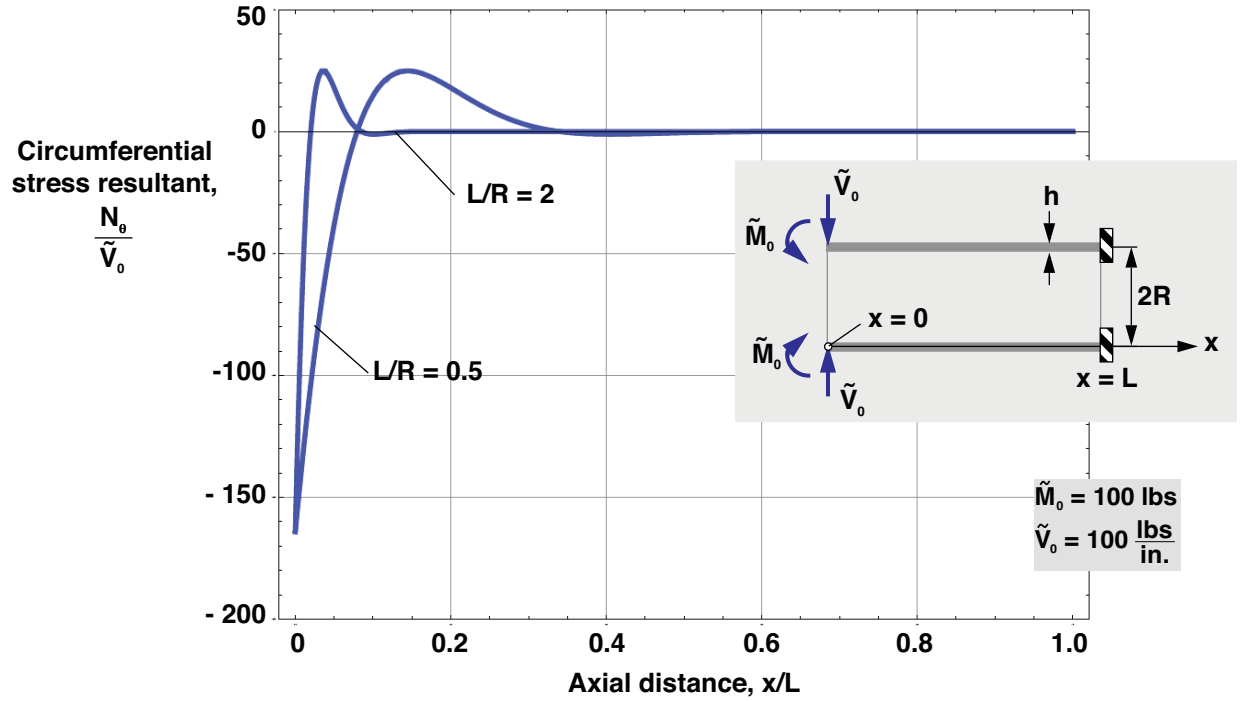

Figure 7. Circumferential stress resultant for laminated cylinder with all 90-deg plies, subjected to edge loads at x = 0, and clamped at x = L (R/h = 100).

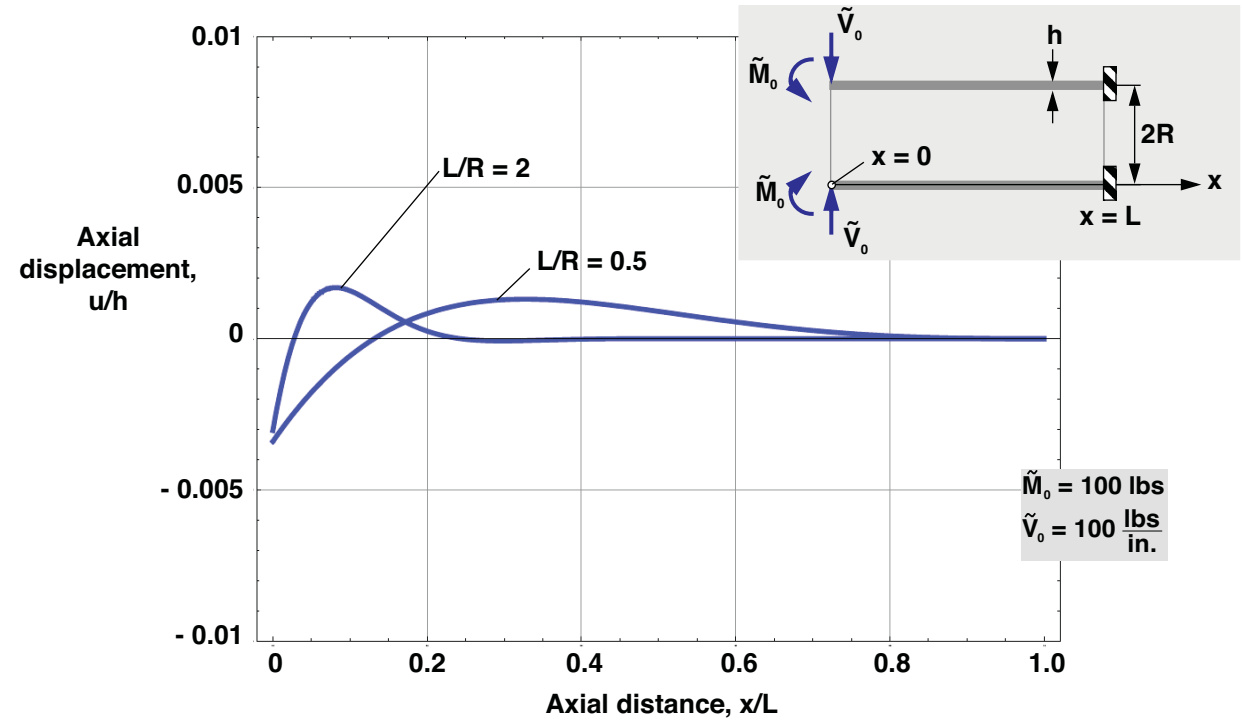

Figure 8. Axial displacement of laminated cylinder with all 10-deg plies, subjected to edge loads at x = 0, and clamped at x = L (R/h = 100).

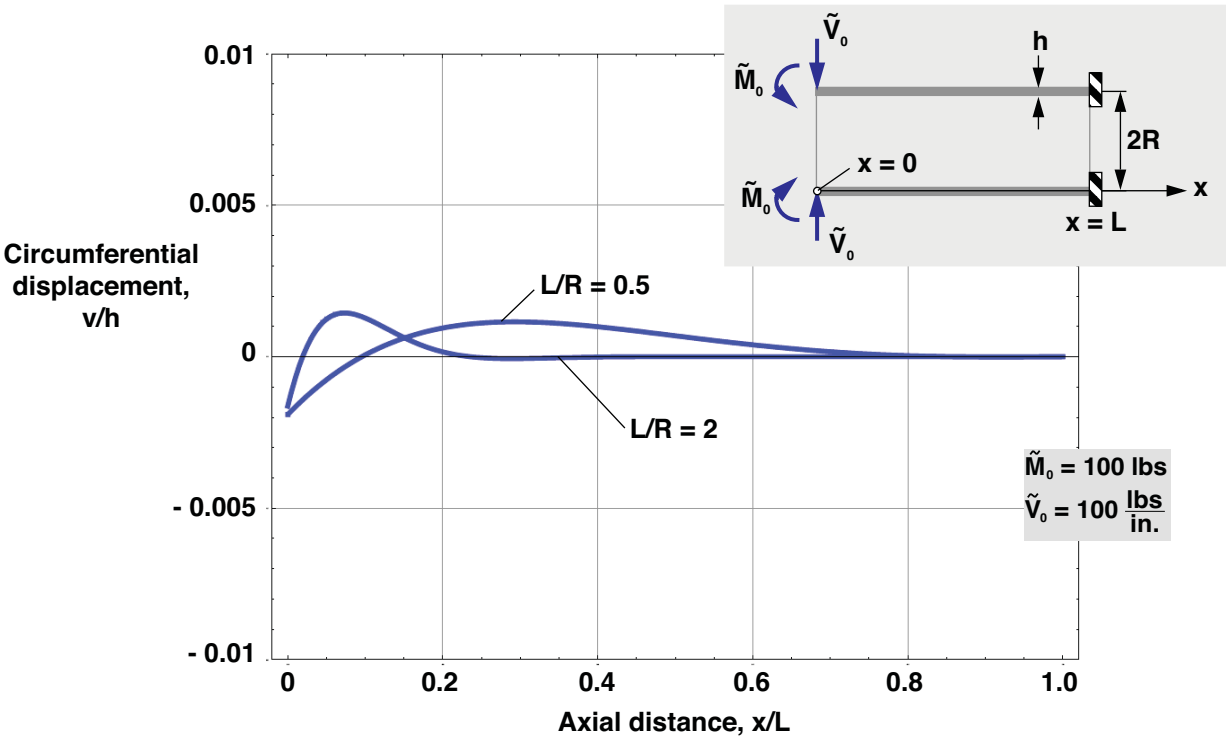

Figure 9. Circumferential displacement of laminated cylinder with all 10-deg plies, subjected to edge loads at x = 0, and clamped at x = L (R/h = 100).

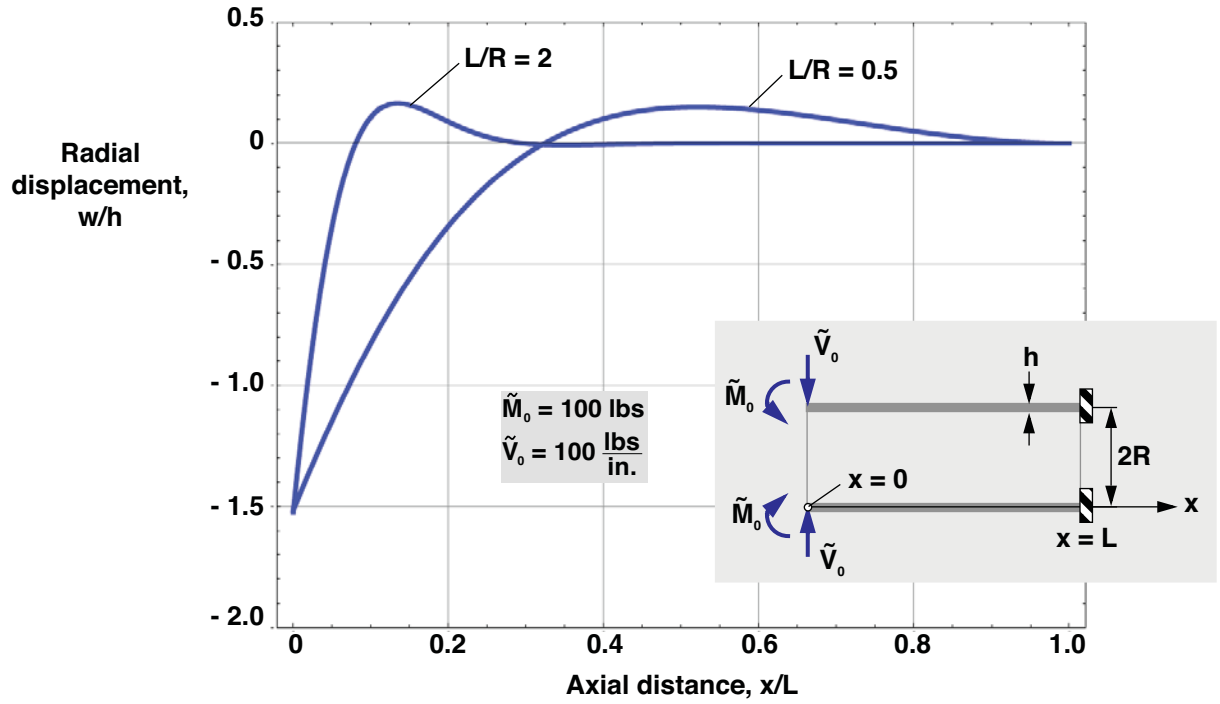

Figure 10. Radial displacement of laminated cylinder with all 10-deg plies, subjected to edge loads at x = 0, and clamped at x = L (R/h = 100).

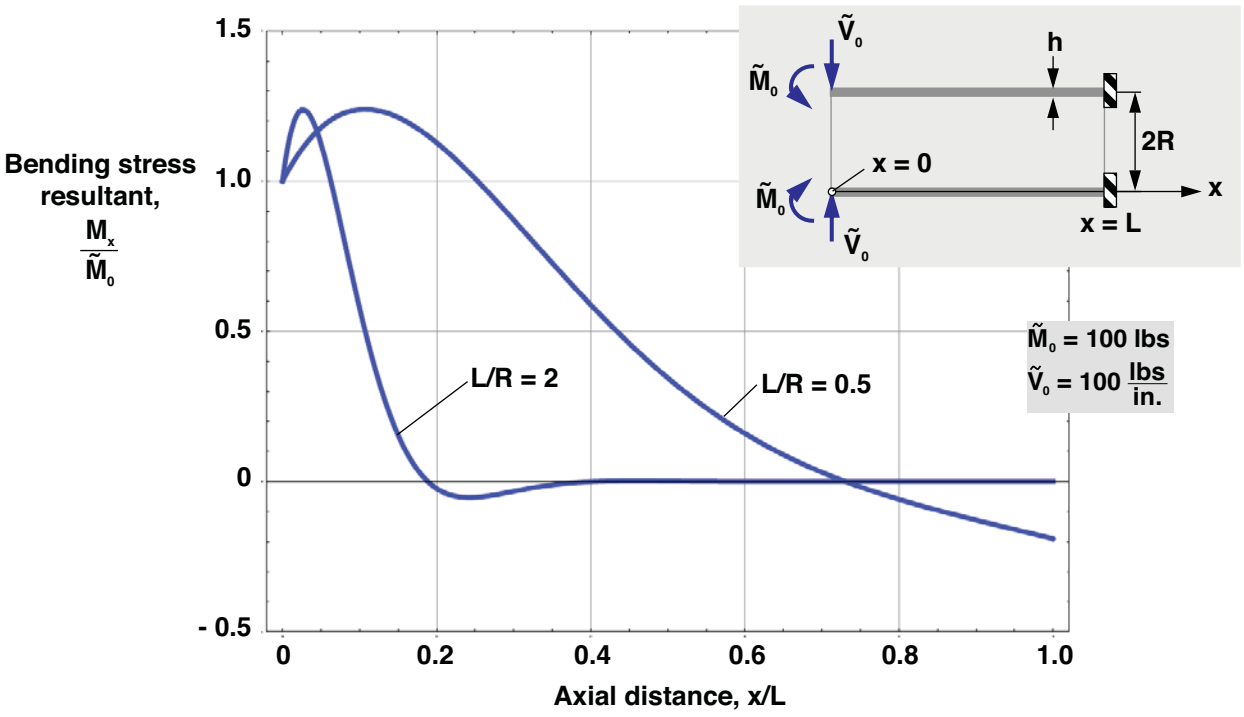

Figure 11. Bending stress resultant for laminated cylinder with all 10-deg plies, subjected to edge loads at x = 0, and clamped at x = L (R/h = 100).

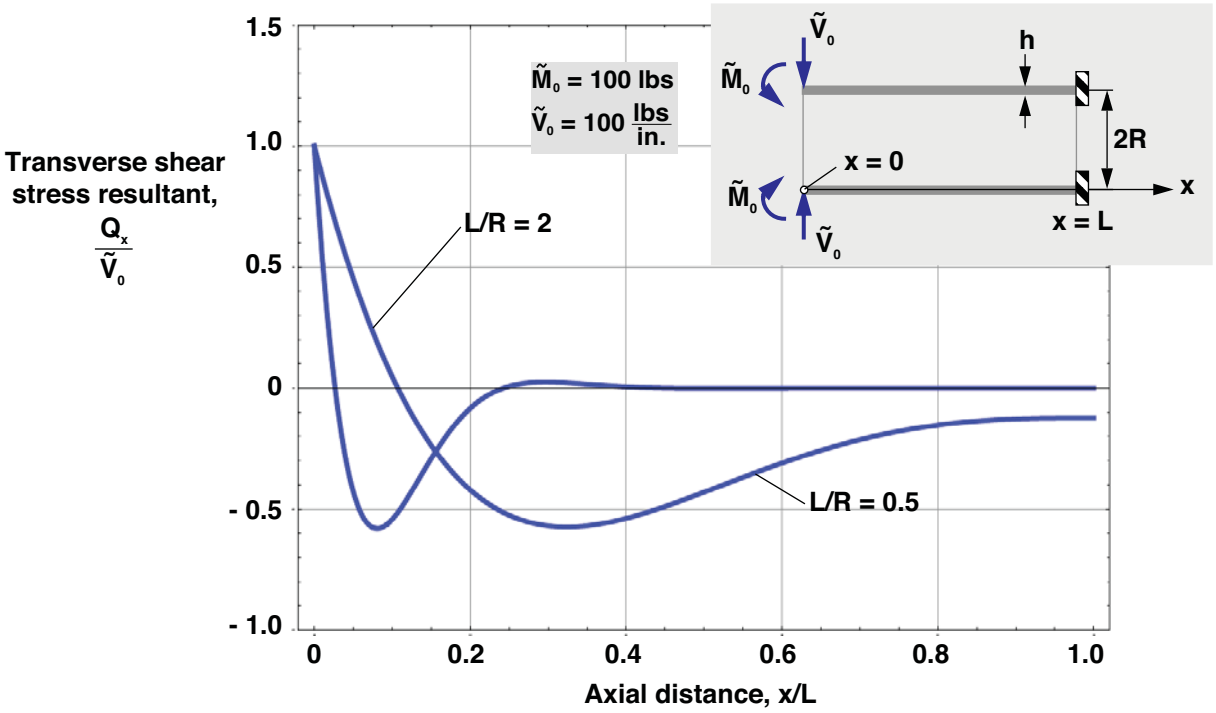

Figure 12. Transverse shear stress resultant for laminated cylinder with all 10-deg plies, subjected to edge loads at x = 0, and clamped at x = L (R/h = 100).

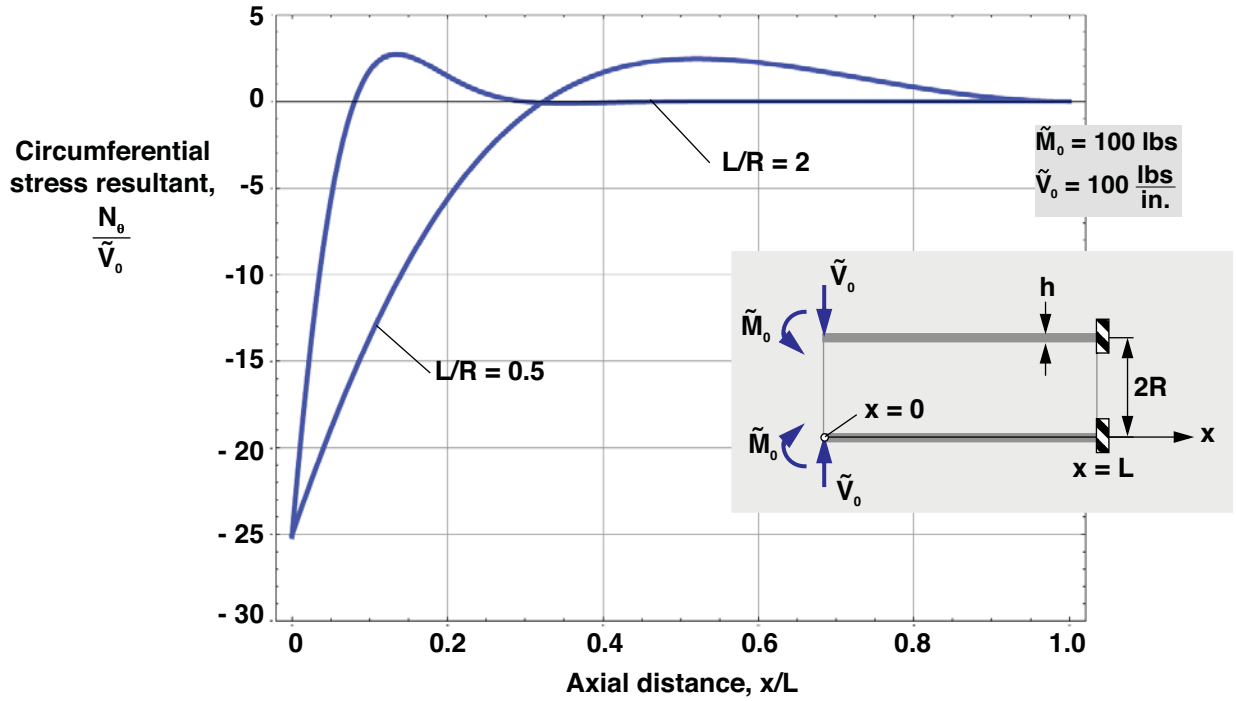

Figure 13. Circumferential stress resultant for laminated cylinder with all 10-deg plies, subjected to edge loads at x = 0, and clamped at x = L (R/h = 100).

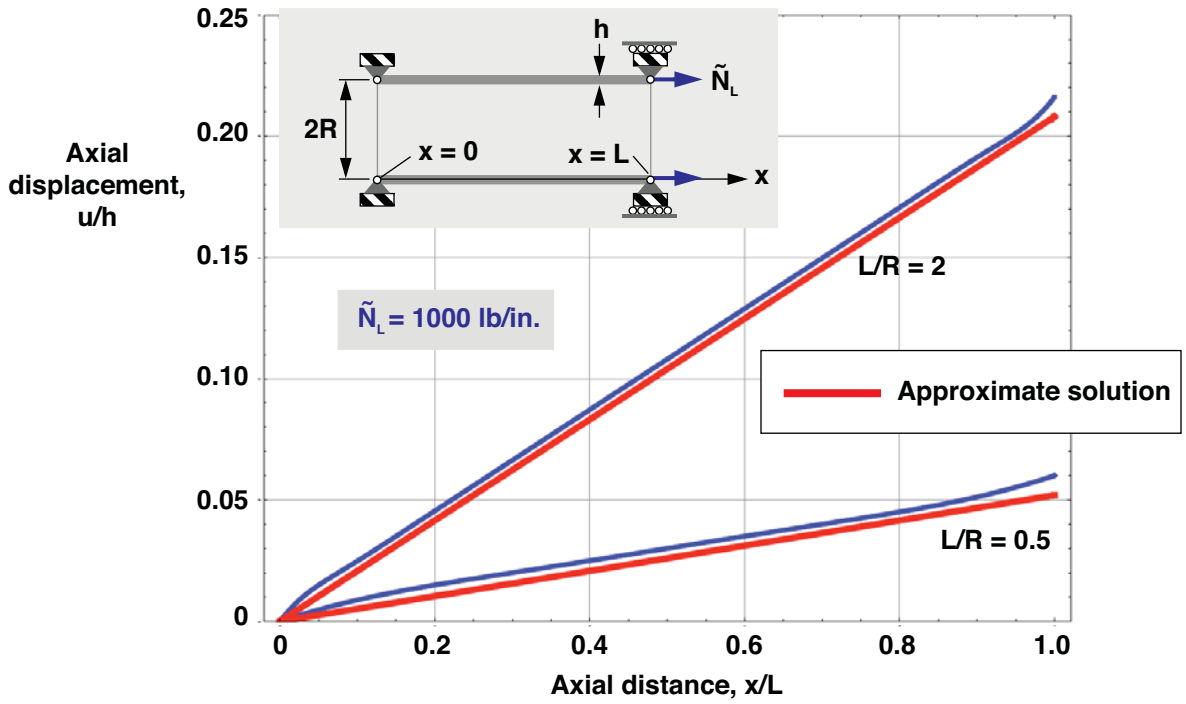

Figure 14. Axial displacement of $[90_2/10_2]_T$ laminated cylinder subjected to an axial edge load at x = L, with u, v, and w fixed at x = 0, and with v and w fixed at x = L (R/h = 100).

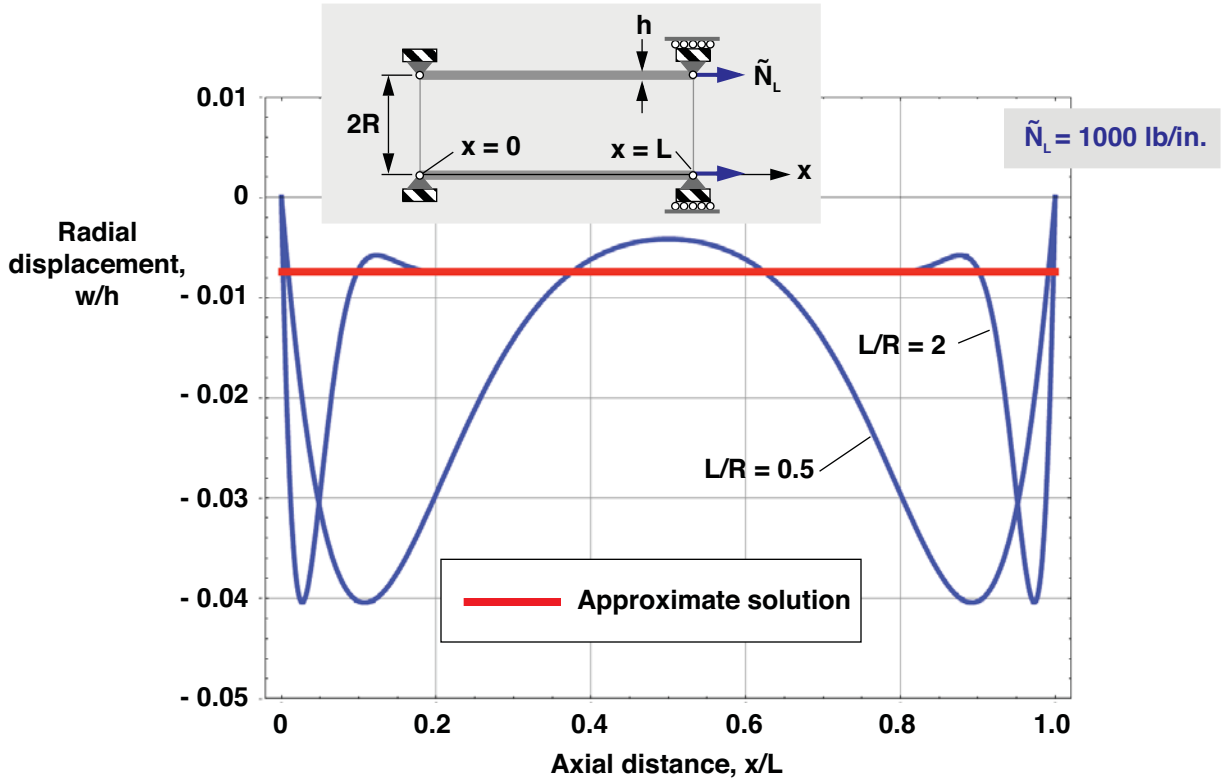

Figure 15. Radial displacement of $[90_2/10_2]_T$ laminated cylinder subjected to an axial edge load at x = L, with u, v, and w fixed at x = 0, and with v and w fixed at x = L (R/h = 100).

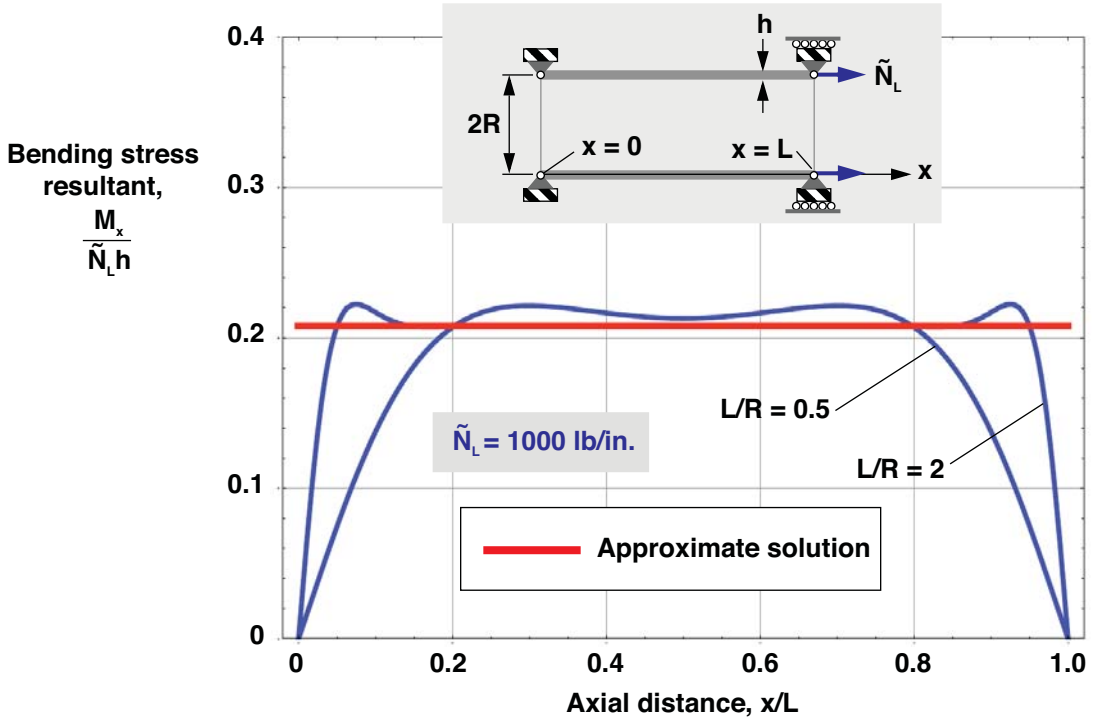

Figure 16. Bending stress resultants of $[90_2/10_2]_T$ laminated cylinder subjected to an axial edge load at x = L, with u, v, and w fixed at x = 0, and with v and w fixed at x = L (R/h = 100).

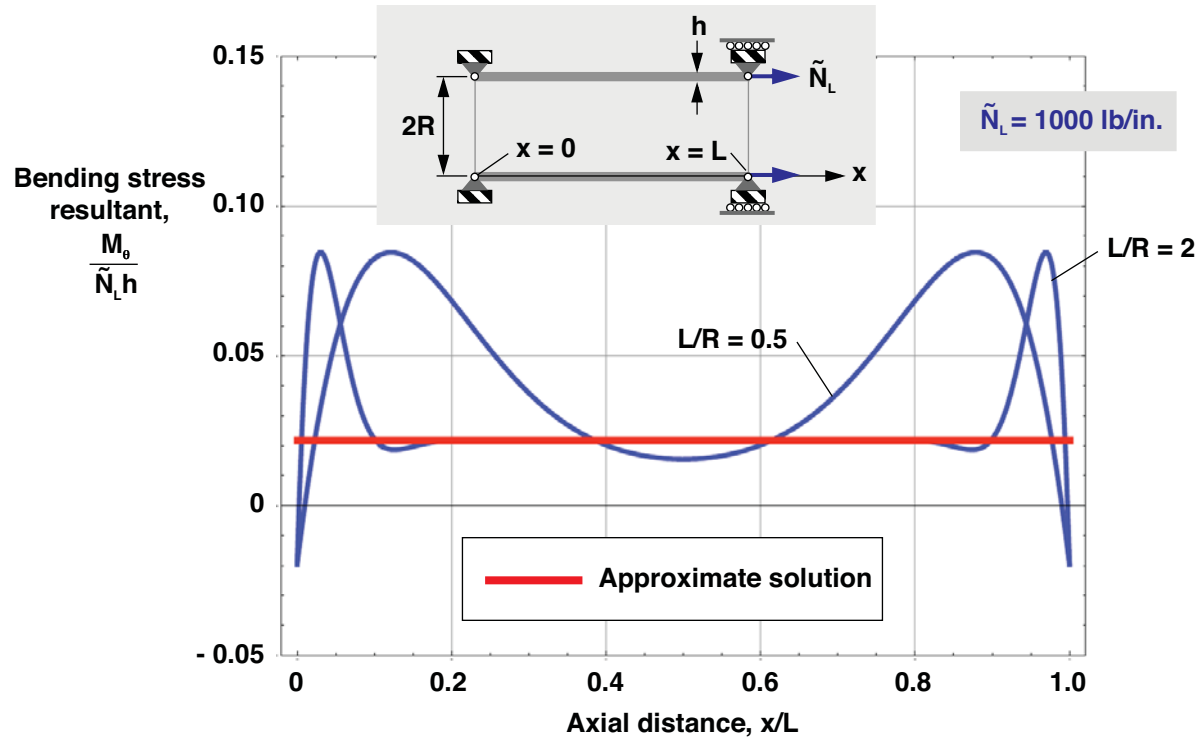

Figure 17. Bending stress resultants of $[90_2/10_2]_T$ laminated cylinder subjected to an axial edge load at x = L, with u, v, and w fixed at x = 0, and with v and w fixed at x = L (R/h = 100).

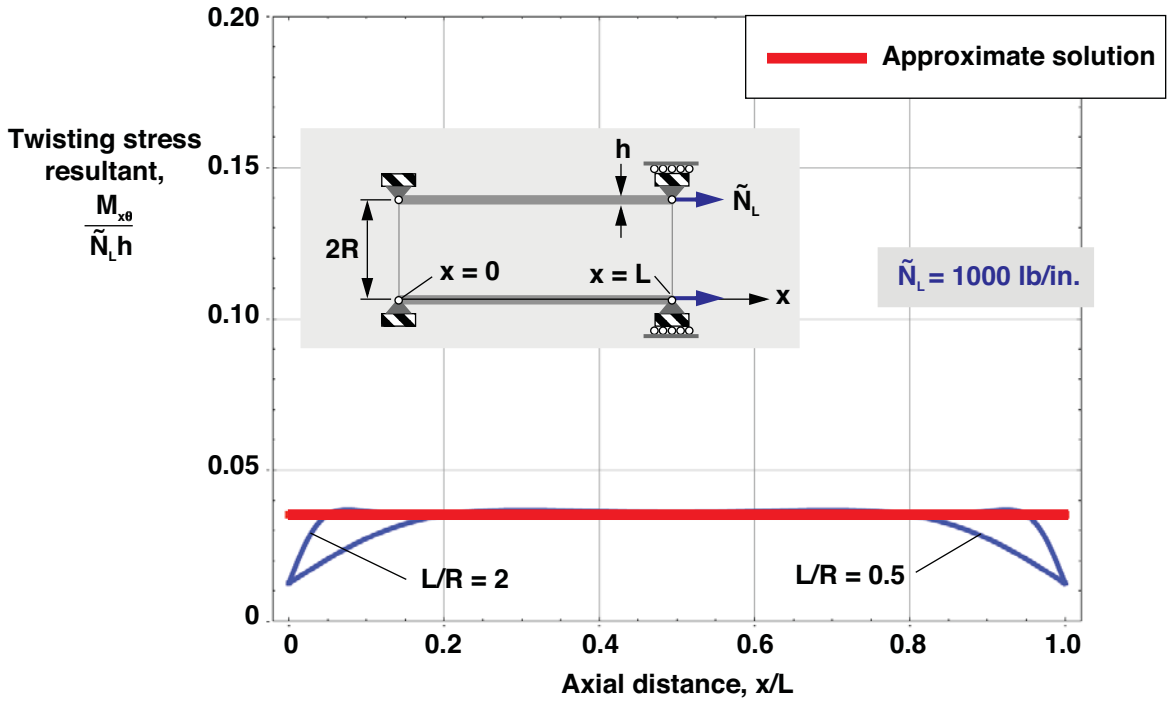

Figure 18. Twisting stress resultants of $[90_2/10_2]_T$ laminated cylinder subjected to an axial edge load at x = L, with u, v, and w fixed at x = 0, and with v and w fixed at x = L (R/h = 100).

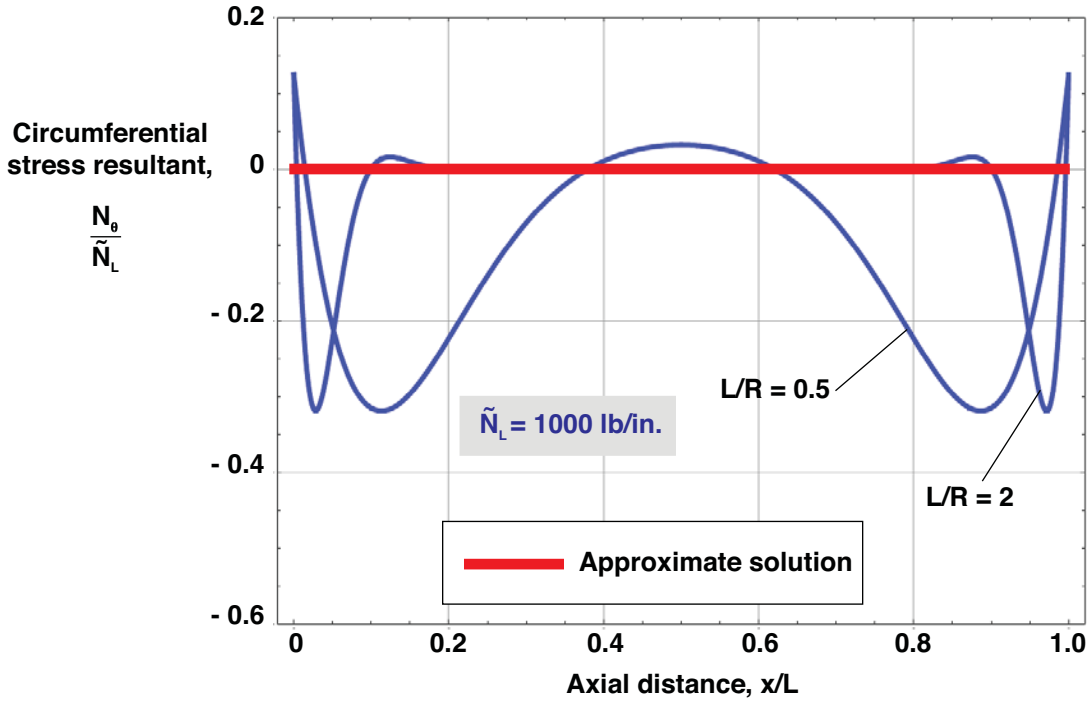

Figure 19. Circumferential stress resultants of $[90_2/10_2]_T$ laminated cylinder subjected to an axial edge load at x = L, with u, v, and w fixed at x = 0, and with v and w fixed at x = L (R/h = 100).

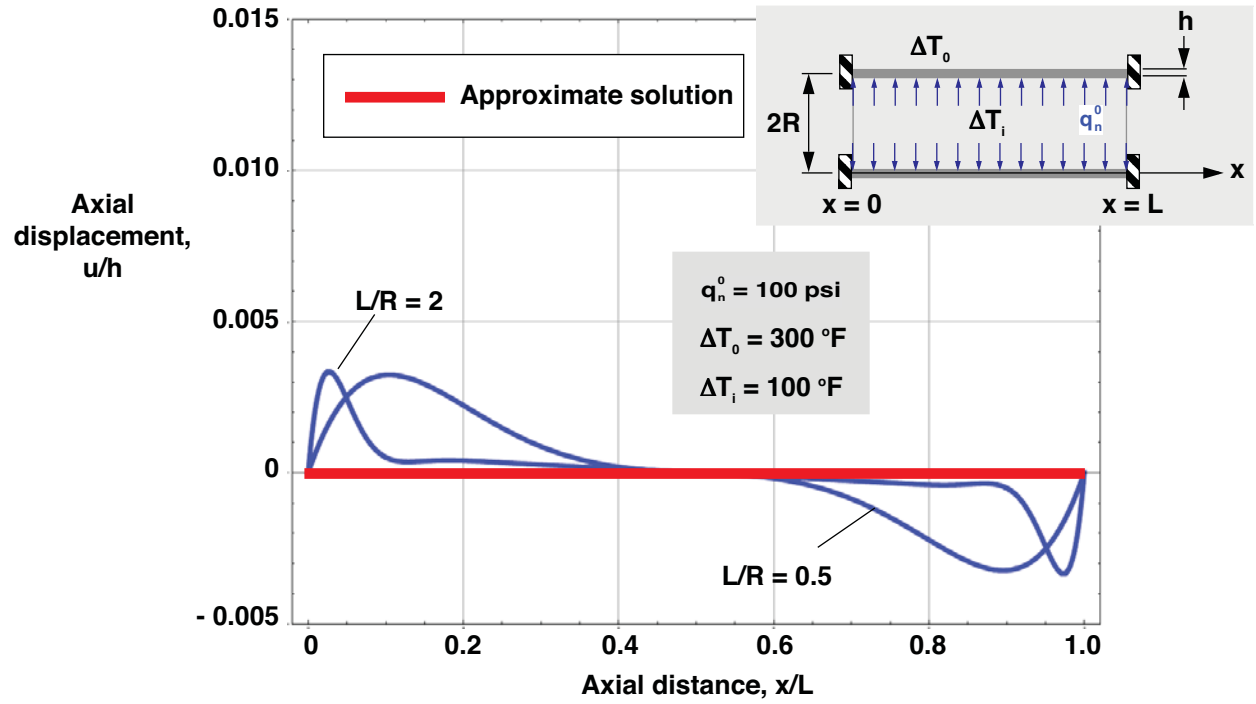

Figure 20. Axial displacement of $[90_2/10_2]_T$ laminated cylinder clamped at both ends and subjected internal pressure and uniform interior and exterior temperature fields (R/h = 100).

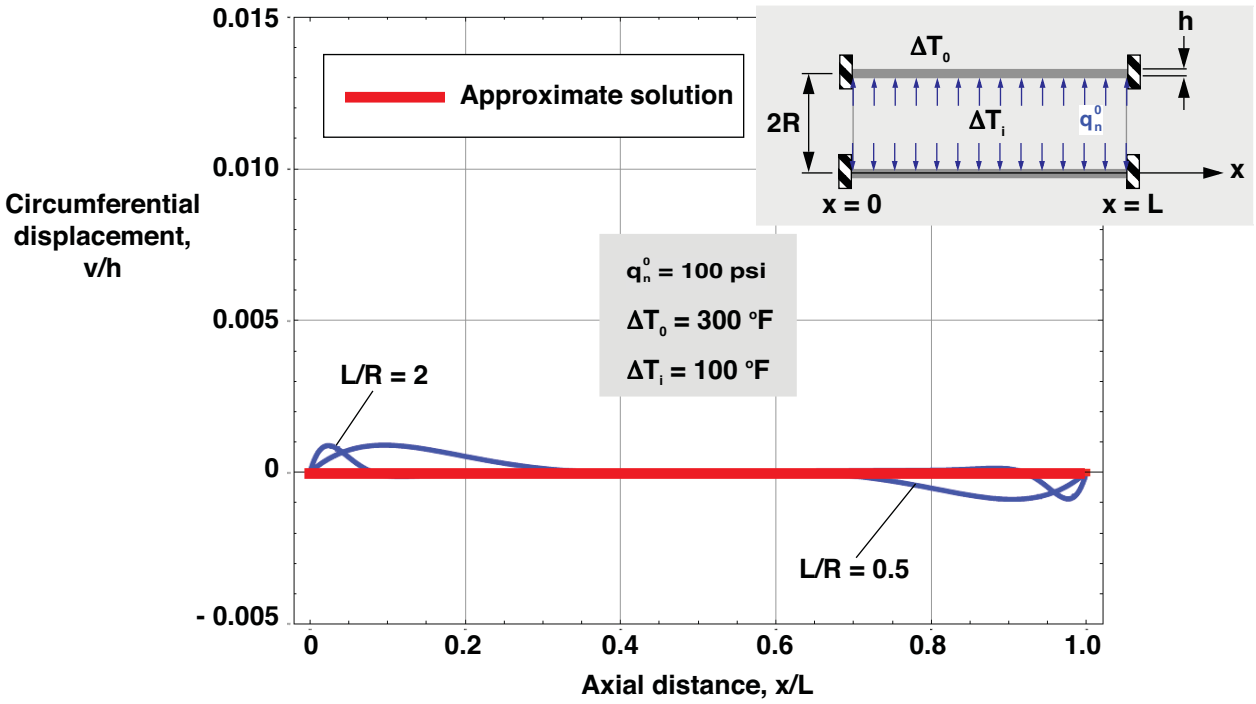

Figure 21. Circumferential displacement of $[90_2/10_2]_T$ laminated cylinder clamped at both ends and subjected internal pressure and uniform interior and exterior temperature fields (R/h = 100).

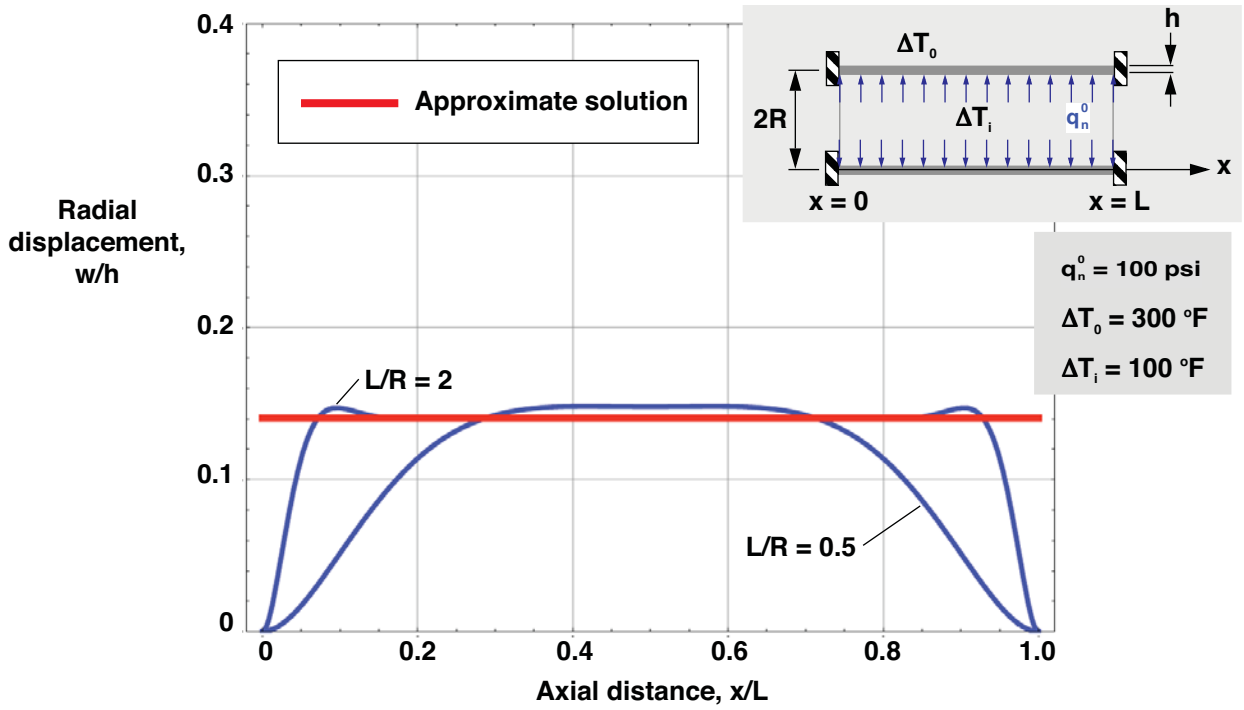

Figure 22. Radial displacement of $[90_2/10_2]_T$ laminated cylinder clamped at both ends and subjected internal pressure and uniform interior and exterior temperature fields (R/h = 100).

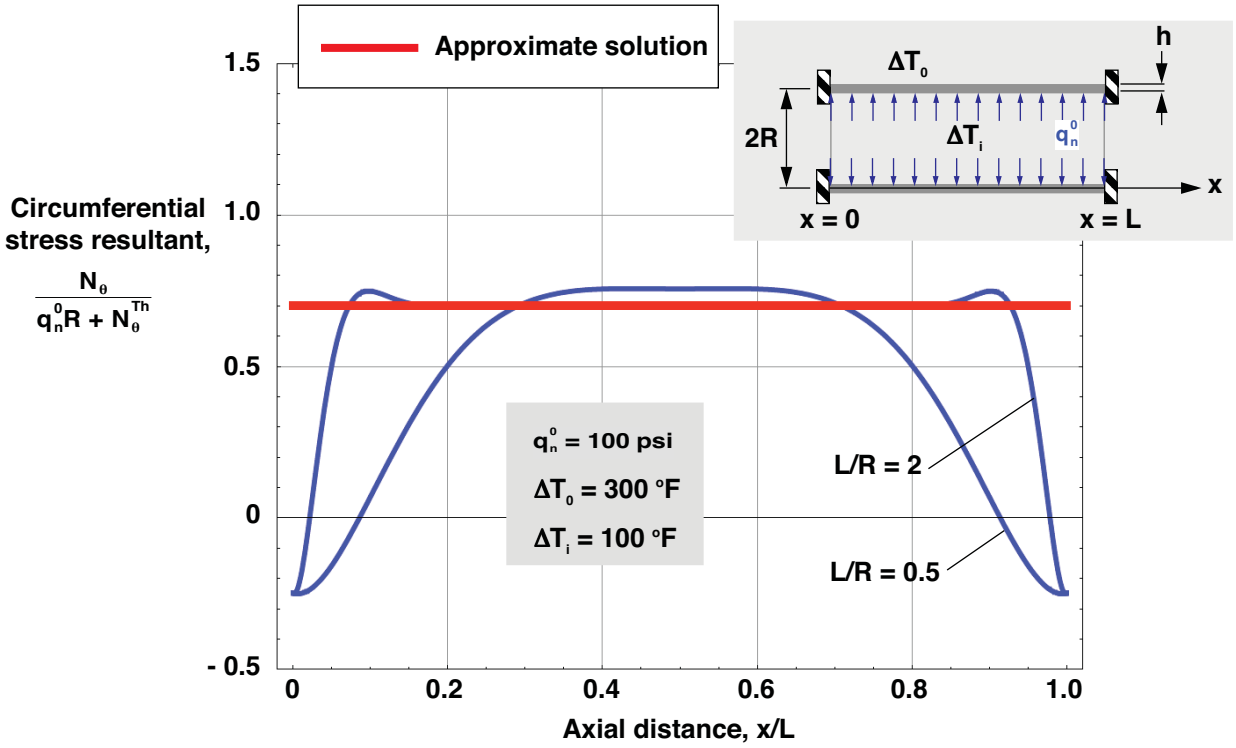

Figure 23. Circumferential stress resultant of $[90_2/10_2]_T$ laminated cylinder clamped at both ends and subjected internal pressure and uniform interior and exterior temperature fields (R/h = 100).

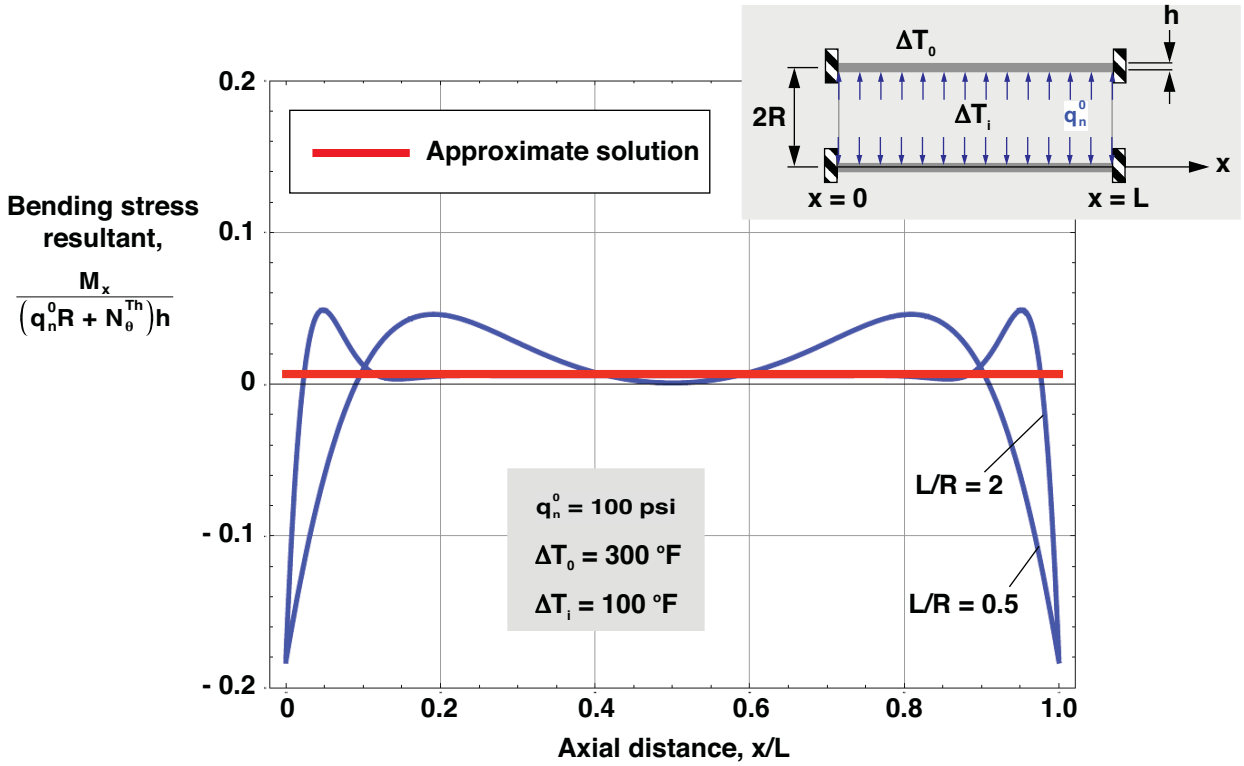

Figure 24. Bending stress resultant of $[90_2/10_2]_T$ laminated cylinder clamped at both ends and subjected to internal pressure and uniform interior and exterior temperature fields (R/h = 100).

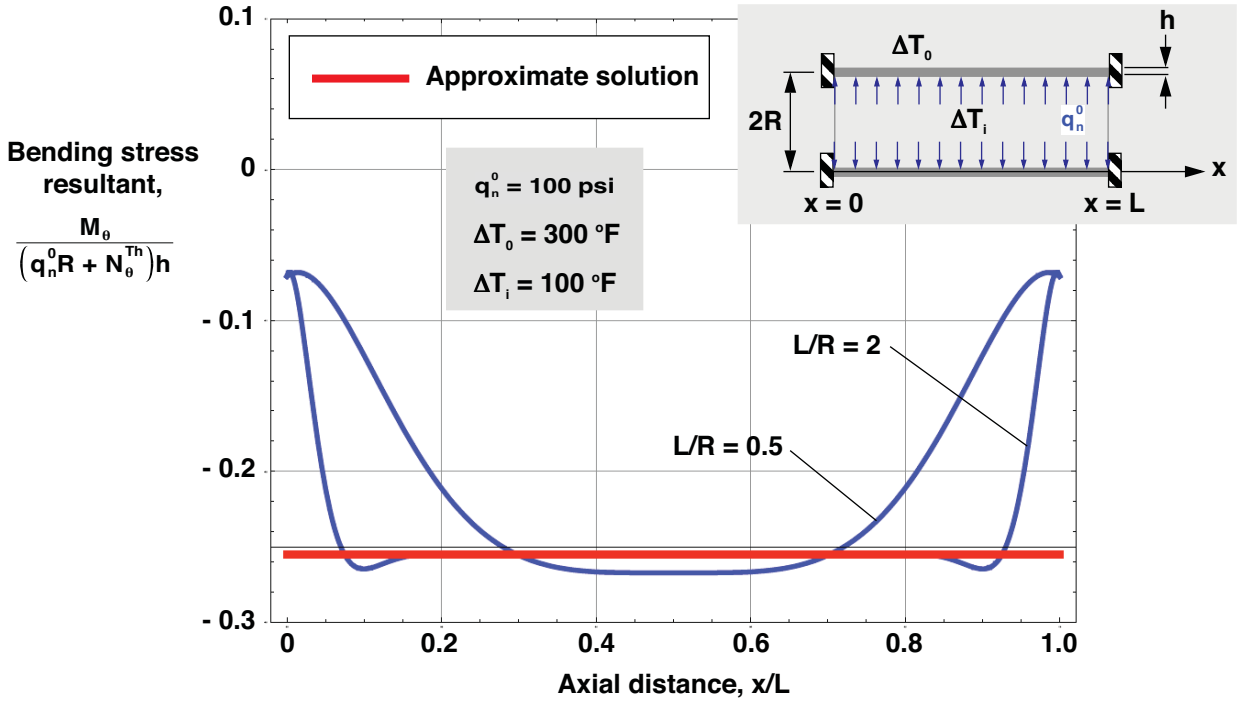

Figure 25. Bending stress resultant of $[90_2/10_2]_T$ laminated cylinder clamped at both ends and subjected to internal pressure and uniform interior and exterior temperature fields (R/h = 100).

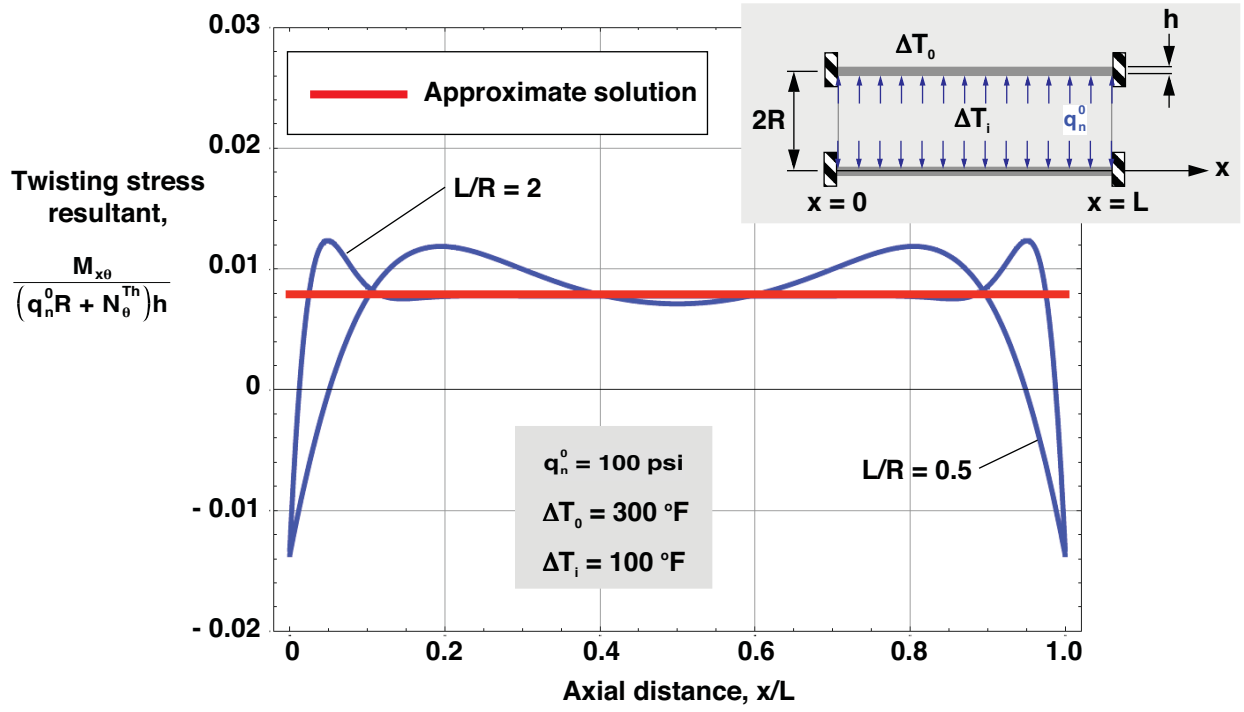

Figure 26. Twisting stress resultant of $[90_2/10_2]_T$ laminated cylinder clamped at both ends and subjected to internal pressure and uniform interior and exterior temperature fields (R/h = 100).

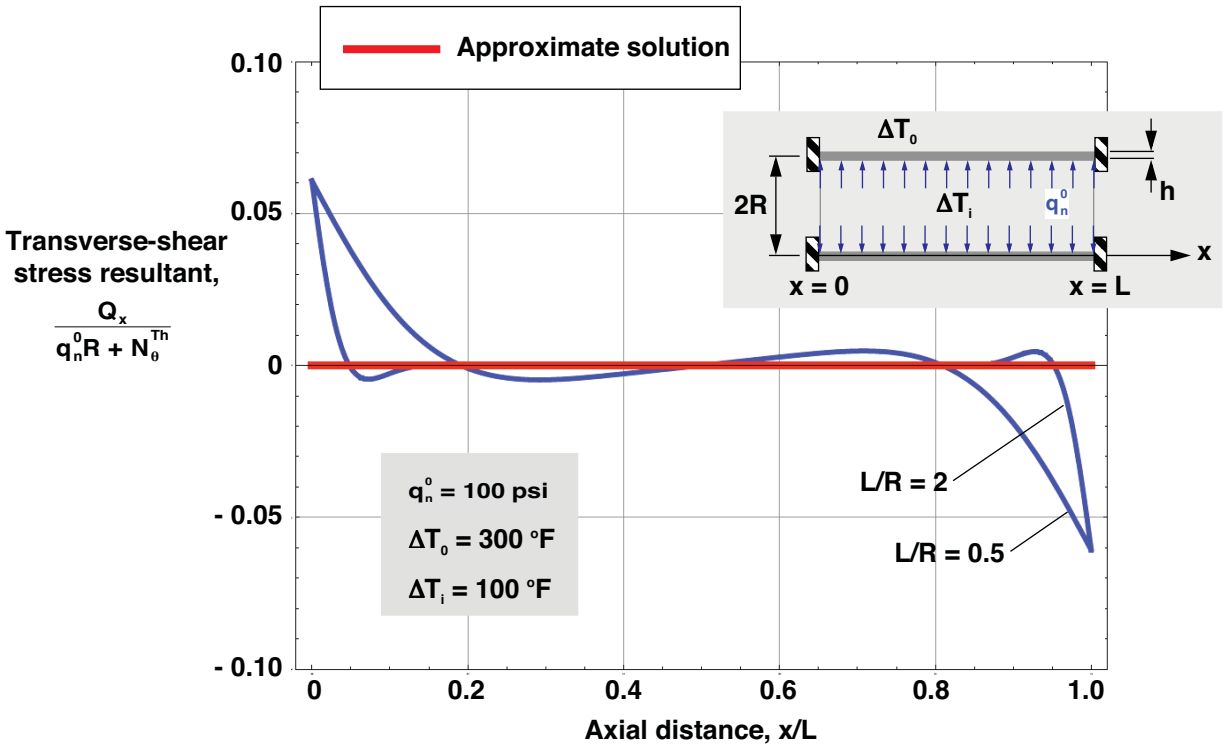

Figure 27. Transverse-shear stress resultant of $[90_2/10_2]_T$ laminated cylinder clamped at both ends and subjected to internal pressure and uniform interior and exterior temperature fields (R/h = 100).

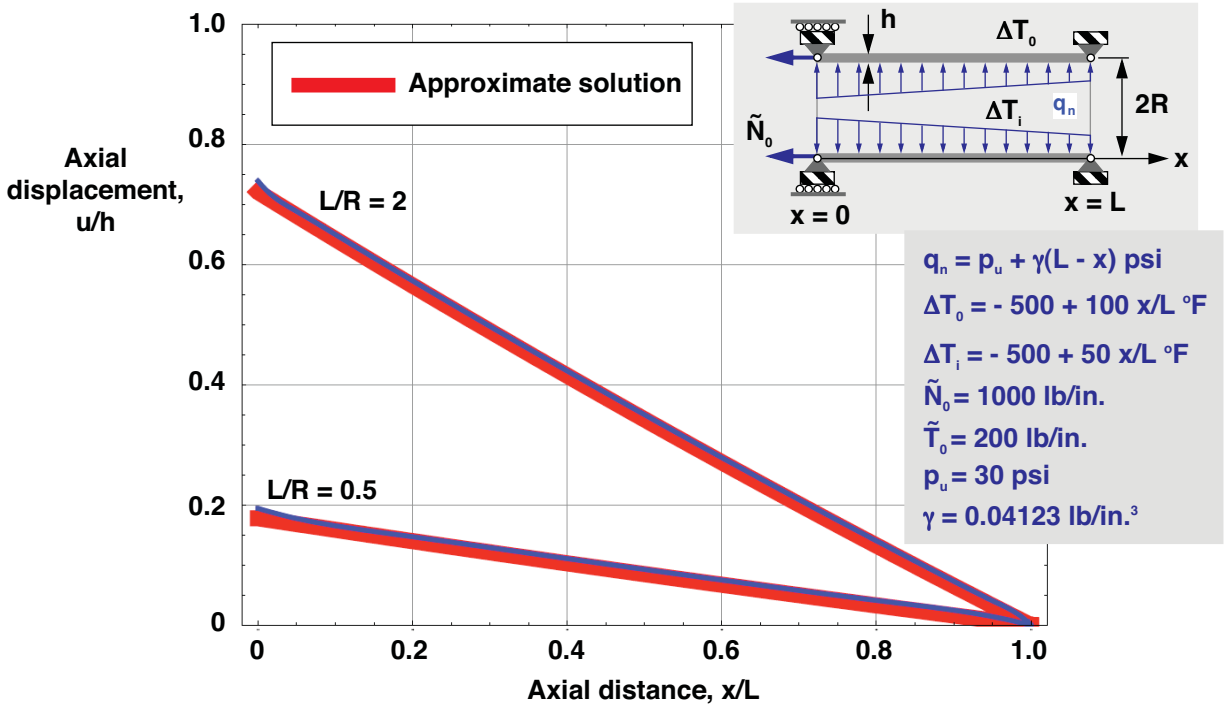

Figure 28. Axial displacement of $[90_2/10_2]_T$ laminated cylinder subjected to edge loads at x = 0, linearly varying pressure and temperatures, with u, v, and w fixed at x = L, and with w fixed at x = 0 (R/h = 330).

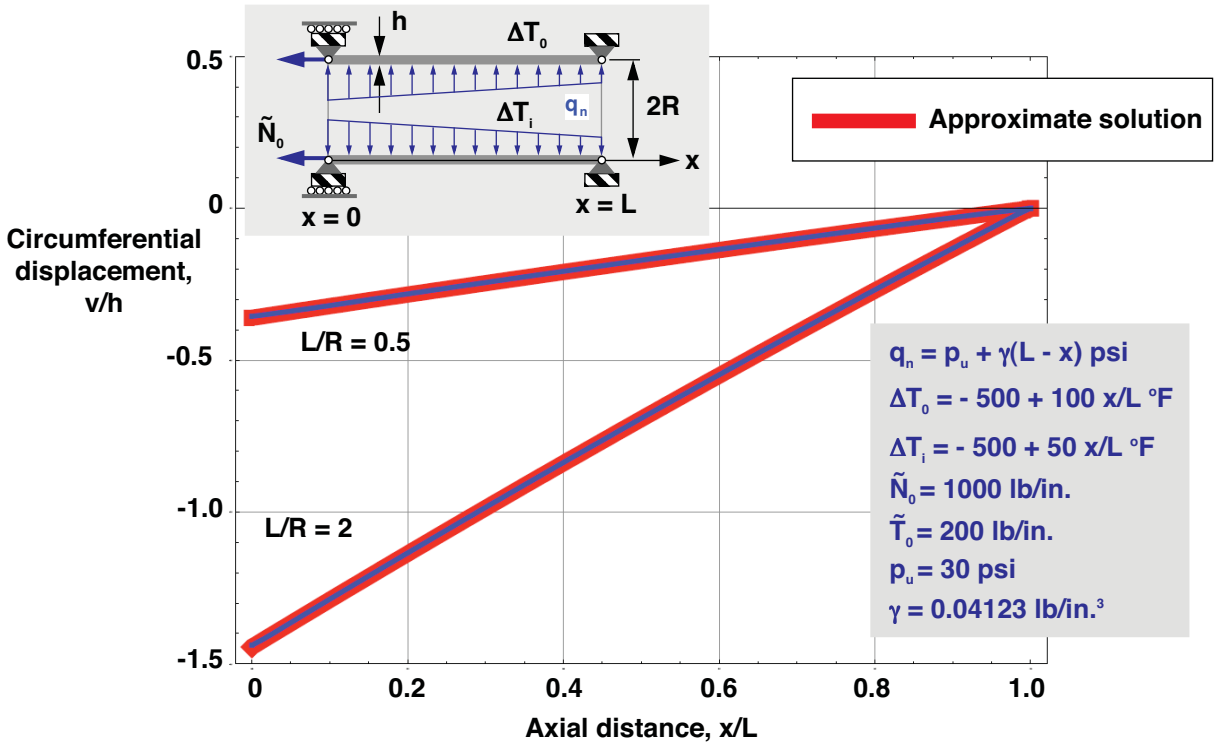

Figure 29. Circumferential displacement of $[90_2/10_2]_T$ laminated cylinder subjected to edge loads at x = 0, linearly varying pressure and temperatures, with u, v, and w fixed at x = L, and with w fixed at x = 0 (R/h = 330).

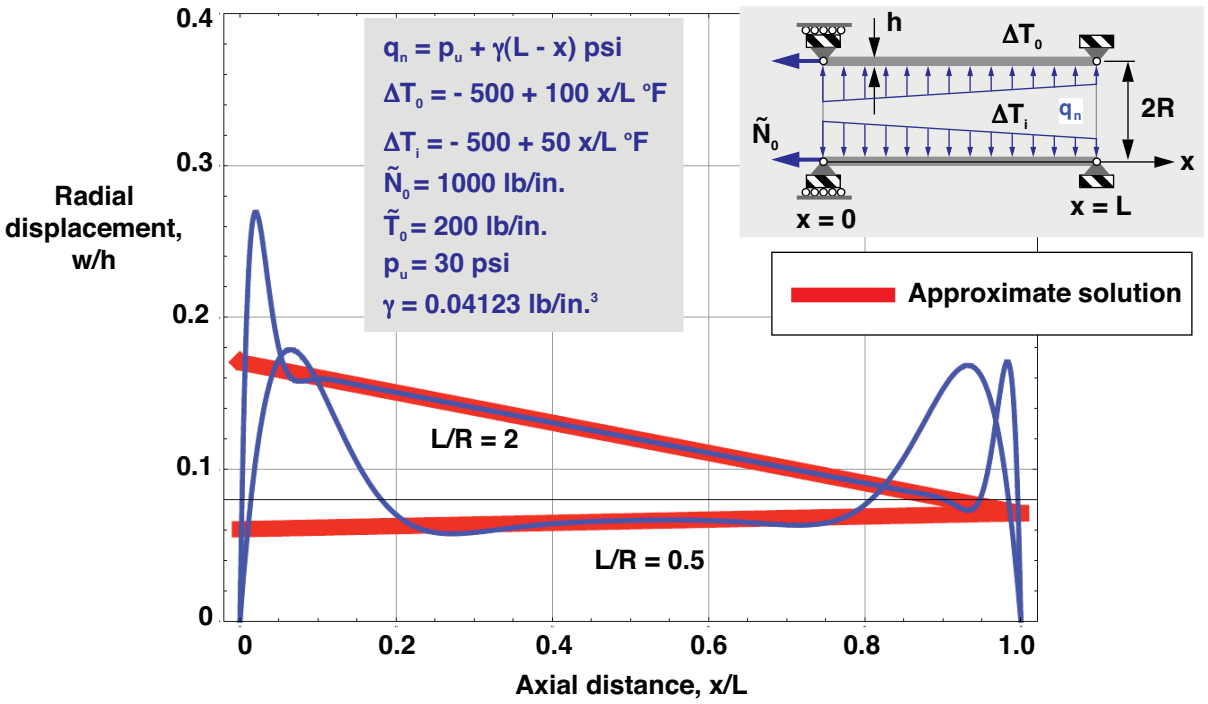

Figure 30. Radial displacement of $[90_2/10_2]_T$ laminated cylinder subjected to edge loads at x = 0, linearly varying pressure and temperatures, with u, v, and w fixed at x = L, and with w fixed at x = 0 (R/h = 330).

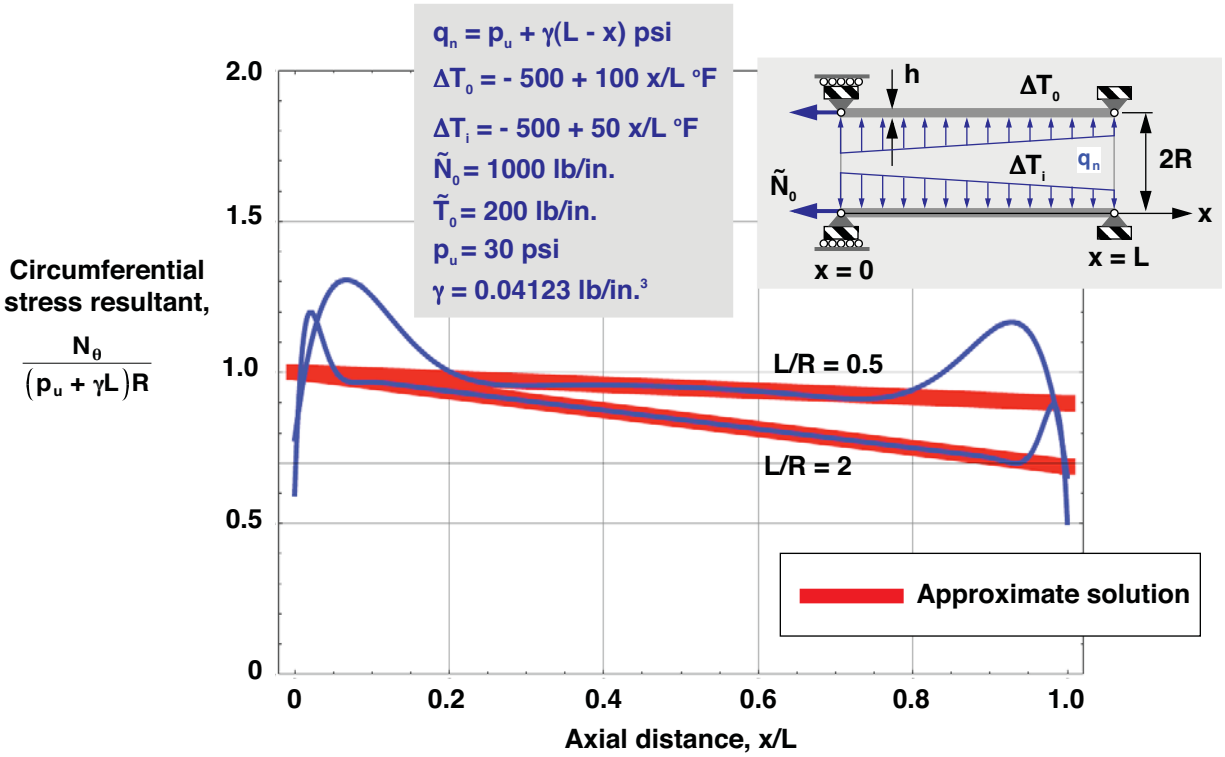

Figure 31. Circumferential stress resultant of $[90_2/10_2]_T$ laminated cylinder subjected to edge loads at x = 0, linearly varying pressure and temperatures, with u, v, and w fixed at x = L, and with w fixed at x = 0 (R/h = 330).

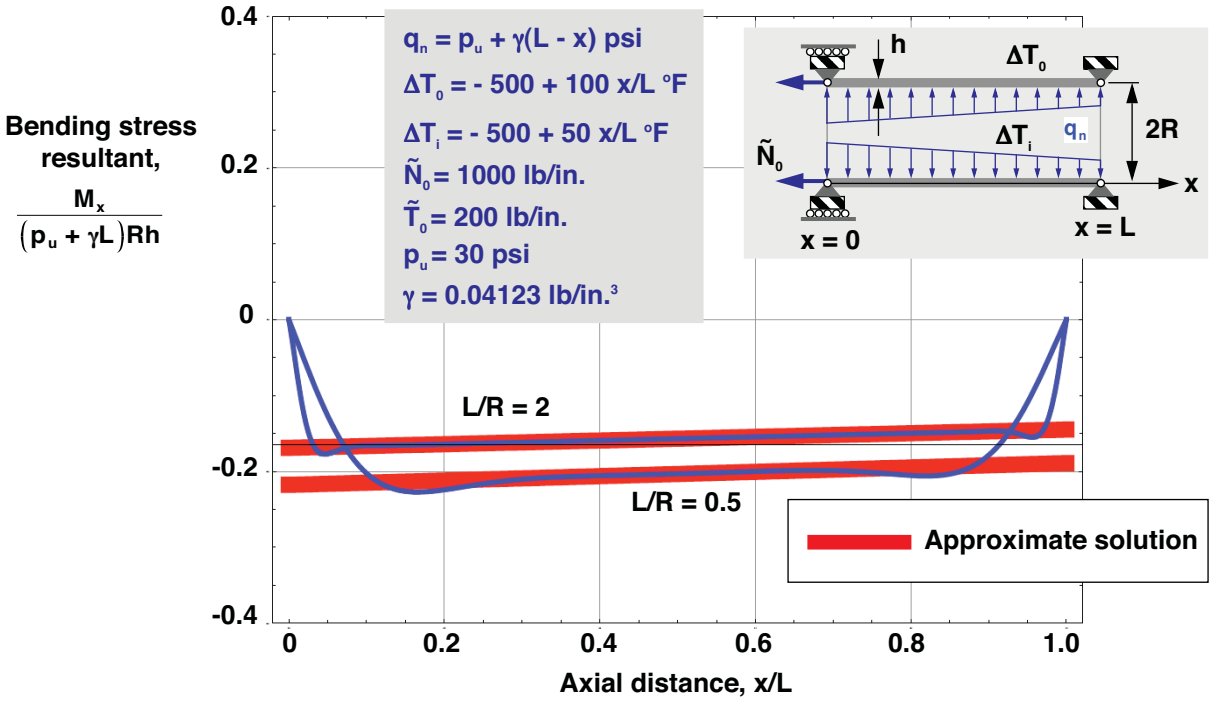

Figure 32. Bending stress resultant of $[90_2/10_2]_T$ laminated cylinder subjected to edge loads at x = 0, linearly varying pressure and temperatures, with u, v, and w fixed at x = L, and with w fixed at x = 0 (R/h = 330).

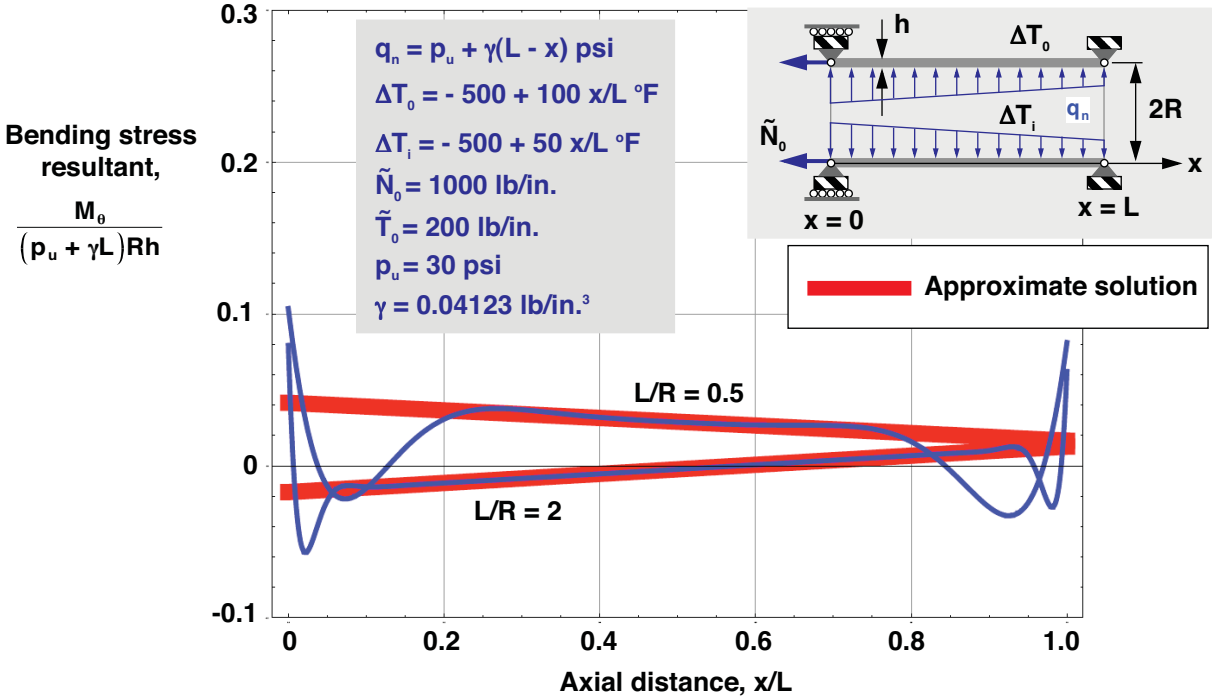

Figure 33. Bending stress resultant of $[90_2/10_2]_T$ laminated cylinder subjected to edge loads at x = 0, linearly varying pressure and temperatures, with u, v, and w fixed at x = L, and with w fixed at x = 0 (R/h = 330).

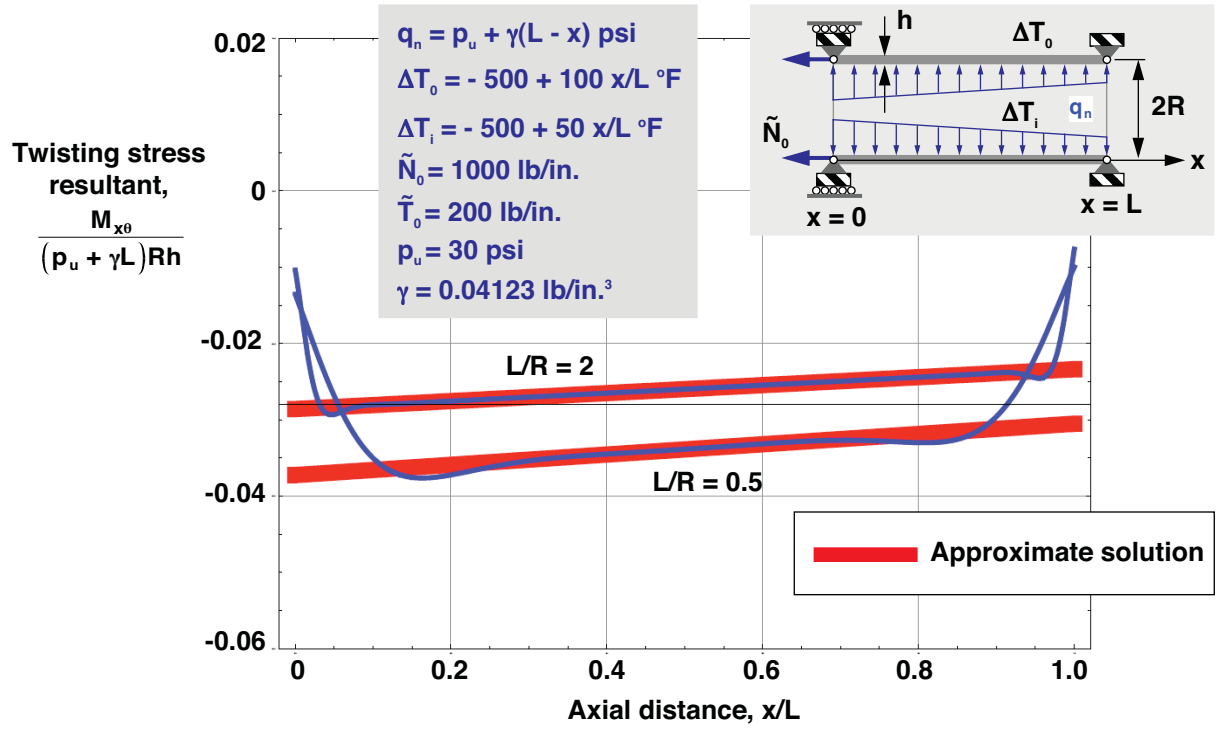

Figure 34. Twisting stress resultant of $[90_2/10_2]_T$ laminated cylinder subjected to edge loads at x = 0, linearly varying pressure and temperatures, with u, v, and w fixed at x = L, and with w fixed at x = 0 (R/h = 330).

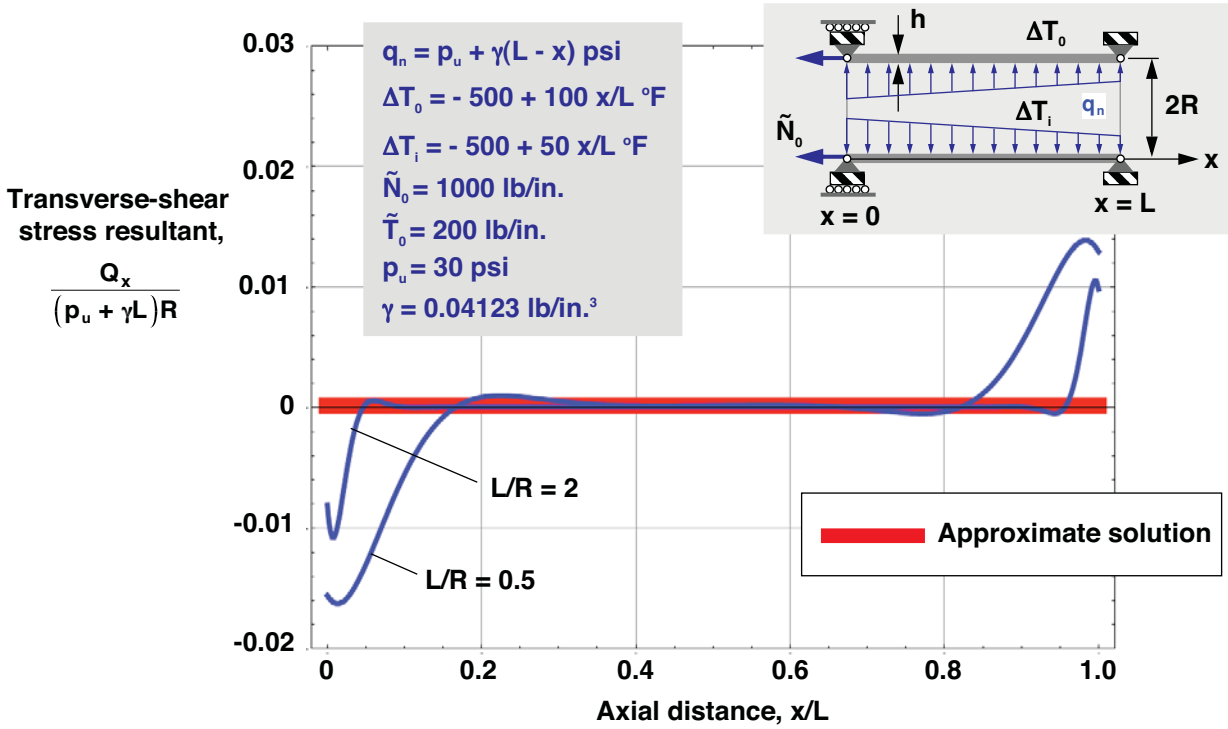

Figure 35. Transverse-shear stress resultant of $[90_2/10_2]_T$ laminated cylinder subjected to edge loads at x = 0, linearly varying pressure and temperatures, with u, v, and w fixed at x = L, and with w fixed at x = 0 (R/h = 330).

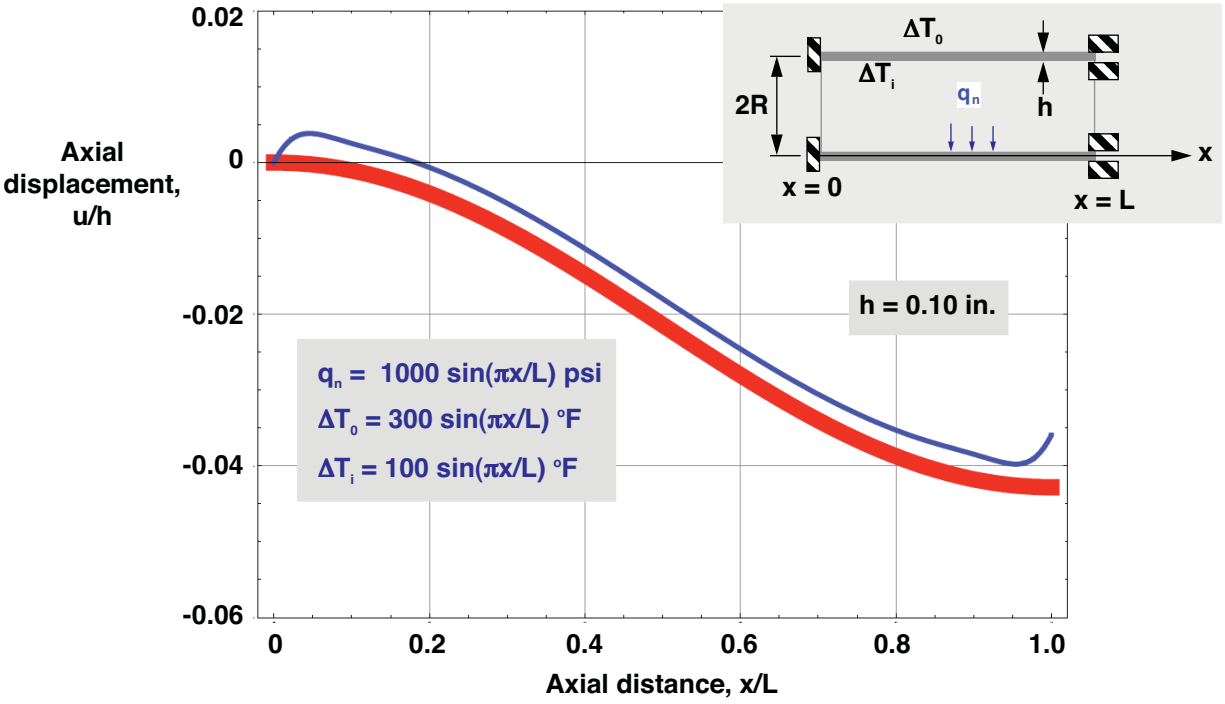

(b) Length-to-radius ratio, L/R = 2

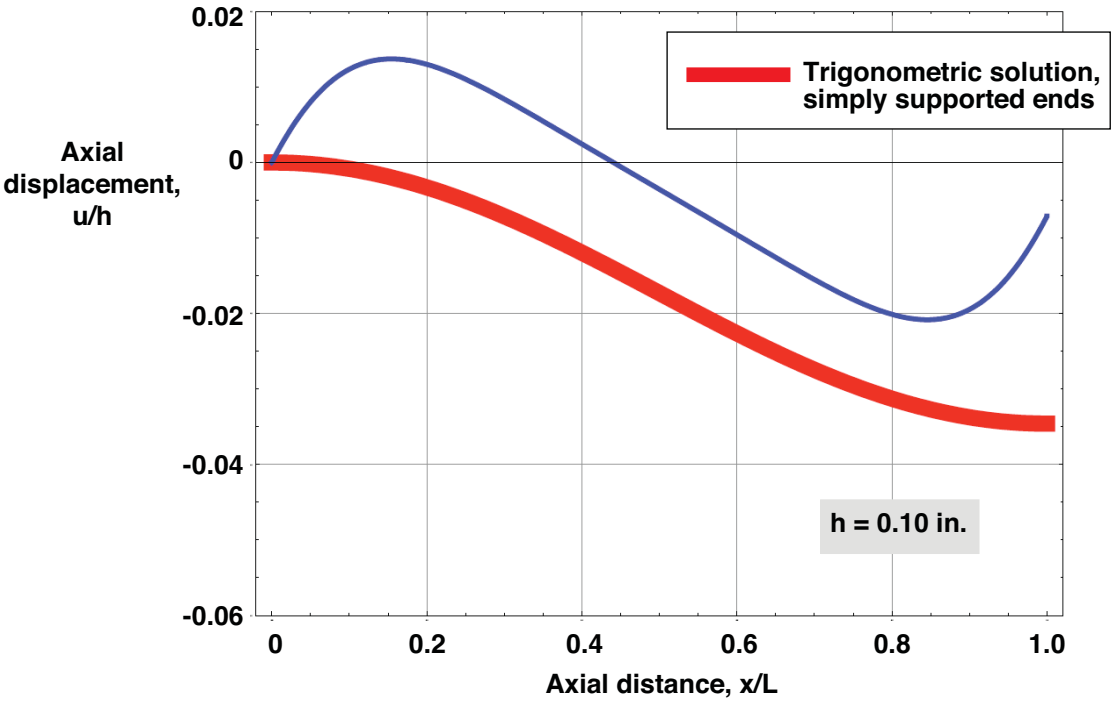

(a) Length-to-radius ratio, L/R = 0.5

Figure 36. Axial displacement of $[90_2/10_2]_T$ laminated cylinder subjected to sinusoidal pressure and temperatures, fixed at x = 0, and partially fixed at x = L to permit unrestrained axial and circumferential motion (R/h = 100).

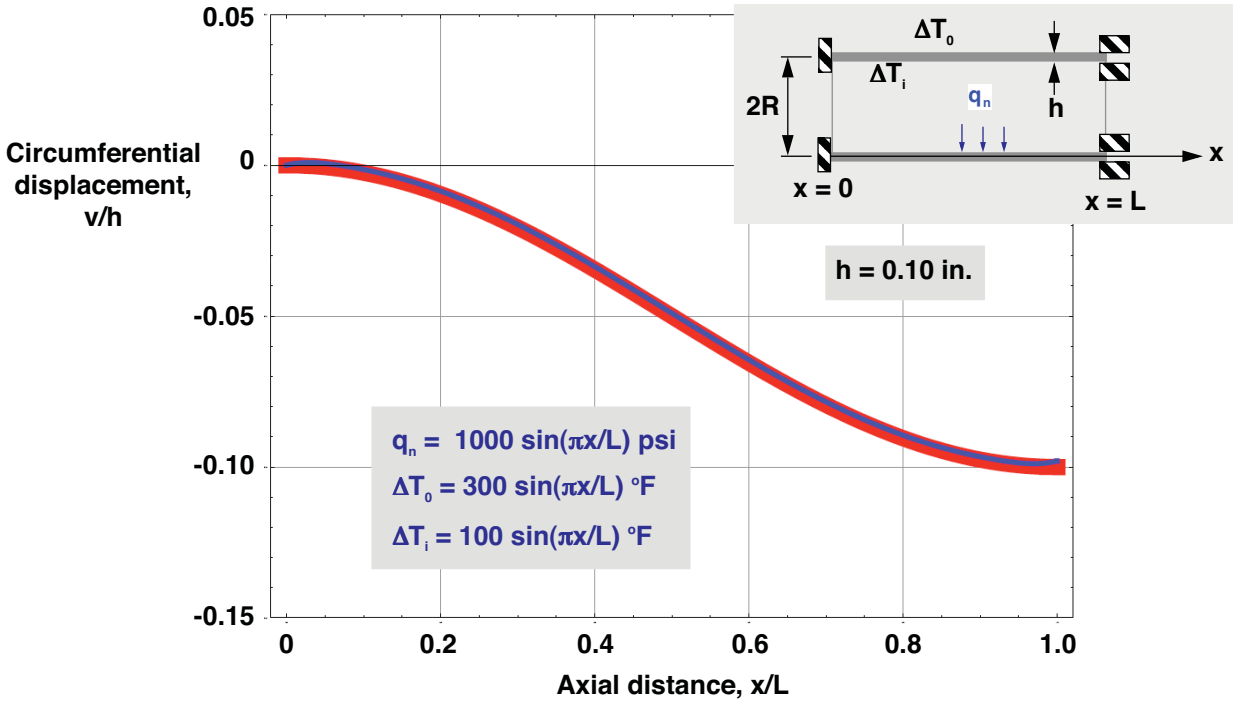

(b) Length-to-radius ratio, L/R = 2

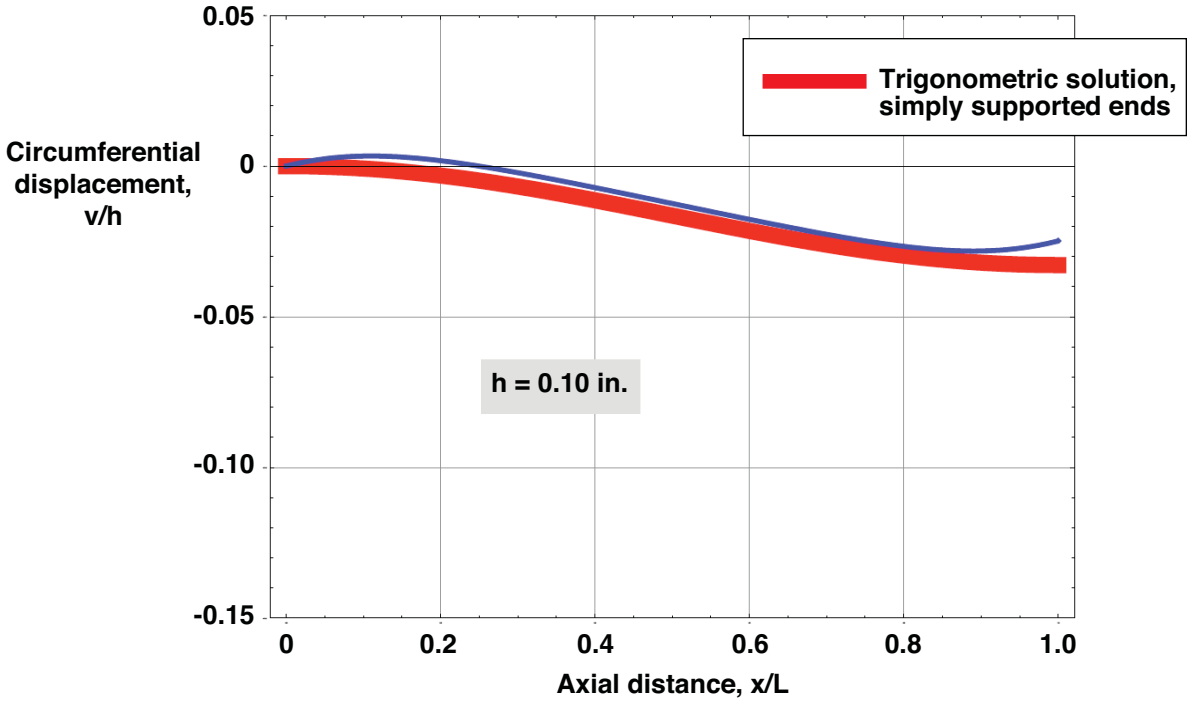

(a) Length-to-radius ratio, L/R = 0.5

Figure 37. Circumferential displacement of $[90_2/10_2]_T$ laminated cylinder subjected to sinusoidal pressure and temperatures, fixed at x = 0, and partially fixed at x = L to permit unrestrained axial and circumferential motion (R/h = 100).

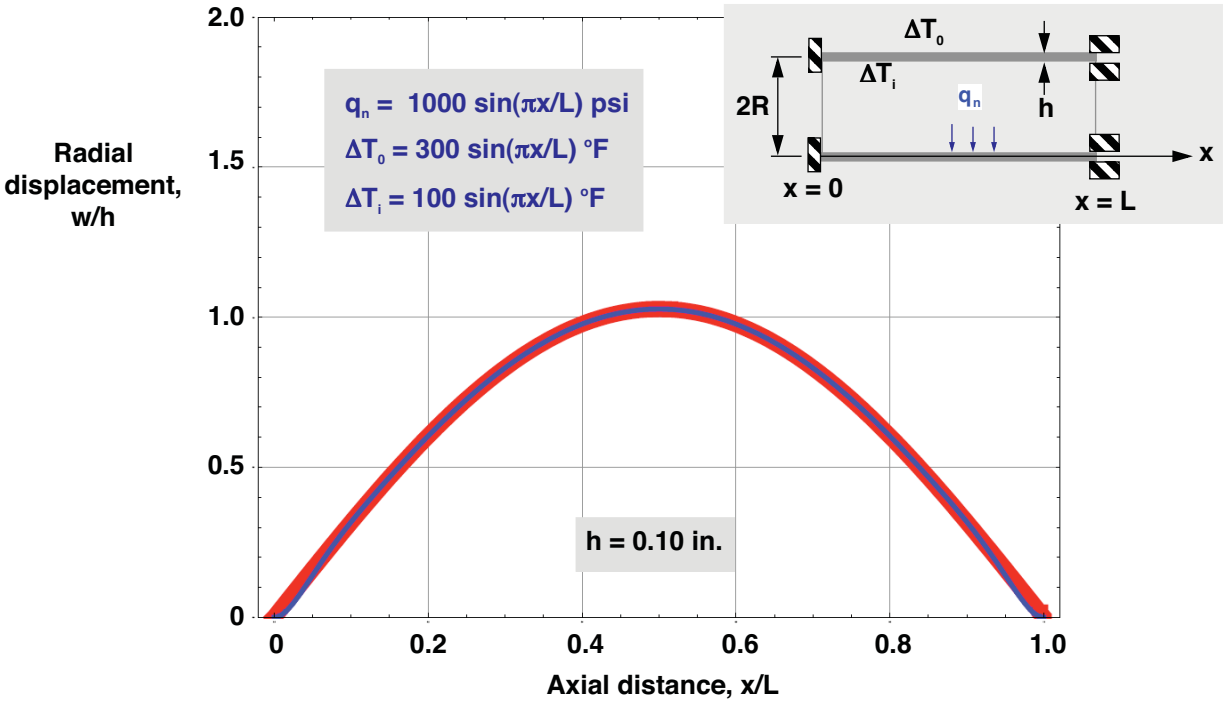

(b) Length-to-radius ratio, L/R = 2

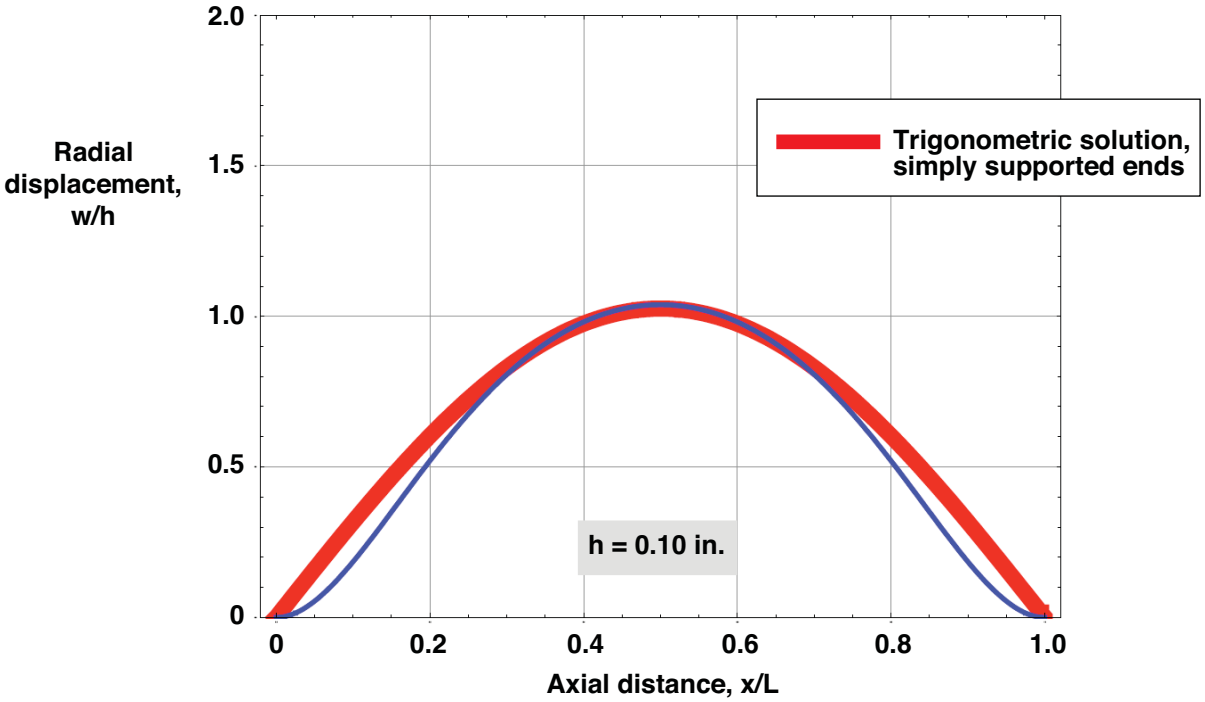

(a) Length-to-radius ratio, L/R = 0.5

Figure 38. Radial displacement of $[90_2/10_2]_T$ laminated cylinder subjected to sinusoidal pressure and temperatures, fixed at x = 0, and partially fixed at x = L to permit unrestrained axial and circumferential motion (R/h = 100).

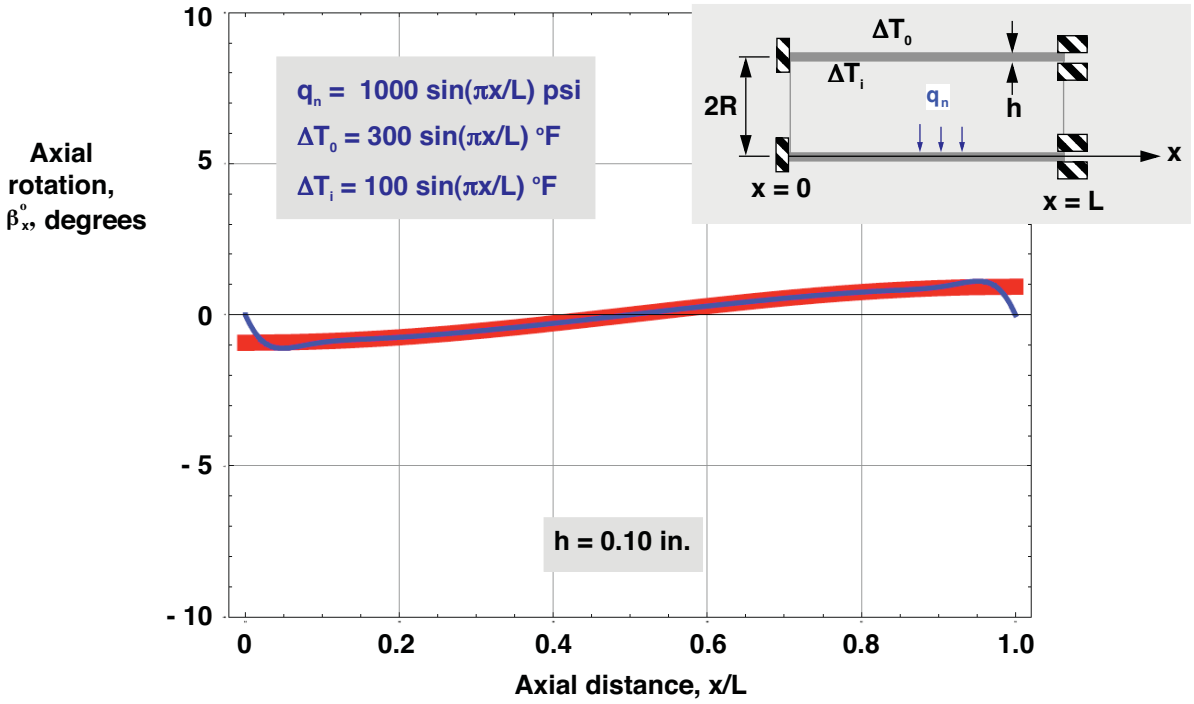

(b) Length-to-radius ratio, L/R = 2

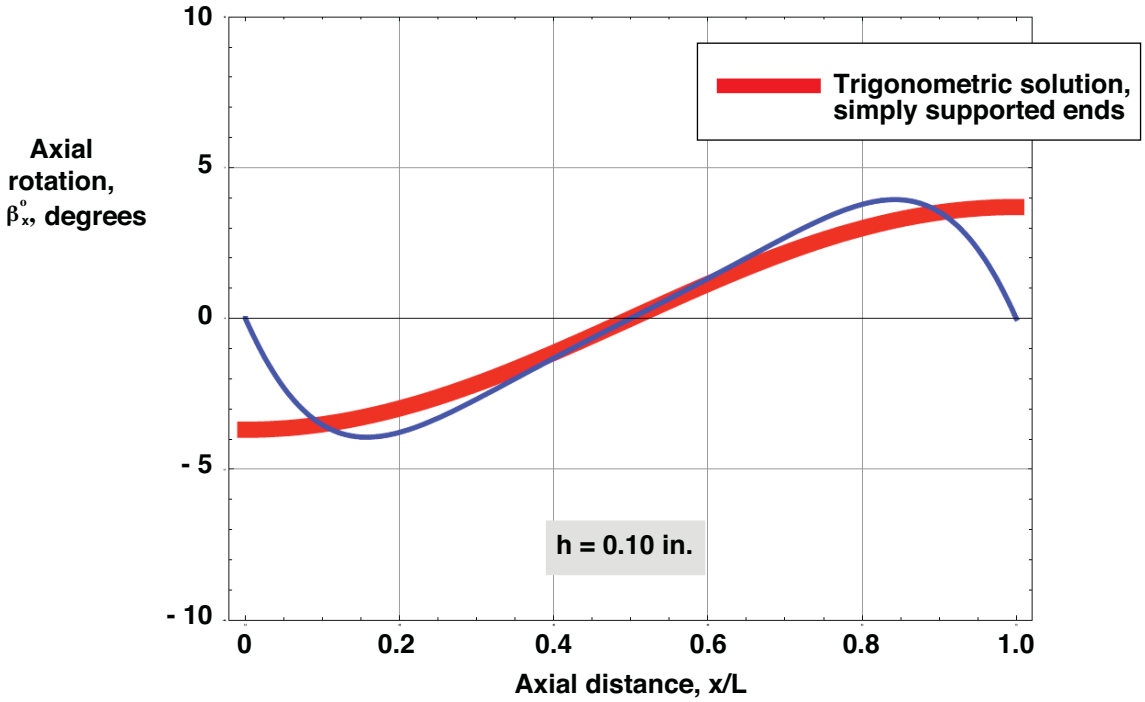

(a) Length-to-radius ratio, L/R = 0.5

Figure 39. Axial rotation of $[90_2/10_2]_T$ laminated cylinder subjected to sinusoidal pressure and temperatures, fixed at x = 0, and partially fixed at x = L to permit unrestrained axial and circumferential motion (R/h = 100).

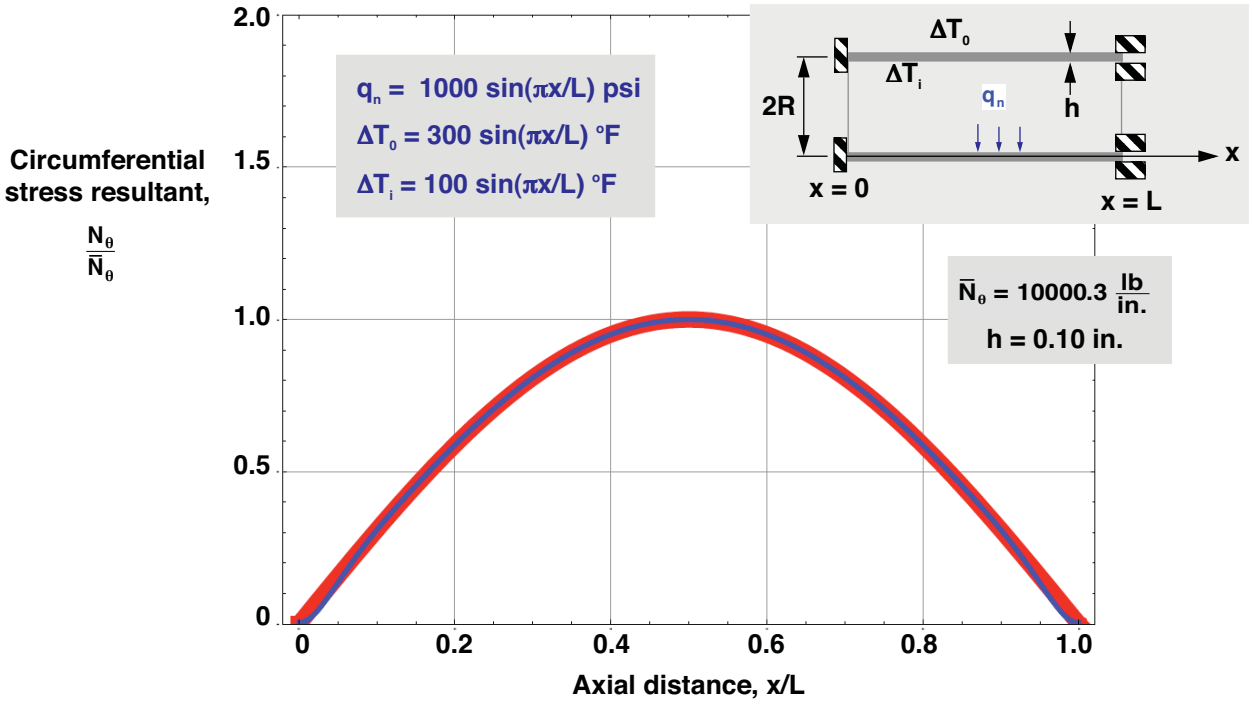

(b) Length-to-radius ratio, L/R = 2

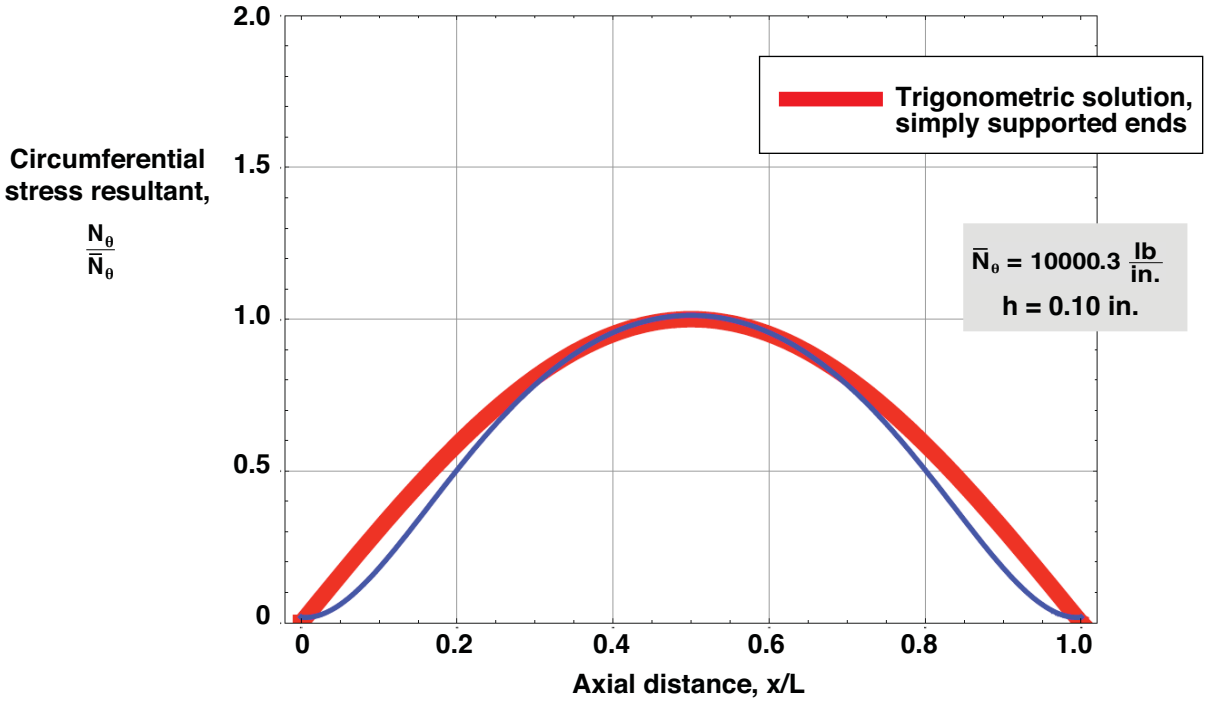

(a) Length-to-radius ratio, L/R = 0.5

Figure 40. Circumferential stress resultant of $[90_2/10_2]_T$ laminated cylinder subjected to sinusoidal pressure and temperatures, fixed at x = 0, and partially fixed at x = L to permit unrestrained axial and circumferential motion (R/h = 100).

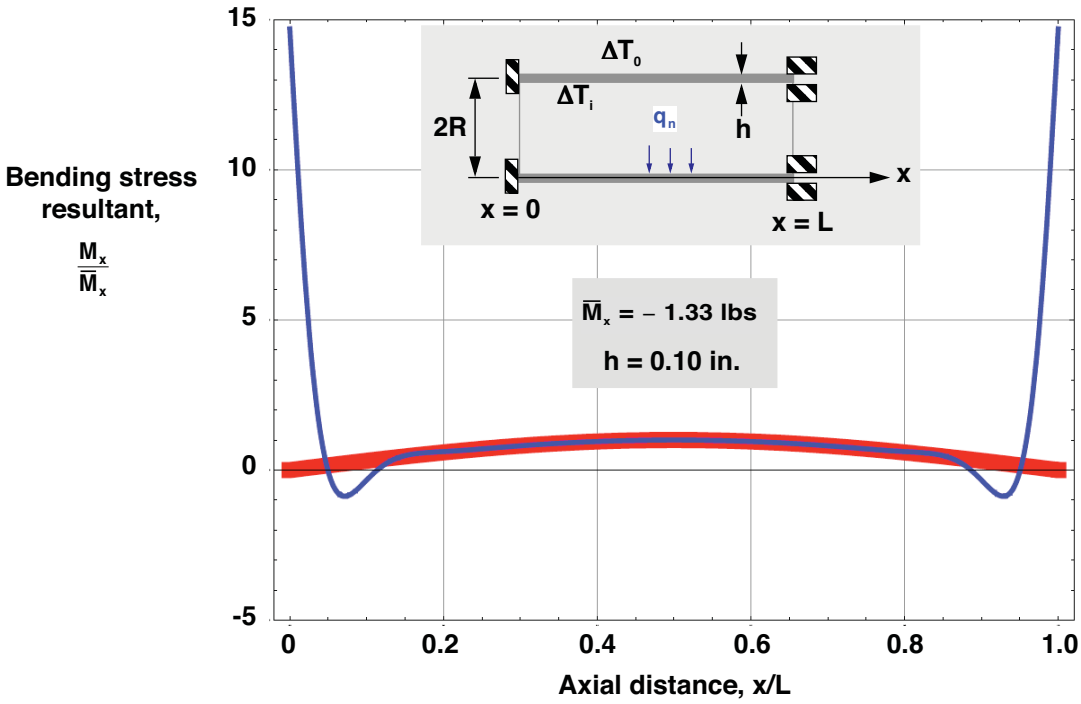

(b) Length-to-radius ratio, L/R = 2

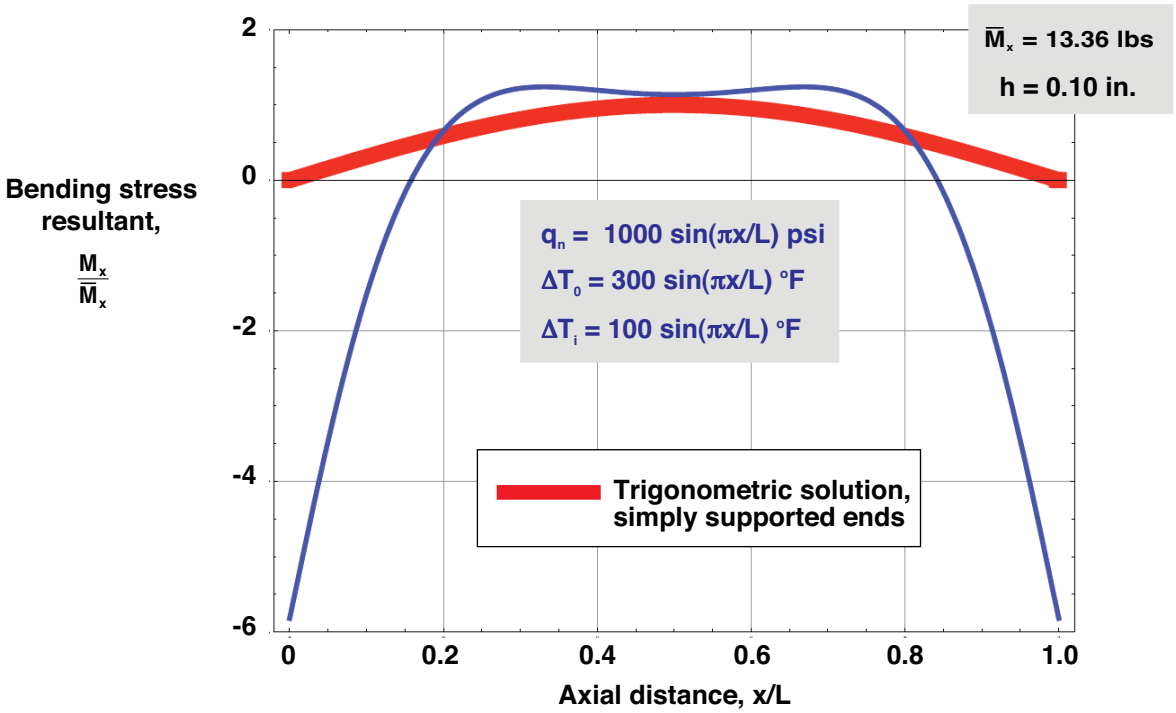

(a) Length-to-radius ratio, L/R = 0.5

Figure 41. Bending stress resultant of $[90_2/10_2]_T$ laminated cylinder subjected to sinusoidal pressure and temperatures, fixed at x = 0, and partially fixed at x = L to permit unrestrained axial and circumferential motion (R/h = 100).

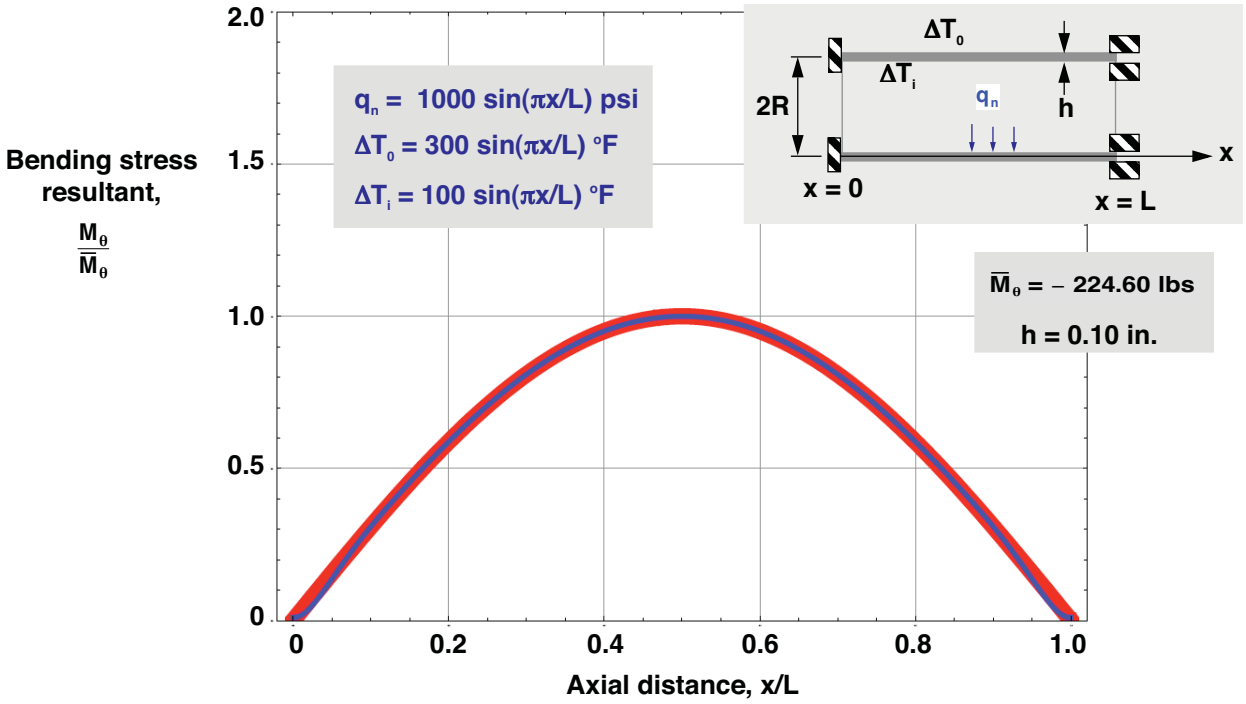

(b) Length-to-radius ratio, L/R = 2

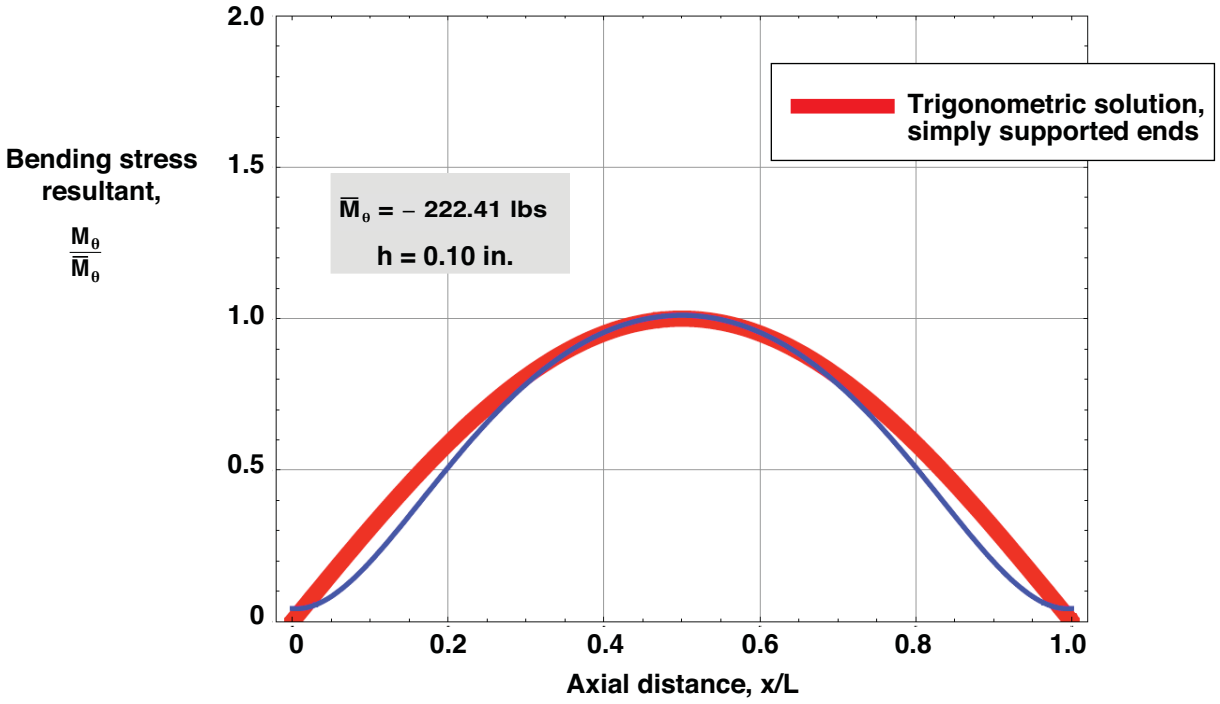

(a) Length-to-radius ratio, L/R = 0.5

Figure 42. Bending stress resultant of $[90_2/10_2]_T$ laminated cylinder subjected to sinusoidal pressure and temperatures, fixed at x = 0, and partially fixed at x = L to permit unrestrained axial and circumferential motion (R/h = 100).

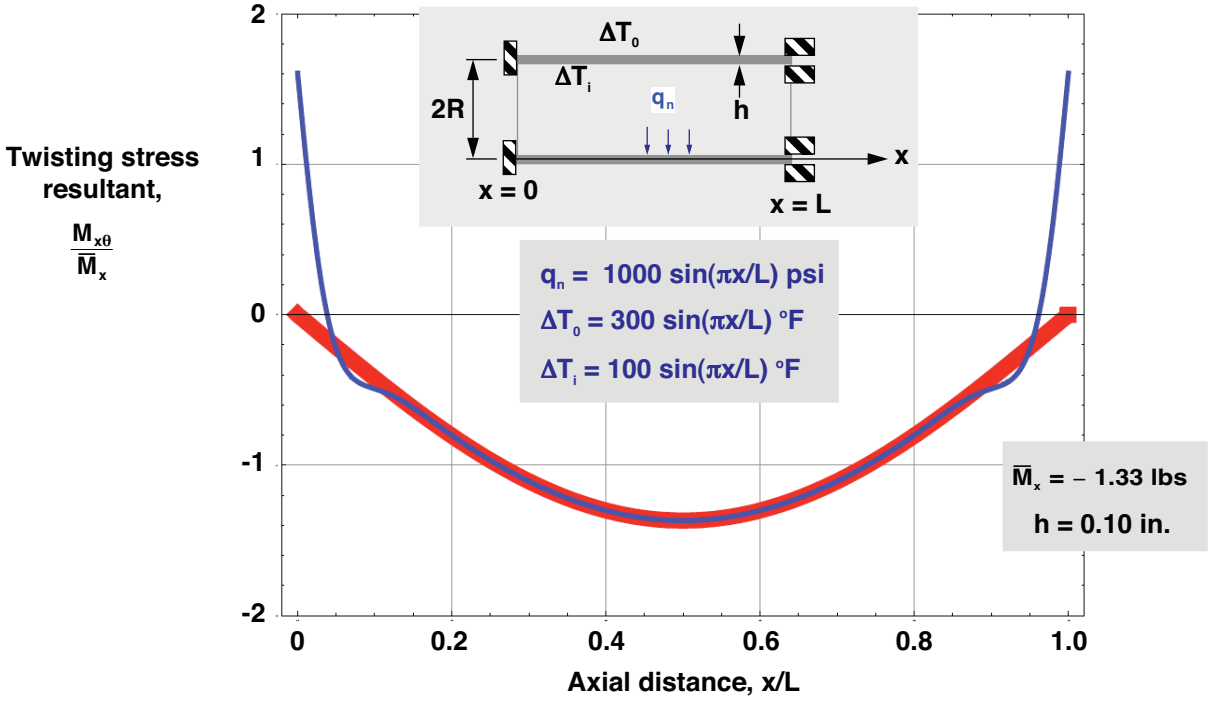

(b) Length-to-radius ratio, L/R = 2

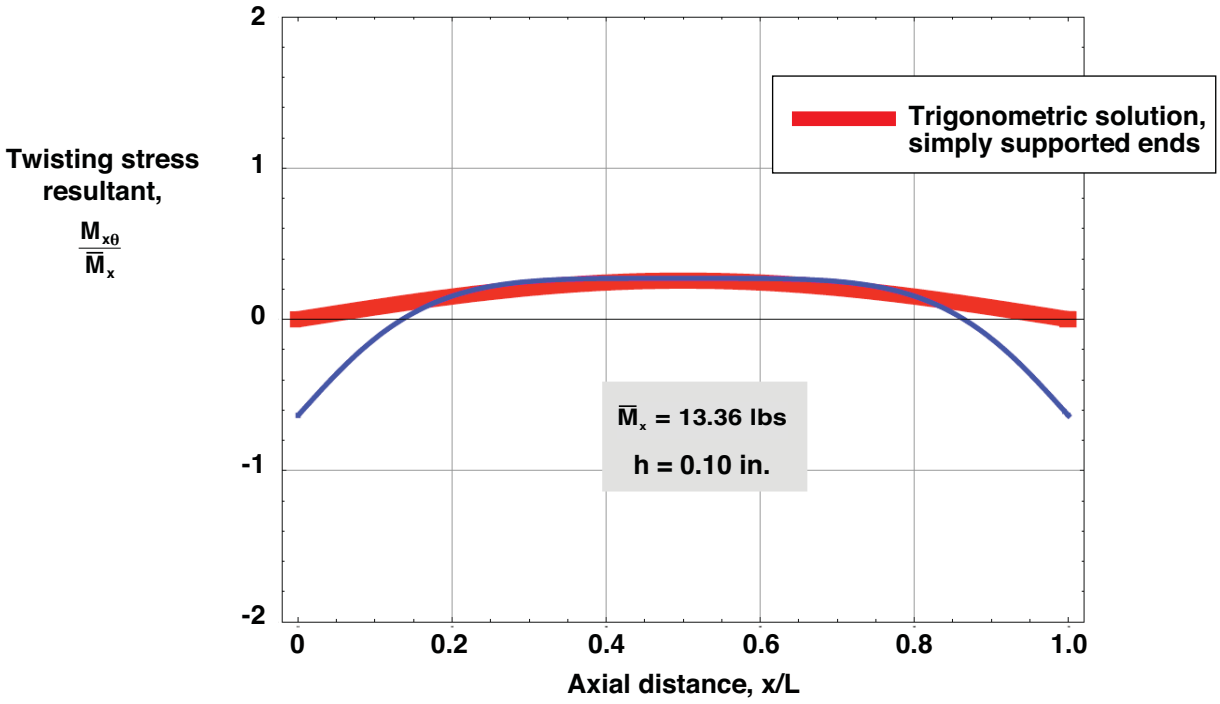

(a) Length-to-radius ratio, L/R = 0.5

Figure 43. Twisting stress resultant of $[90_2/10_2]_T$ laminated cylinder subjected to sinusoidal pressure and temperatures, fixed at x = 0, and partially fixed at x = L to permit unrestrained axial and circumferential motion (R/h = 100).

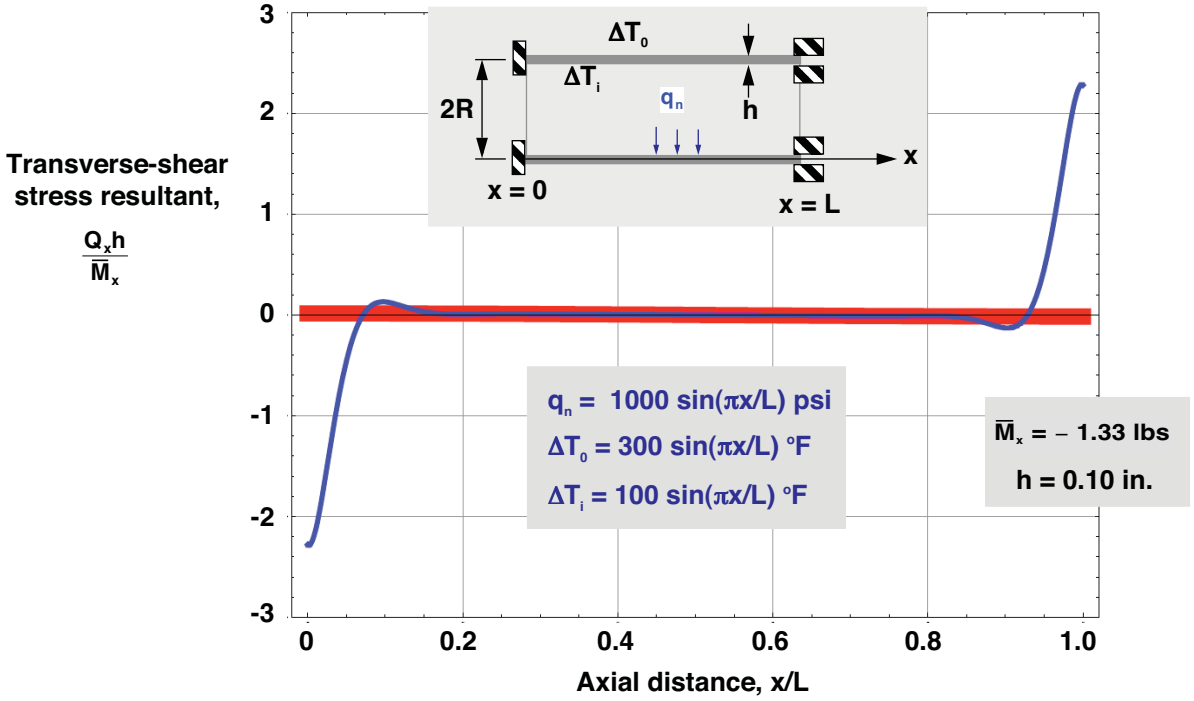

(b) Length-to-radius ratio, L/R = 2

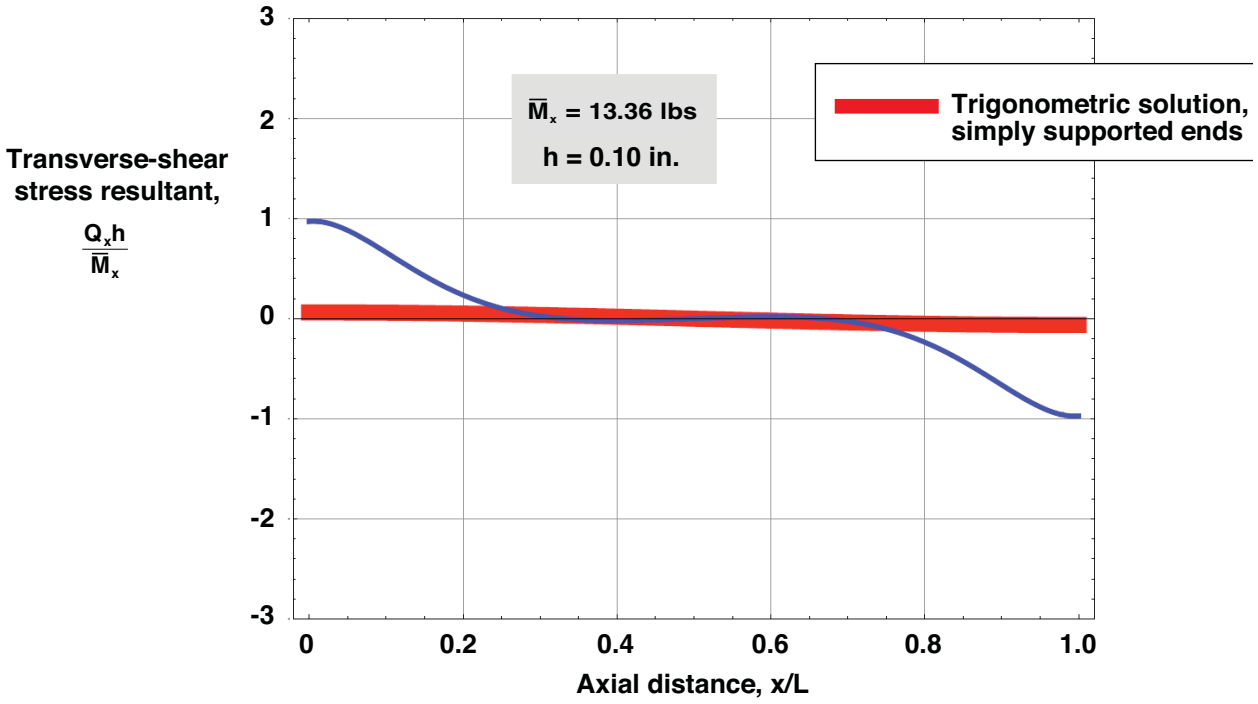

(a) Length-to-radius ratio, L/R = 0.5

Figure 44. NTransverse-shear stress resultant of $[90_2/10_2]_T$ laminated cylinder subjected to sinusoidal pressure and temperatures, fixed at x = 0, and partially fixed at x = L to permit unrestrained axial and circumferential motion (R/h = 100).

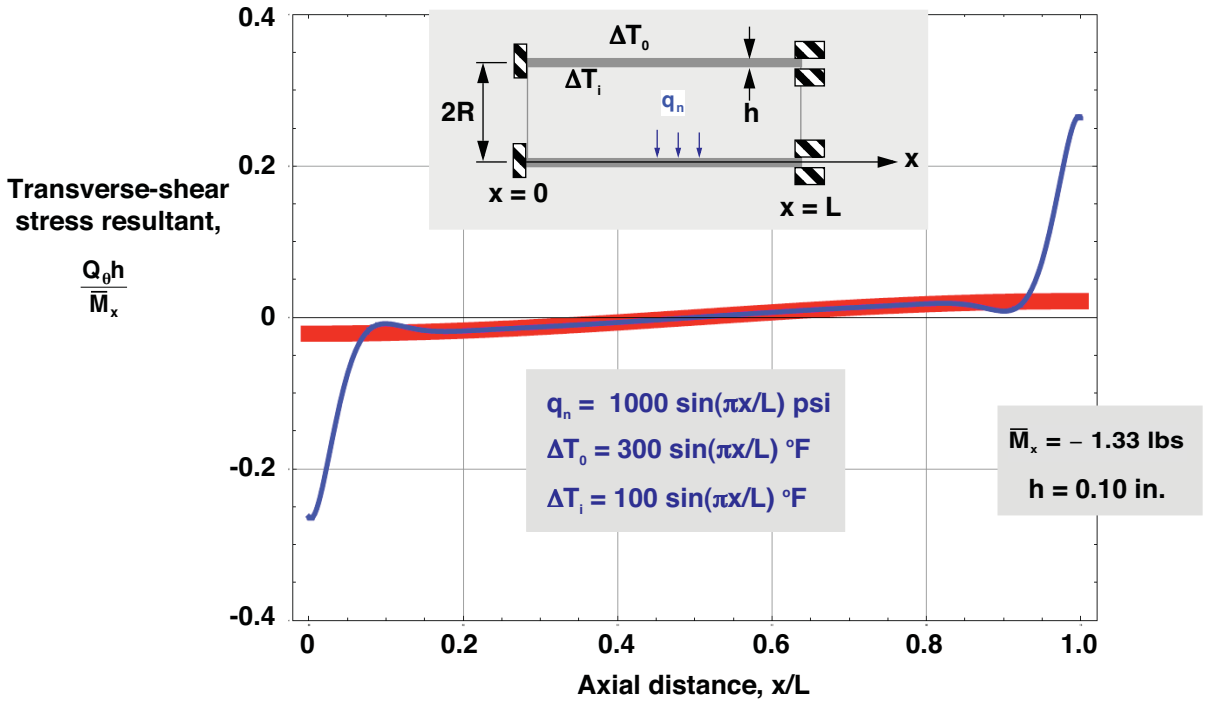

(b) Length-to-radius ratio, L/R = 2

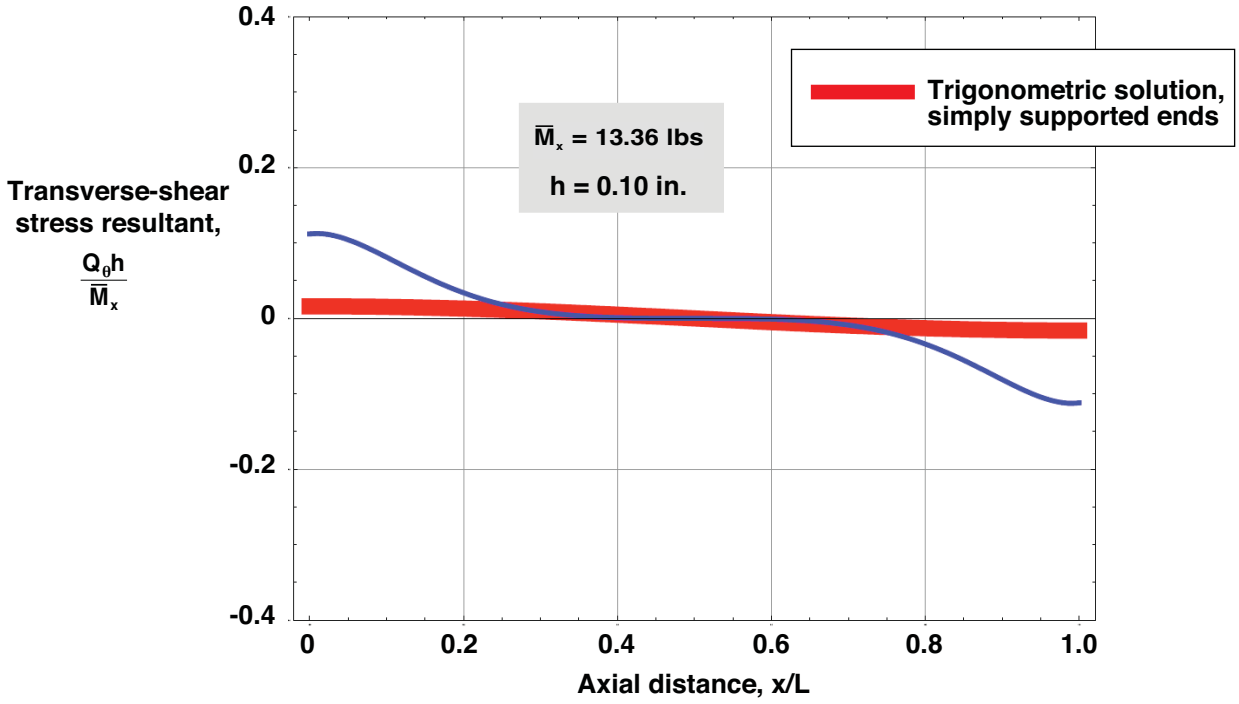

(a) Length-to-radius ratio, L/R = 0.5

Figure 45. Transverse-shear stress resultant of $[90_2/10_2]_T$ laminated cylinder subjected to sinusoidal pressure and temperatures, fixed at x = 0, and partially fixed at x = L to permit unrestrained axial and circumferential motion (R/h = 100).

Appendix A
Sanders-Koiter Equations

The linear Sanders-Koiter shell equations[24,25] are presented in this appendix for a right-circular cylinder with a radius that is given by R. For these equations, x is the axial coordinate, θ is the circumferential coordinate, and z is the radial coordinate, as shown in figure 3. First, the equilibrium equations are presented, then the kinematic equations and the constitutive equations are presented. Last, the boundary conditions are given for a complete right-circular cylinder at an edge that is given by a constant value of x.

Equilibrium Equations

The equilibrium equations are given in a form similar to those found in Ref. 24; that is,

$$\frac{\partial N_x}{\partial x} + \frac{1}{R}\frac{\partial N_{x\theta}}{\partial \theta} - \frac{c_2}{2R^2}\frac{\partial M_{x\theta}}{\partial \theta} + q_x = 0 \tag{A1}$$

$$\frac{\partial N_{x\theta}}{\partial x} + \frac{1}{R}\frac{\partial N_\theta}{\partial \theta} + \frac{c_1}{R}Q_\theta + \frac{c_2}{2R}\frac{\partial M_{x\theta}}{\partial x} + q_\theta = 0 \tag{A2}$$

$$\frac{\partial Q_x}{\partial x} + \frac{1}{R}\frac{\partial Q_\theta}{\partial \theta} - \frac{N_\theta}{R} + q_n = 0 \tag{A3}$$

$$\frac{\partial M_x}{\partial x} + \frac{1}{R}\frac{\partial M_{x\theta}}{\partial \theta} - Q_x = 0 \tag{A4}$$

$$\frac{\partial M_{x\theta}}{\partial x} + \frac{1}{R}\frac{\partial M_\theta}{\partial \theta} - Q_\theta = 0 \tag{A5}$$

where N_x, N_θ, and $N_{x\theta}$ are the membrane stress resultants; Q_x and Q_θ are the transverse shear-stress resultants; M_x, M_θ, and $M_{x\theta}$ are the bending stress resultants; q_x, q_θ, and q_n are the applied surface tractions; and c_1 and c_2 are constants that identify the equations of other shell theories that are considered herein. In particular, the Sanders-Koiter equations are given by $c_1 = c_2 = 1$ and the Love-Kirchhoff equations are give by $c_1 = 1$ and $c_2 = 0$. Donnell's equations are given by $c_1 = c_2 = 0$. This convention is used throughout the present study.

Kinematic Equations

The kinematic equations are given by

$$\varepsilon_x^o = \frac{\partial u}{\partial x} \tag{A6}$$

$$\varepsilon_\theta^o = \frac{1}{R}\frac{\partial v}{\partial \theta} + \frac{w}{R} \tag{A7}$$

$$\gamma_{x\theta}^o = \frac{\partial v}{\partial x} + \frac{1}{R}\frac{\partial u}{\partial \theta} \tag{A8}$$

$$\beta_x^o = -\frac{\partial w}{\partial x} \tag{A9}$$

$$\beta_\theta^o = \frac{c_1}{R} v - \frac{1}{R}\frac{\partial w}{\partial \theta} \tag{A10}$$

$$\beta_n^o = \frac{c_2}{2}\left(\frac{\partial v}{\partial x} - \frac{1}{R}\frac{\partial u}{\partial \theta}\right) \tag{A11}$$

$$\kappa_x^o = \frac{\partial \beta_x^o}{\partial x} = -\frac{\partial^2 w}{\partial x^2} \tag{A12}$$

$$\kappa_\theta^o = \frac{1}{R}\frac{\partial \beta_\theta^o}{\partial \theta} = \frac{c_1}{R^2}\frac{\partial v}{\partial \theta} - \frac{1}{R^2}\frac{\partial^2 w}{\partial \theta^2} \tag{A13}$$

$$\kappa_{x\theta}^o = \frac{1}{R}\left(\frac{\partial \beta_x^o}{\partial \theta} + \beta_n^o\right) + \frac{\partial \beta_\theta^o}{\partial x} = -\frac{2}{R}\frac{\partial^2 w}{\partial x \partial \theta} + \frac{1}{R}\left(c_1 + \frac{1}{2}c_2\right)\frac{\partial v}{\partial x} - \frac{c_2}{2R^2}\frac{\partial u}{\partial \theta} \tag{A14}$$

where u, v, and w are the axial, circumferential, and radial displacements of a point of the shell middle surface; ε_x^o, ε_θ^o, and $\gamma_{x\theta}^o$ are the membrane strains; β_x^o, β_θ^o, and β_n^o are the rotations; and κ_x^o, κ_θ^o, and $\kappa_{x\theta}^o$ are the bending strains. The displacement w is positive when it is outward from the cylinder reference surface.

Constitutive Equations

The isothermal constitutive equations are given in matrix form by

$$\begin{Bmatrix} N_x \\ N_\theta \\ N_{x\theta} \\ \hdashline M_x \\ M_\theta \\ M_{x\theta} \end{Bmatrix} = \left[\begin{array}{ccc:ccc} A_{11} & A_{12} & A_{16} & B_{11} & B_{12} & B_{16} \\ A_{12} & A_{22} & A_{26} & B_{12} & B_{22} & B_{26} \\ A_{16} & A_{26} & A_{66} & B_{16} & B_{26} & B_{66} \\ \hdashline B_{11} & B_{12} & B_{16} & D_{11} & D_{12} & D_{16} \\ B_{12} & B_{22} & B_{26} & D_{12} & D_{22} & D_{26} \\ B_{16} & B_{26} & B_{66} & D_{16} & D_{26} & D_{66} \end{array}\right] \begin{Bmatrix} \varepsilon_x^o \\ \varepsilon_\theta^o \\ \gamma_{x\theta}^o \\ \hdashline \kappa_x^o \\ \kappa_\theta^o \\ \kappa_{x\theta}^o \end{Bmatrix} - \begin{Bmatrix} N_x^{Th} \\ N_\theta^{Th} \\ N_{x\theta}^{Th} \\ \hdashline M_x^{Th} \\ M_\theta^{Th} \\ M_{x\theta}^{Th} \end{Bmatrix} \tag{A15}$$

where the subscripted A, B, and D terms of the matrix are the stiffnesses of laminated composite shells that are obtained from the Love-Kirchhoff shell theory. Moreover, the constitutive terms in Eq. (A15) are identical to those for laminated-composite plates that are given in Ref. 34 on pp. 198 and 243-244. The terms with the superscript "Th" are the ficticious thermal stress resultants.

Boundary Conditions

The boundary conditions for an edge that is defined by a constant value of the axial coordinate x are given by

$$N_x = \tilde{N}(\theta) \quad \text{or} \quad u = \tilde{u}(\theta) \tag{A16}$$

$$N_{x\theta} + \frac{1}{R}\left(c_1 + \frac{1}{2}c_2\right)M_{x\theta} = \tilde{T}(\theta) \quad \text{or} \quad v = \tilde{v}(\theta) \tag{A17}$$

$$Q_x + \frac{1}{R}\frac{\partial M_{x\theta}}{\partial \theta} = \tilde{V}(\theta) \quad \text{or} \quad w = \tilde{w}(\theta) \tag{A18}$$

$$M_x = \tilde{M}(\theta) \quad \text{or} \quad \beta_x^o = \tilde{\beta}(\theta) \tag{A19}$$

where $\tilde{u}(\theta)$, $\tilde{v}(\theta)$, and $\tilde{w}(\theta)$ are applied edge displacements; $\tilde{\beta}(\theta)$ is an applied edge rotation; and $\tilde{N}(\theta)$, $\tilde{T}(\theta)$, $\tilde{V}(\theta)$, and $\tilde{M}(\theta)$ are applied edge loads.

Appendix B
Equations for Axisymmetry

The linear Sanders-Koiter shell equations that are presented in Appendix A for a right-circular cylinder with a radius R are specialized in this appendix for the case of axisymmetric behavior. For these equations, x and θ denote the axial and circumferential coordinates, respectively. The specialization to axial symmetry is conducted by eliminating all terms in the equations of Appendix A that are differentiatied with respect to the circumferential coordinate, θ. First, the equilibrium equations, the kinematic equations, and the constitutive equations are presented. Then, the boundary conditions are given for a complete right-circular cylinder at an edge that is given by a constant value of x.

Equilibrium Equations

The equilibrium equations for axisymmetric behavior are given by

$$\frac{dN_x}{dx} + q_x(x) = 0 \tag{B1}$$

$$\frac{dN_{x\theta}}{dx} + \frac{c_1}{R}Q_\theta + \frac{c_2}{2R}\frac{dM_{x\theta}}{dx} + q_\theta(x) = 0 \tag{B2}$$

$$\frac{dQ_x}{dx} - \frac{N_\theta}{R} + q_n(x) = 0 \tag{B3}$$

$$\frac{dM_x}{dx} - Q_x = 0 \tag{B4}$$

$$\frac{dM_{x\theta}}{dx} - Q_\theta = 0 \tag{B5}$$

where the membrane stress resultants N_x, N_θ, and $N_{x\theta}$; the transverse shear-stress resultants Q_x and Q_θ; the bending stress resultants M_x, M_θ, and $M_{x\theta}$; and the applied surface tractions q_x, q_θ, and q_n are functions of only the axial coordinate, x.

Kinematic Equations

The kinematic equations are given by

$$\varepsilon_x^o = \frac{du}{dx} \tag{B6}$$

$$\varepsilon_\theta^o = \frac{w}{R} \tag{B7}$$

$$\gamma_{x\theta}^{o} = \frac{dv}{dx} \tag{B8}$$

$$\beta_{x}^{o} = -\frac{dw}{dx} \tag{B9}$$

$$\beta_{\theta}^{o} = \frac{c_1}{R} v \tag{B10}$$

$$\beta_{n}^{o} = \frac{c_2}{2}\frac{dv}{dx} \tag{B11}$$

$$\kappa_{x}^{o} = \frac{d\beta_{x}^{o}}{dx} = -\frac{d^2 w}{dx^2} \tag{B12}$$

$$\kappa_{\theta}^{o} = 0 \tag{B13}$$

$$\kappa_{x\theta}^{o} = \frac{1}{R}\beta_{n}^{o} + \frac{d\beta_{\theta}^{o}}{dx} = \frac{1}{R}\left(c_1 + \frac{1}{2}c_2\right)\frac{dv}{dx} \tag{B14}$$

where the middle-surface displacements u, v, and w; the membrane strains ε_{x}^{o}, ε_{θ}^{o}, and $\gamma_{x\theta}^{o}$; the rotations β_{x}^{o}, β_{θ}^{o}, and β_{n}^{o}; and the bending strains κ_{x}^{o}, κ_{θ}^{o}, and $\kappa_{x\theta}^{o}$ are functions of only the axial coordinate, x.

Constitutive Equations

The constitutive equations reduce to

$$\begin{Bmatrix} N_x \\ N_\theta \\ \hdashline N_{x\theta} \\ M_x \\ M_\theta \\ M_{x\theta} \end{Bmatrix} = \left[\begin{array}{ccc:ccc} A_{11} & A_{12} & A_{16} & B_{11} & B_{12} & B_{16} \\ A_{12} & A_{22} & A_{26} & B_{12} & B_{22} & B_{26} \\ A_{16} & A_{26} & A_{66} & B_{16} & B_{26} & B_{66} \\ \hdashline B_{11} & B_{12} & B_{16} & D_{11} & D_{12} & D_{16} \\ B_{12} & B_{22} & B_{26} & D_{12} & D_{22} & D_{26} \\ B_{16} & B_{26} & B_{66} & D_{16} & D_{26} & D_{66} \end{array}\right] \begin{Bmatrix} \varepsilon_{x}^{o} \\ \varepsilon_{\theta}^{o} \\ \hdashline \gamma_{x\theta}^{o} \\ \kappa_{x}^{o} \\ 0 \\ \kappa_{x\theta}^{o} \end{Bmatrix} - \begin{Bmatrix} N_{x}^{Th} \\ N_{\theta}^{Th} \\ \hdashline N_{x\theta}^{Th} \\ M_{x}^{Th} \\ M_{\theta}^{Th} \\ M_{x\theta}^{Th} \end{Bmatrix} \tag{B15}$$

For thin shells, it is convenient to introduce a temperature-change function

$$\Delta T(x, z) = \Theta_0(x) + z\,\Theta_1(x) \tag{B16a}$$

such that

$$\Theta_0(x) = \frac{1}{2}\left[\Delta T\left(x, \frac{h}{2}\right) + \Delta T\left(x, -\frac{h}{2}\right)\right] \tag{B16b}$$

$$\Theta_1(x) = \frac{1}{h}\left[\Delta T\left(x, \frac{h}{2}\right) - \Delta T\left(x, -\frac{h}{2}\right)\right] \tag{B16c}$$

and

$$\begin{Bmatrix} N_x^{Th} \\ N_\theta^{Th} \\ N_{x\theta}^{Th} \\ \hdashline M_x^{Th} \\ M_\theta^{Th} \\ M_{x\theta}^{Th} \end{Bmatrix} = \Theta_0(x) \begin{Bmatrix} n_x^{Th} \\ n_\theta^{Th} \\ n_{x\theta}^{Th} \\ \hdashline c_x^{Th} \\ c_\theta^{Th} \\ c_{x\theta}^{Th} \end{Bmatrix} + \Theta_1(x) \begin{Bmatrix} c_x^{Th} \\ c_\theta^{Th} \\ c_{x\theta}^{Th} \\ \hdashline m_x^{Th} \\ m_\theta^{Th} \\ m_{x\theta}^{Th} \end{Bmatrix} \tag{B17}$$

where the two vectors on the right-hand-side of the equal sign are the constants that result from substituting equation (B16) into expressions for the ficticious thermal stress resultants, like those given on pp. 243-244 of reference 34.

Boundary Conditions

The boundary conditions for an edge that is defined by a constant value of the axial coordinate, x, are given by

$$N_x = \tilde{N} \quad \text{or} \quad u = \tilde{u} \tag{B18}$$

$$N_{x\theta} + \frac{1}{R}\left(c_1 + \frac{1}{2}c_2\right)M_{x\theta} = \tilde{T} \quad \text{or} \quad v = \tilde{v} \tag{B19}$$

$$Q_x = \tilde{V} \quad \text{or} \quad w = \tilde{w} \tag{B20}$$

$$M_x = \tilde{M} \quad \text{or} \quad \beta_x^o = \tilde{\beta} \tag{B21}$$

where the applied edge displacements $\tilde{u}$, $\tilde{v}$, and $\tilde{w}$; the applied edge rotation $\tilde{\beta}$; and the applied edge loads $\tilde{N}$, $\tilde{T}$, $\tilde{V}$, and $\tilde{M}$ are all constants.

Appendix C
Approximate Solution for Uniform Axial End Load

For this example, the boundary conditions are specified as

$$u(0) = 0 \tag{C1a}$$

$$v(0) = 0 \tag{C1b}$$

$$w(0) = 0 \tag{C1c}$$

$$M_x(0) = 0 \tag{C1d}$$

at $x = 0$ and

$$N_x(L) = \tilde{N}_L \tag{C2a}$$

$$v(L) = 0 \tag{C2b}$$

$$w(L) = 0 \tag{C2c}$$

$$M_x(L) = 0 \tag{C2d}$$

at $x = L$. The only applied load is that defined by equation (C2a). An approximate solution is found by applying the equations of linear membrane theory, in which the bending boundary layer is ignored such that the radial displacement is presumed to be constant valued. First, equation (B1) gives a constant value for the axial stress resultant N_x. Thus, the boundary condition given by equation (C2a) yields the result $N_x(x) = \tilde{N}_L$. Similarly, equation (5) yields $\hat{T}(x) = \bar{T}_0$, where $\bar{T}_0$ is an unknown constant. However, because this problem does not have a boundary condition specified for $\hat{T}(x)$, the problem is statically indeterminate. Next, the transverse-shear stress resultant Q_x, that arises from variations in the bending stress resultant M_x (see equation (B4)), is neglected in equation (B3) to get $N_\theta(x) = 0$. Similarly, the derivatives of the radial displacement w vanish and, as a result, the rotation $\beta_x^\circ = 0$ the bending strain $\kappa_x^\circ = 0$. The matrix constitutive equation given by equation (14) reduces to

$$\begin{Bmatrix} u'(x) \\ v'(x) \end{Bmatrix} = \begin{bmatrix} \bar{a}_{11} & \bar{a}_{16} \\ \bar{a}_{16} & \bar{a}_{66} \end{bmatrix} \begin{Bmatrix} \tilde{N}_L \\ \bar{T}_0 \end{Bmatrix} + \begin{Bmatrix} \bar{\ell}_{12} \\ \bar{\ell}_{62} \end{Bmatrix} \frac{W}{R} \tag{C3}$$

In addition, equation (16a) reduces to

$$A_{22}\frac{w}{R} = -A_{12}u' - \bar{A}_{26}v' \tag{C4}$$

Substituting equation (C4) into (C3) yields

$$\begin{bmatrix} \left(A_{22} + A_{12}\bar{\ell}_{12}\right) & \bar{A}_{26}\bar{\ell}_{12} \\ A_{12}\bar{\ell}_{62} & \left(A_{22} + \bar{A}_{26}\bar{\ell}_{62}\right) \end{bmatrix} \begin{Bmatrix} u' \\ v' \end{Bmatrix} = A_{22}\begin{bmatrix} \bar{a}_{11} & \bar{a}_{16} \\ \bar{a}_{16} & \bar{a}_{66} \end{bmatrix} \begin{Bmatrix} \tilde{N}_L \\ \bar{T}_0 \end{Bmatrix} \tag{C5}$$

Integration of these equations reveals that u(x) and v(x) are linear functions. The only possible way that the boundary conditions given by (C1b) and (C2b) can be satisfied is for $v(x) = 0$. Thus, equation (C5) can be expressed as (see equations (13))

$$\begin{Bmatrix} \tilde{N}_L \\ \bar{T}_0 \end{Bmatrix} = \begin{bmatrix} A_{11} & \bar{A}_{16} \\ \bar{A}_{16} & \bar{A}_{66} \end{bmatrix} \begin{Bmatrix} u'(x) \\ 0 \end{Bmatrix} + \begin{Bmatrix} A_{12} \\ \bar{A}_{26} \end{Bmatrix} \frac{w}{R} \tag{C6}$$

In addition, equation (C4) gives

$$u' = -\frac{A_{22}}{A_{12}}\frac{w}{R} \tag{C7}$$

Substituting equation (C7) into the first of equations (C6) gives the result

$$\frac{w}{R} = -\frac{A_{12}\tilde{N}_L}{A_{11}A_{22} - A_{12}^2} \tag{C8}$$

Next, substituting equation (C8) into equation (C7), integrating, and applying boundary-condition equation (C1a) gives the result

$$u(x) = \frac{A_{22}\tilde{N}_L x}{A_{11}A_{22} - A_{12}^2} \tag{C9}$$

Substituting equations (C8) and (C9) into the second of equations (C6) gives

$$\bar{T}_0 = \frac{A_{22}\bar{A}_{16} - A_{12}\bar{A}_{26}}{A_{11}A_{22} - A_{12}^2}\tilde{N}_L \tag{C10}$$

Approximations to the bending stress resultants are obtained by substituting $v(x) = 0$ and equations (C8) and (C9) into equations (17a), (82), and (88) to get

$$M_x(x) = \frac{A_{22}B_{11} - A_{12}B_{12}}{A_{11}A_{22} - A_{12}^2}\,\tilde{N}_L \tag{C11}$$

$$M_\theta(x) = \frac{A_{22}B_{12} - A_{12}B_{22}}{A_{11}A_{22} - A_{12}^2}\,\tilde{N}_L \tag{C12}$$

$$M_{x\theta}(x) = \frac{A_{22}B_{16} - A_{12}B_{26}}{A_{11}A_{22} - A_{12}^2}\,\tilde{N}_L \tag{C13}$$

Because these bending stress resultants are constants, it follows that the transverse-shear stress resultants Q_x and Q_θ are zero valued (see equations (B4) and (B5)). An approximation to $N_{x\theta}$ is obtained by substituting $\hat{T}(x) = \overline{T}_0$ and equation (C13) into equation (4).

Appendix D
Approximate Solution for Uniform Pressure and Temperatures

For this example, the boundary conditions are specified as

$$u(0) = 0 \tag{D1a}$$

$$v(0) = 0 \tag{D1b}$$

$$w(0) = 0 \tag{D1c}$$

$$\beta_x^o(0) = 0 \tag{D1d}$$

at $x = 0$ and

$$u(L) = 0 \tag{D2a}$$

$$v(L) = 0 \tag{D2b}$$

$$w(L) = 0 \tag{D2c}$$

$$\beta_x^o(L) = 0 \tag{D2d}$$

at $x = L$. The applied mechanical load is given by $q_n(x) = q_n^0$ and the applied thermal load is given by $\Theta_0(x) = H_0$ and $\Theta_1(x) = G_0$. For these loading conditions, equations (1b) and (7b) yield $\bar{N}_1(x) = 0$ and $\bar{T}_1(x) = 0$. Likewise, equations (100) reduce to

$$N_x^{Th}(x) = H_0 n_x^{Th} + G_0 c_x^{Th} \tag{D3a}$$

$$N_\theta^{Th}(x) = H_0 n_\theta^{Th} + G_0 c_\theta^{Th} \tag{D3b}$$

$$M_x^{Th}(x) = H_0 c_x^{Th} + G_0 m_x^{Th} \tag{D3c}$$

$$\hat{T}^{Th}(x) = H_0 \bar{n}_{x\theta}^{Th} + G_0 \bar{c}_{x\theta}^{Th} \tag{D3d}$$

In addition, equation (B17) yields

$$N_{x\theta}^{Th}(x) = H_0 n_{x\theta}^{Th} + G_0 c_{x\theta}^{Th} \tag{D3e}$$

$$M_{\theta}^{Th}(x) = H_0 c_{\theta}^{Th} + G_0 m_{\theta}^{Th} \tag{D3f}$$

$$M_{x\theta}^{Th}(x) = H_0 c_{x\theta}^{Th} + G_0 m_{x\theta}^{Th} \tag{D3g}$$

An approximate solution is found by applying the equations of linear membrane theory, in which the bending boundary layer is ignored such that the radial displacement is presumed to be constant valued. First, equations (1) and (7) give constant values for the axial stress resultant , $N_x(x) = \bar{N}_0$, and the torsional stress resultant, $\hat{T}(x) = \bar{T}_0$, where $\bar{N}_0$ and $\bar{T}_0$ are unknown constants. Because this problem does not have any stress-resultant boundary conditions, the problem is statically indeterminate. Next, the transverse-shear stress resultant Q_x, that arises from variations in the bending stress resultant M_x (see equation (B4)), is neglected in equation (B3) to get $N_\theta(x) = q_n^0 R$. Similarly, the derivatives of the radial displacement w vanish and, as a result, the rotation $\beta_x^o = 0$ and the bending strain $\kappa_x^o = 0$. The matrix constitutive equation given by equation (14) reduces to

$$\begin{Bmatrix} u'(x) \\ v'(x) \end{Bmatrix} = \begin{bmatrix} \bar{a}_{11} & \bar{a}_{16} \\ \bar{a}_{16} & \bar{a}_{66} \end{bmatrix} \begin{Bmatrix} \bar{N}_0 + N_x^{Th}(x) \\ \bar{T}_0 + \hat{T}^{Th}(x) \end{Bmatrix} + \begin{Bmatrix} \bar{\ell}_{12} \\ \bar{\ell}_{62} \end{Bmatrix} \frac{w}{R} \tag{D4}$$

In addition, equation (16a) reduces to

$$A_{22} \frac{w}{R} = q_n^0 R + N_\theta^{Th} - A_{12} u' - \bar{A}_{26} v' \tag{D5}$$

Substituting equation (D5) into (D4) yields

$$\begin{bmatrix} \left(A_{22} + A_{12}\bar{\ell}_{12}\right) & \bar{A}_{26}\bar{\ell}_{12} \\ A_{12}\bar{\ell}_{62} & \left(A_{22} + \bar{A}_{26}\bar{\ell}_{62}\right) \end{bmatrix} \begin{Bmatrix} u' \\ v' \end{Bmatrix} = A_{22} \begin{bmatrix} \bar{a}_{11} & \bar{a}_{16} \\ \bar{a}_{16} & \bar{a}_{66} \end{bmatrix} \begin{Bmatrix} \bar{N}_0 + N_x^{Th} \\ \bar{T}_0 + \hat{T}^{Th} \end{Bmatrix} + \begin{Bmatrix} \bar{\ell}_{12} \\ \bar{\ell}_{62} \end{Bmatrix} \left(q_n^0 R + N_\theta^{Th}\right) \tag{D6}$$

Integration of these equations reveals that u(x) and v(x) are linear functions. The only possible way that the boundary conditions given by (D1a), (D1b), (D2a), and (D2b) can be satisfied is for u(x) = 0 and v(x) = 0. Thus, the left-hand-side of equation (D4) vanishes and the resulting equations are expressed as (see equations (13))

$$\begin{Bmatrix} \overline{N}_0 \\ \overline{T}_0 \end{Bmatrix} = \begin{Bmatrix} A_{12} \\ \overline{A}_{26} \end{Bmatrix} \frac{w}{R} - \begin{Bmatrix} N_x^{Th} \\ \hat{T}^{Th} \end{Bmatrix} \tag{D7}$$

In addition, equation (D5) reduces to

$$A_{22} \frac{w}{R} = q_n^0 R + N_\theta^{Th} \tag{D8}$$

Substituting equation (D8) into (D7) gives the results

$$\begin{Bmatrix} \overline{N}_0 \\ \overline{T}_0 \end{Bmatrix} = \left(\frac{q_n^0 R + N_\theta^{Th}}{A_{22}} \right) \begin{Bmatrix} A_{12} \\ \overline{A}_{26} \end{Bmatrix} - \begin{Bmatrix} N_x^{Th} \\ \hat{T}^{Th} \end{Bmatrix} \tag{D9}$$

Approximations to the bending stress resultants are obtained by substituting u(x) = 0, v(x) = 0, and equations (D8) into equations (17a), (82), and (88) to get

$$M_x = \frac{B_{12}}{A_{22}} \left(q_n^0 R + N_\theta^{Th} \right) - M_x^{Th} \tag{D10}$$

$$M_\theta = \frac{B_{22}}{A_{22}} \left(q_n^0 R + N_\theta^{Th} \right) - M_\theta^{Th} \tag{D11}$$

$$M_{x\theta} = \frac{B_{26}}{A_{22}} \left(q_n^0 R + N_\theta^{Th} \right) - M_{x\theta}^{Th} \tag{D12}$$

Because these bending stress resultants are constants, if follows that the transverse-shear stress resultants Q_x and Q_θ are zero valued (see equations (B4) and (B5). An approximation to $N_{x\theta}$ is obtained by substituting $\hat{T}(x) = \overline{T}_0$ and equation (D12) into equation (4).

Appendix E
Approximate Solution for Linearly Varying Pressure and Temperatures

For this example, the boundary conditions are specified as

$$N_x(0) = \tilde{N}_0 \tag{E1a}$$

$$\hat{T}(0) = \tilde{T}_0 \tag{E1b}$$

$$w(0) = 0 \tag{E1c}$$

$$M_x(0) = 0 \tag{E1d}$$

at $x = 0$ and

$$u(L) = 0 \tag{E2a}$$

$$v(L) = 0 \tag{E2b}$$

$$w(L) = 0 \tag{E2c}$$

$$M_x(L) = 0 \tag{E2d}$$

at $x = L$. The applied pressure load given by $q_n(x) = q_n^0 + q_n^1 x$ and the applied thermal load is given by $\Theta_0(x) = H_0 + H_1 x$ and $\Theta_1(x) = G_0 + G_1 x$. For these loading conditions, equations (1b) and (7b) yield $\bar{N}_1(x) = 0$ and $\bar{T}_1(x) = 0$. Likewise, equations (100) reduce to

$$N_x^{Th}(x) = \left(H_0 n_x^{Th} + G_0 c_x^{Th}\right) + \left(H_1 n_x^{Th} + G_1 c_x^{Th}\right)x \tag{E3a}$$

$$N_\theta^{Th}(x) = \left(H_0 n_\theta^{Th} + G_0 c_\theta^{Th}\right) + \left(H_1 n_\theta^{Th} + G_1 c_\theta^{Th}\right)x \tag{E3b}$$

$$M_x^{Th}(x) = \left(H_0 c_x^{Th} + G_0 m_x^{Th}\right) + \left(H_1 c_x^{Th} + G_1 m_x^{Th}\right)x \tag{E3c}$$

$$\hat{T}^{Th}(x) = \left(H_0 \bar{n}_{x\theta}^{Th} + G_0 \bar{c}_{x\theta}^{Th}\right) + \left(H_1 \bar{n}_{x\theta}^{Th} + G_1 \bar{c}_{x\theta}^{Th}\right)x \tag{E3d}$$

An approximate solution is found by applying the equations of linear membrane theory, in which

the bending boundary layer is ignored such that the radial displacement is presumed to vary like the pressure and temperature fields; that is,

$$w(x) = W_0 + W_1\, x \tag{E4}$$

First, equations (1) and (7) give constant values for the axial stress resultant , $N_x(x) = \bar{N}_0$, and the torsional stress resultant, $\hat{T}(x) = \bar{T}_0$, where $\bar{N}_0$ and $\bar{T}_0$ constants determined from applying boundary-condition equations (E1a) and (E1b). Applying these boundary conditions yields

$$N_x(x) = \bar{N}_0 = \tilde{N}_0 \tag{E5a}$$

$$\hat{T}(x) = \bar{T}_0 = \tilde{T}_0 \tag{E5b}$$

By using equations (E3), (E4), and (E5), the matrix constitutive equation given by equation (14) is reduced to

$$\begin{Bmatrix} u'(x) \\ v'(x) \end{Bmatrix} = \begin{bmatrix} \bar{a}_{11} & \bar{a}_{16} \\ \bar{a}_{16} & \bar{a}_{66} \end{bmatrix} \begin{Bmatrix} \tilde{N}_0 + H_0 n_x^{Th} + G_0 c_x^{Th} + \left(H_1 n_x^{Th} + G_1 c_x^{Th}\right) x \\ \tilde{T}_0 + H_0 \bar{n}_{x\theta}^{Th} + G_0 \bar{c}_{x\theta}^{Th} + \left(H_1 \bar{n}_{x\theta}^{Th} + G_1 \bar{c}_{x\theta}^{Th}\right) x \end{Bmatrix} + \begin{Bmatrix} \bar{\ell}_{12} \\ \bar{\ell}_{62} \end{Bmatrix} \frac{W_0 + W_1\, x}{R} \tag{E6}$$

Integrating these equations and applying boundary-condition equations (E2a) and (E2b) gives

$$\begin{Bmatrix} u(x) \\ v(x) \end{Bmatrix} = \begin{bmatrix} \bar{a}_{11} & \bar{a}_{16} \\ \bar{a}_{16} & \bar{a}_{66} \end{bmatrix} \begin{Bmatrix} \left(\tilde{N}_0 + H_0 n_x^{Th} + G_0 c_x^{Th}\right)(x - L) + \frac{1}{2}\left(H_1 n_x^{Th} + G_1 c_x^{Th}\right)\left(x^2 - L^2\right) \\ \left(\tilde{T}_0 + H_0 \bar{n}_{x\theta}^{Th} + G_0 \bar{c}_{x\theta}^{Th}\right)(x - L) + \frac{1}{2}\left(H_1 \bar{n}_{x\theta}^{Th} + G_1 \bar{c}_{x\theta}^{Th}\right)\left(x^2 - L^2\right) \end{Bmatrix} + \begin{Bmatrix} \bar{\ell}_{12} \\ \bar{\ell}_{62} \end{Bmatrix} \frac{2W_0(x - L) + W_1\left(x^2 - L^2\right)}{2R} \tag{E7}$$

The remaining part of the solution is the determination of the constants W_0 and W_1. These constants are found by first noting that P_0 appearing equation (40), and given by equation (29b) reduces to the constant

$$P_0 = -\frac{1}{RD_{11}\,\ell}\left[\left(A_{12}\bar{a}_{11} + \bar{A}_{26}\bar{a}_{16}\right)\tilde{N}_0 + \left(A_{12}\bar{a}_{16} + \bar{A}_{26}\bar{a}_{66}\right)\tilde{T}_0\right] \tag{E8}$$

Likewise, equation (102a) reduces to

$$P_1(x) = Y_0 + Y_1\, x \tag{E9}$$

for the given loading conditions, where

$$Y_0 = \frac{1}{D_{11}\,\epsilon}\left[q_n^0 + \frac{H_0}{R}\left(n_\theta^{Th} - n_x^{Th}\left(A_{12}\bar{a}_{11} + \overline{A}_{26}\bar{a}_{16}\right) - \bar{n}_{x\theta}^{Th}\left(A_{12}\bar{a}_{16} + \overline{A}_{26}\bar{a}_{66}\right)\right)\right. \\ \left. + \frac{G_0}{R}\left(c_\theta^{Th} - c_x^{Th}\left(A_{12}\bar{a}_{11} + \overline{A}_{26}\bar{a}_{16}\right) - \bar{c}_{x\theta}^{Th}\left(A_{12}\bar{a}_{16} + \overline{A}_{26}\bar{a}_{66}\right)\right)\right] \tag{E10a}$$

$$Y_1 = \frac{1}{D_{11}\,\epsilon}\left[q_n^1 + \frac{H_1}{R}\left(n_\theta^{Th} - n_x^{Th}\left(A_{12}\bar{a}_{11} + \overline{A}_{26}\bar{a}_{16}\right) - \bar{n}_{x\theta}^{Th}\left(A_{12}\bar{a}_{16} + \overline{A}_{26}\bar{a}_{66}\right)\right)\right. \\ \left. + \frac{G_1}{R}\left(c_\theta^{Th} - c_x^{Th}\left(A_{12}\bar{a}_{11} + \overline{A}_{26}\bar{a}_{16}\right) - \bar{c}_{x\theta}^{Th}\left(A_{12}\bar{a}_{16} + \overline{A}_{26}\bar{a}_{66}\right)\right)\right] \tag{E10b}$$

Substituting equations (E4), (E7), and (E9) into equation (40) yields

$$W_0 = \frac{P_0 + Y_0}{4T^2} \tag{E11a}$$

$$W_1 = \frac{Y_1}{4T^2} \tag{E11a}$$

Approximations to the stress resultants $N_\theta(x)$, $M_x(x)$, $M_\theta(x)$, and $M_{x\theta}(x)$ are determined by substituting equations (E4) and (E7) into equation (16a), (17a), (82), and (88), respectively. Approximations to the transverse-shear stress resultants are then obtained by substituting the resulting expressions for $M_x(x)$ and $M_{x\theta}(x)$ into equations (B4) and (B5), respectively. An approximate expression for $N_{x\theta}$ is obtained by substituting equation (E5b) and the expression for $M_{x\theta}(x)$ into equation (4).

Appendix F
Exact Solution for Sinusoidal Pressure and Temperatures

For this example, the boundary conditions are specified as

$$u(0) = 0 \tag{F1a}$$

$$v(0) = 0 \tag{F1b}$$

$$w(0) = 0 \tag{F1c}$$

$$M_x(0) = 0 \tag{F1d}$$

at $x = 0$ and

$$N_x(L) = 0 \tag{F2a}$$

$$\hat{T}(L) = 0 \tag{F2b}$$

$$w(L) = 0 \tag{F2c}$$

$$M_x(L) = 0 \tag{F2d}$$

at $x = L$. It should be noted that these boundary conditions are for simply supported ends rather than the clamped ends considered in the corresponding example presented herein. The applied mechanical load given by $q_n(x) = q_n^s \sin(\frac{\pi x}{L})$ and the applied thermal load is given by $\Theta_0(x) = H_s \sin(\frac{\pi x}{L})$ and $\Theta_1(x) = G_s \sin(\frac{\pi x}{L})$. For these loading conditions, equations (1b) and (7b) yield $\bar{N}_1(x) = 0$ and $\bar{T}_1(x) = 0$. Likewise, equations (100) reduce to

$$N_x^{Th}(x) = \left(H_s n_x^{Th} + G_s c_x^{Th}\right)\sin(\frac{\pi x}{L}) \tag{F3a}$$

$$N_\theta^{Th}(x) = \left(H_s n_\theta^{Th} + G_s c_\theta^{Th}\right)\sin(\frac{\pi x}{L}) \tag{F3b}$$

$$M_x^{Th}(x) = \left(H_s c_x^{Th} + G_s m_x^{Th}\right)\sin(\frac{\pi x}{L}) \tag{F3c}$$

$$\hat{T}^{Th}(x) = \left(H_s \bar{n}_{x\theta}^{Th} + G_s \bar{c}_{x\theta}^{Th}\right)\sin(\frac{\pi x}{L}) \tag{F3d}$$

In addition, equation (B17) yields

$$N_{x\theta}^{Th}(x) = \left(H_s n_{x\theta}^{Th} + G_s c_{x\theta}^{Th}\right)\sin\left(\frac{\pi x}{L}\right) \tag{F3e}$$

$$M_{\theta}^{Th}(x) = \left(H_s c_{\theta}^{Th} + G_s m_{\theta}^{Th}\right)\sin\left(\frac{\pi x}{L}\right) \tag{F3f}$$

$$M_{x\theta}^{Th}(x) = \left(H_s c_{x\theta}^{Th} + G_s m_{x\theta}^{Th}\right)\sin\left(\frac{\pi x}{L}\right) \tag{F3g}$$

Applying boundary-condition equations (F2a) and (F2b) to equations (1a) and (7a) gives $\bar{N}_0 = 0$ and $\bar{T}_0 = 0$. Thus, $N_x(x) = 0$ and $\hat{T}(x) = 0$. Next, the radial displacement is presumed to be given by

$$w(x) = W\sin\left(\frac{\pi x}{L}\right) \tag{F4}$$

where W is a constant to be determined. By using equations (F3) and (F4), equations (14) become

$$\begin{Bmatrix} u'(x) \\ v'(x) \end{Bmatrix} = \left\{ \begin{bmatrix} \bar{a}_{11} & \bar{a}_{16} \\ \bar{a}_{16} & \bar{a}_{66} \end{bmatrix} \begin{Bmatrix} H_s n_x^{Th} + G_s c_x^{Th} \\ H_s \bar{n}_{x\theta}^{Th} + G_s \bar{c}_{x\theta}^{Th} \end{Bmatrix} + \frac{W}{R} \begin{Bmatrix} \bar{\ell}_{12} \\ \bar{\ell}_{62} \end{Bmatrix} + \frac{W\pi^2}{L^2} \begin{Bmatrix} \bar{\varepsilon}_{12} \\ \bar{\varepsilon}_{62} \end{Bmatrix} \right\} \sin\left(\frac{\pi x}{L}\right) \tag{F5}$$

Integrating these two equations and applying boundary-condition equations (F1a) and (F1b) gives

$$\begin{Bmatrix} u(x) \\ v(x) \end{Bmatrix} = \left\{ \begin{bmatrix} \bar{a}_{11} & \bar{a}_{16} \\ \bar{a}_{16} & \bar{a}_{66} \end{bmatrix} \begin{Bmatrix} H_s n_x^{Th} + G_s c_x^{Th} \\ H_s \bar{n}_{x\theta}^{Th} + G_s \bar{c}_{x\theta}^{Th} \end{Bmatrix} + \frac{W}{R} \begin{Bmatrix} \bar{\ell}_{12} \\ \bar{\ell}_{62} \end{Bmatrix} + \frac{W\pi^2}{L^2} \begin{Bmatrix} \bar{\varepsilon}_{12} \\ \bar{\varepsilon}_{62} \end{Bmatrix} \right\} \frac{L}{\pi}\left[1 - \cos\left(\frac{\pi x}{L}\right)\right] \tag{F6}$$

Substituting equations (F3)-(F5) into equation (17a) gives

$$M_x(x) = \bar{M}_x \sin\left(\frac{\pi x}{L}\right) \tag{F7a}$$

where

$$\begin{aligned} \bar{M}_x = H_s\Big[B_{11}\left(\bar{a}_{11} n_x^{Th} + \bar{a}_{16}\bar{n}_{x\theta}^{Th}\right) + \bar{B}_{16}\left(\bar{a}_{16} n_x^{Th} + \bar{a}_{66}\bar{n}_{x\theta}^{Th}\right) - c_x^{Th}\Big] \\ + G_s\Big[B_{11}\left(\bar{a}_{11} c_x^{Th} + \bar{a}_{16}\bar{c}_{x\theta}^{Th}\right) + \bar{B}_{16}\left(\bar{a}_{16} c_x^{Th} + \bar{a}_{66}\bar{c}_{x\theta}^{Th}\right) - m_x^{Th}\Big] \\ + \frac{W}{R}\left[\frac{R\pi^2}{L^2} D_{11} + B_{12} + B_{11}\left(\bar{\ell}_{12} + \frac{R\pi^2}{L^2}\bar{\varepsilon}_{12}\right) + \bar{B}_{16}\left(\bar{\ell}_{62} + \frac{R\pi^2}{L^2}\bar{\varepsilon}_{62}\right)\right] \end{aligned} \tag{F7b}$$

Inspection of equation (F7) reveals that boundary-condition equations (F1d) and (F2d) are also satisfied.

The remaining part of the solution is the determination of the constant W. This constant is found by first noting that $P_0 = 0$ in equation (40) and equation (102a) reduces to

$$P_1(x) = Y_{s1} \sin\left(\frac{\pi x}{L}\right) \tag{F8}$$

for the given loading conditions, where Y_{s1} is given by equation (102e). Substituting equations (F4) and (F8), and $P_0 = 0$, into equation (40) yields

$$W = \frac{Y_{s1} L^4}{\pi^4 - 4S\,\pi^2 L^2 + 4T^2 L^4} \tag{F9}$$

The remaining stress resultants are determined by substituting equations (F3)-(F5), (97), and (B17) into equation (16a), (82), and (88). The results are:

$$N_\theta(x) = \overline{N}_\theta \sin\left(\frac{\pi x}{L}\right) \tag{F10a}$$

with

$$\begin{aligned}\overline{N}_\theta = H_s\Big[& A_{12}\left(\bar{a}_{11} n_x^{Th} + \bar{a}_{16} \bar{n}_{x\theta}^{Th}\right) + \overline{A}_{26}\left(\bar{a}_{16} n_x^{Th} + \bar{a}_{66} \bar{n}_{x\theta}^{Th}\right) - n_\theta^{Th}\Big] \\ & + G_s\Big[A_{12}\left(\bar{a}_{11} c_x^{Th} + \bar{a}_{16} \bar{c}_{x\theta}^{Th}\right) + \overline{A}_{26}\left(\bar{a}_{16} c_x^{Th} + \bar{a}_{66} \bar{c}_{x\theta}^{Th}\right) - c_\theta^{Th}\Big] \\ & + \frac{W}{R}\left[\frac{R\pi^2}{L^2} B_{12} + A_{22} + A_{12}\left(\bar{\ell}_{12} + \frac{R\pi^2}{L^2}\bar{\varepsilon}_{12}\right) + \overline{A}_{26}\left(\bar{\ell}_{62} + \frac{R\pi^2}{L^2}\bar{\varepsilon}_{62}\right)\right]\end{aligned} \tag{F10b}$$

$$M_\theta(x) = \overline{M}_\theta \sin\left(\frac{\pi x}{L}\right) \tag{F11a}$$

with

$$\begin{aligned}\overline{M}_\theta = H_s\Big[& B_{12}\left(\bar{a}_{11} n_x^{Th} + \bar{a}_{16} \bar{n}_{x\theta}^{Th}\right) + \overline{B}_{26}\left(\bar{a}_{16} n_x^{Th} + \bar{a}_{66} \bar{n}_{x\theta}^{Th}\right) - c_\theta^{Th}\Big] \\ & + G_s\Big[B_{12}\left(\bar{a}_{11} c_x^{Th} + \bar{a}_{16} \bar{c}_{x\theta}^{Th}\right) + \overline{B}_{26}\left(\bar{a}_{16} c_x^{Th} + \bar{a}_{66} \bar{c}_{x\theta}^{Th}\right) - m_\theta^{Th}\Big] \\ & + \frac{W}{R}\left[\frac{R\pi^2}{L^2} D_{12} + B_{22} + B_{12}\left(\bar{\ell}_{12} + \frac{R\pi^2}{L^2}\bar{\varepsilon}_{12}\right) + \overline{B}_{26}\left(\bar{\ell}_{62} + \frac{R\pi^2}{L^2}\bar{\varepsilon}_{62}\right)\right]\end{aligned} \tag{F11b}$$

$$M_{x\theta}(x) = \overline{M}_{x\theta} \sin\left(\frac{\pi x}{L}\right) \tag{F12a}$$

with

$$\begin{aligned}\overline{M}_{x\theta} = H_s\Big[& B_{16}\left(\bar{a}_{11} n_x^{Th} + \bar{a}_{16} \bar{n}_{x\theta}^{Th}\right) + \overline{B}_{66}\left(\bar{a}_{16} n_x^{Th} + \bar{a}_{66} \bar{n}_{x\theta}^{Th}\right) - c_{x\theta}^{Th}\Big] \\ & + G_s\Big[B_{16}\left(\bar{a}_{11} c_x^{Th} + \bar{a}_{16} \bar{c}_{x\theta}^{Th}\right) + \overline{B}_{66}\left(\bar{a}_{16} c_x^{Th} + \bar{a}_{66} \bar{c}_{x\theta}^{Th}\right) - m_{x\theta}^{Th}\Big] \\ & + \frac{W}{R}\left[\frac{R\pi^2}{L^2} D_{16} + B_{26} + B_{16}\left(\bar{\ell}_{12} + \frac{R\pi^2}{L^2}\bar{\varepsilon}_{12}\right) + \overline{B}_{66}\left(\bar{\ell}_{62} + \frac{R\pi^2}{L^2}\bar{\varepsilon}_{62}\right)\right]\end{aligned} \tag{F12b}$$

Likewise, equations (B4) and (B5) give

$$Q_x(x) = \frac{\pi}{L}\,\overline{M}_x \cos\left(\frac{\pi x}{L}\right) \tag{F13}$$

and

$$Q_\theta(x) = \frac{\pi}{L}\,\overline{M}_{x\theta} \cos\left(\frac{\pi x}{L}\right) \tag{F14}$$

An expression for $N_{x\theta}$ is obtained by substituting $\hat{T}(x) = 0$ and equations (F12b) into equation (4).

REPORT DOCUMENTATION PAGE

Form Approved
OMB No. 0704-0188

1. REPORT DATE *(DD-MM-YYYY)*	2. REPORT TYPE	3. DATES COVERED *(From - To)*
01- 02 - 2011	Technical Publication	

4. TITLE AND SUBTITLE

The Exact Solution for Linear Thermoelastic Axisymmetric Deformations of Generally Laminated Circular Cylindrical Shells

5a. CONTRACT NUMBER

5b. GRANT NUMBER

5c. PROGRAM ELEMENT NUMBER

6. AUTHOR(S)

Nemeth, Michael P.; Schultz, Marc R.

5d. PROJECT NUMBER

5e. TASK NUMBER

5f. WORK UNIT NUMBER

869021.04.07.01.13

7. PERFORMING ORGANIZATION NAME(S) AND ADDRESS(ES)

NASA Langley Research Center
Hampton, VA 23681-2199

8. PERFORMING ORGANIZATION REPORT NUMBER

L-20112

9. SPONSORING/MONITORING AGENCY NAME(S) AND ADDRESS(ES)

National Aeronautics and Space Administration
Washington, DC 20546-0001

10. SPONSOR/MONITOR'S ACRONYM(S)

NASA

11. SPONSOR/MONITOR'S REPORT NUMBER(S)

NASA/TP-2012-217342

12. DISTRIBUTION/AVAILABILITY STATEMENT

Unclassified Unlimited
Subject Category 39
Availability: NASA CASI (443) 757-5802

13. SUPPLEMENTARY NOTES

14. ABSTRACT

A detailed exact solution is presented for laminated-composite circular cylinders with general wall construction and that undergo axisymmetric deformations. The overall solution is formulated in a general, systematic way and is based on the solution of a single fourth-order, nonhomogeneous ordinary differential equation with constant coefficients in which the radial displacement is the dependent variable. Moreover, the effects of general anisotropy are included and positive-definiteness of the strain energy is used to define uniquely the form of the basis functions spanning the solution space of the ordinary differential equation. Loading conditions are considered that include axisymmetric edge loads, surface tractions, and temperature fields. Likewise, all possible axisymmetric boundary conditions are considered. Results are presented for five examples that demonstrate a wide range of behavior for specially orthotropic and fully anisotropic cylinders.

15. SUBJECT TERMS

Anisotropic shells; Bending boundary layer; Cylindrical shells; Edge effects

16. SECURITY CLASSIFICATION OF:			17. LIMITATION OF ABSTRACT	18. NUMBER OF PAGES	19a. NAME OF RESPONSIBLE PERSON
a. REPORT	b. ABSTRACT	c. THIS PAGE			STI Help Desk (email: help@sti.nasa.gov)
					19b. TELEPHONE NUMBER *(Include area code)*
U	U	U	UU	104	(443) 757-5802